Julius-Maximilians-
UNIVERSITÄT
WÜRZBURG

EP 3

Current Heating in Quasi-ballistic Channels: Thermoelectrics and Hydrodynamic Flow

Laurens W. Molenkamp

Physikalisches Institut, EP3
Universität Würzburg

EP3

Onsager Coefficients

- I electric current density
- J particle current density
- J_Q heat flux, heat current density
- μ chemical potential
- T temperature
- V voltage, electrostatic potential difference

$$\begin{pmatrix} I/-e \\ J_Q \end{pmatrix} = \begin{pmatrix} J \\ J_Q \end{pmatrix} = \begin{pmatrix} -\frac{L_{11}}{T} & -\frac{L_{12}}{T^2} \\ -\frac{L_{21}}{T} & -\frac{L_{22}}{T^2} \end{pmatrix} \begin{pmatrix} \nabla\mu - e\nabla V \\ \nabla T \end{pmatrix}$$

From: R.D. Barnard *Thermoelectricity in Metals and Alloys* (1972)

$$L_{11} = \frac{\sigma T}{e^2}$$

$$L_{12} = L_{21}$$

$$L_{12} = -\frac{ST^2\sigma}{e} = -\frac{\Pi T \sigma}{e}$$

$$L_{22} = T^2\left(\kappa + T\sigma S^2\right)$$

Thermoelectric Properties

"fluxes" $\begin{pmatrix} I \\ Q \end{pmatrix} = \begin{pmatrix} G & L \\ M & K \end{pmatrix} \begin{pmatrix} \Delta\mu / e \\ \Delta T \end{pmatrix}$ "forces"

Onsager-relation: $M = -LT$

$$\boxed{\begin{pmatrix} -\Delta V \\ Q \end{pmatrix} = \begin{pmatrix} R & S \\ \Pi & -\kappa \end{pmatrix} \begin{pmatrix} I \\ \Delta T \end{pmatrix}}$$

Diffusion Thermopower

$$S \equiv \left(\frac{\Delta\mu / e}{\Delta T} \right)_{I=0} = -\frac{L}{G}$$

$$\Pi \equiv \left(\frac{Q}{I} \right)_{\Delta T=0} = \frac{M}{G} = ST$$

$$\kappa \equiv -\left(\frac{Q}{\Delta T} \right)_{I=0} = -K\left(1 + \frac{S^2 GT}{K} \right)$$

Thermoelectric Properties

Landauer-Büttiker-Formalism:

$$G = -\frac{2e^2}{h}\int_0^\infty dE\,\frac{\partial f}{\partial E}t(E)$$

$$L = -\frac{2e^2}{h}\frac{k_B}{e}\int_0^\infty dE\,\frac{\partial f}{\partial E}t(E)\frac{(E-E_F)}{k_BT}$$

$$\frac{(E-E_F)}{k_BT}\left(\frac{\partial f}{\partial E}\right)$$

odd function in E
➔ L large for $t(E)$
asymmetric around E_F

$$\frac{K}{T} = \frac{2e^2}{h}\left(\frac{k_B}{e}\right)^2\int_0^\infty dE\,\frac{\partial f}{\partial E}t(E)\left[\frac{(E-E_F)}{k_BT}\right]^2$$

$$S \equiv \left(\frac{\Delta\mu/e}{\Delta T}\right)_{I=0} = -\frac{L}{G}$$

$$\Rightarrow S = -\frac{\langle E\rangle}{eT}$$

Thermopower (S)

- Kelvin-Onsager relation (1931)

$$S = -\frac{L}{G}\bigg|_{I=0} = \frac{\Pi}{T} = -\frac{\langle E \rangle}{eT}$$

$(\Delta Q = T\Delta \mathbf{S})$ thermal energy to transfer one electron from a hot to a cold reservoir

- Heike's formula

$$S = -\frac{1}{e}\Delta \mathbf{S} = -\frac{1}{e}k_B\left(\ln g_f - \ln g_i\right)$$

(spin) entropy contribution

- Mott relation

$$S = -\frac{\pi^2}{3}\frac{k_B}{q}\frac{k_B T}{G}\frac{dG}{dE}\bigg|_{E_F}$$

linear response

Thermopower (S)

Measuring Thermopower

$$S \equiv -\lim_{\Delta T \to 0} \left. \frac{\Delta V_{th}}{\Delta T} \right|_{I=0}$$

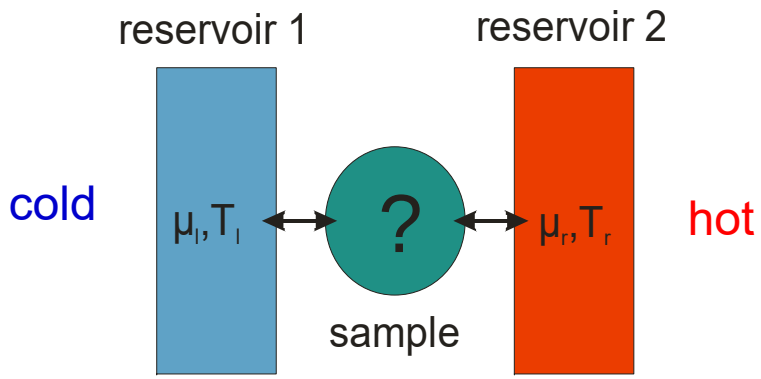

Thermopower Measurement

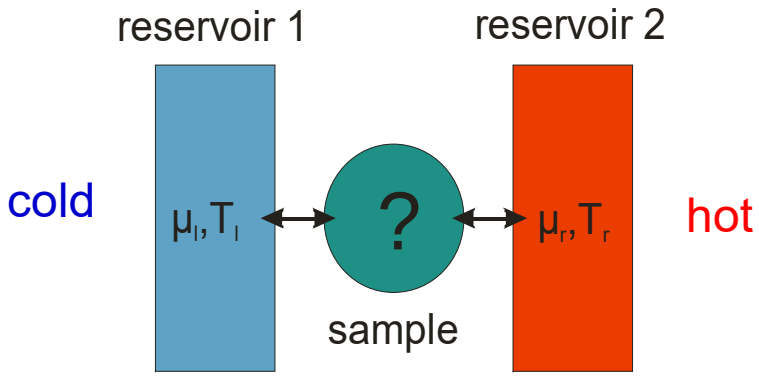

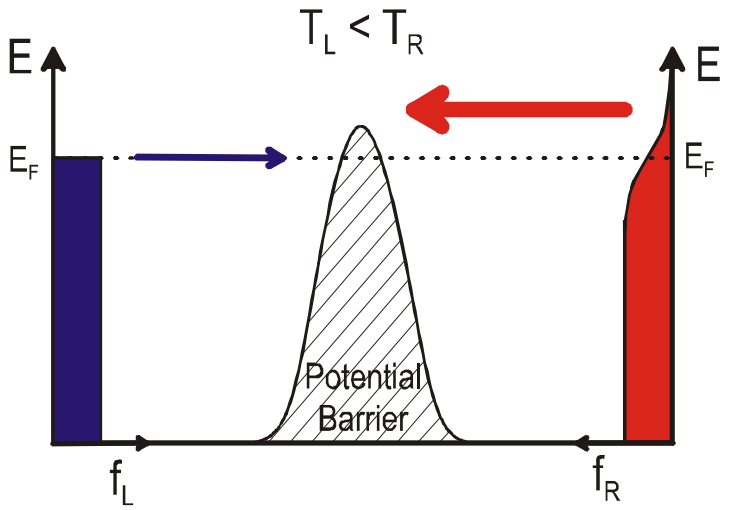

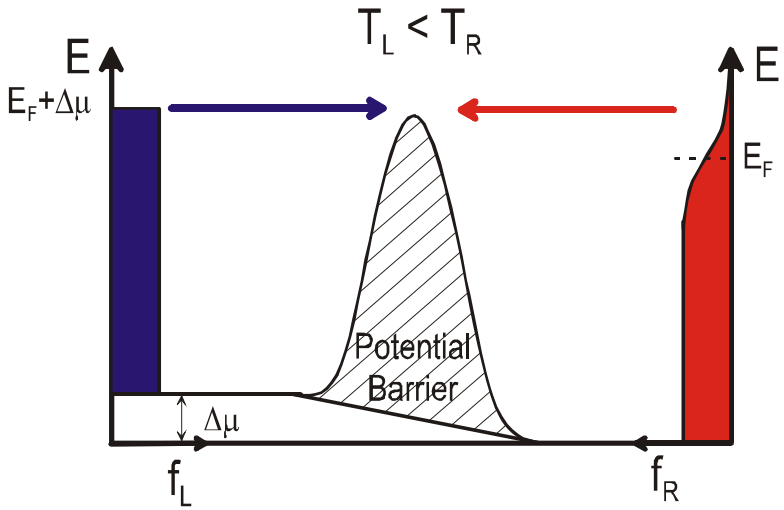

$$S := -\lim_{\Delta T \to 0} \frac{V_{th}}{\Delta T}\bigg|_{I=0}$$

Current Heating Technique

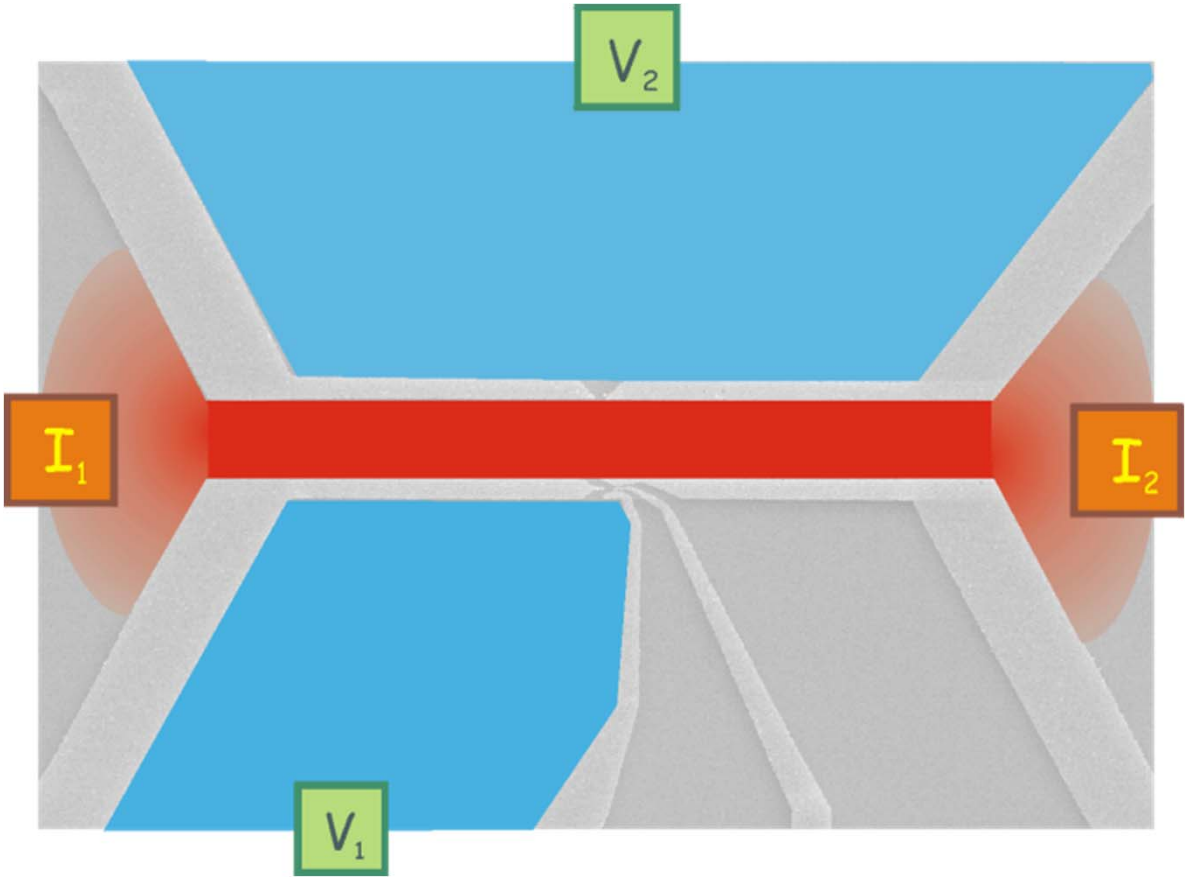

$$V_{th} = V_1 - V_2 = \left(S_{dot} - S_{qpc}\right)\left(T_e - T_L\right)$$

Current Heating Technique

$$V_{th} = V_1 - V_2 = \left(S_{dot} - S_{qpc}\right)\left(T_e - T_L\right)$$

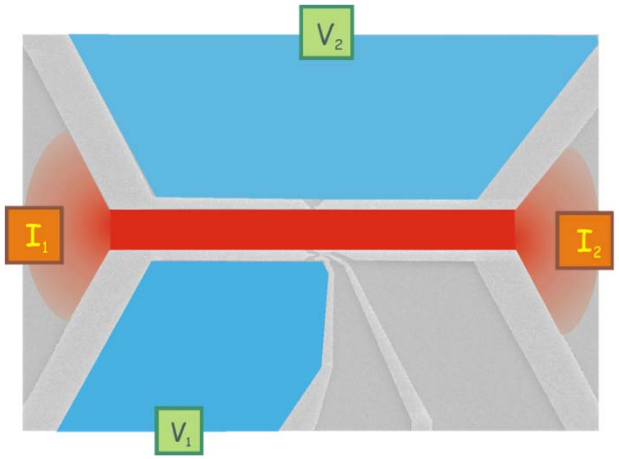

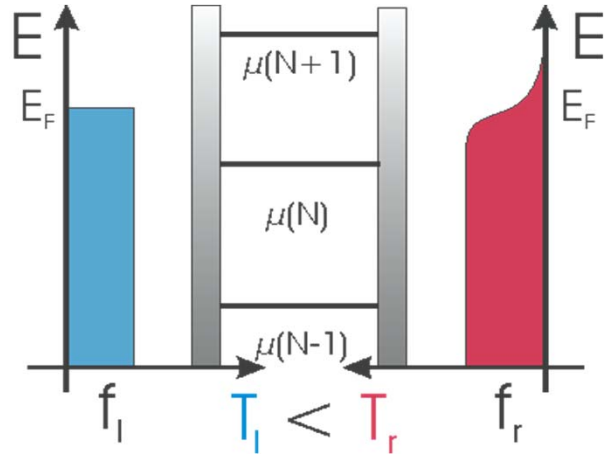

- energy dissipation at the channel entrance
- only hot electron gas within channel
  (1 ps ≈ τ_{ee} << τ_{eph} ≈ 0.2 ns)
- energy relaxation in the reservoir
- diffusion thermopower

  ΔT = 10 mK, Δx = 500 nm ➔ 20 K/mm

- QD and QPC create thermovoltages which can be measured as voltage difference between V_1 and V_2

  V_1-V_2 = (S_{QD} -S_{QPC}) ΔT = S_{QD} ΔT

  S_{QPC} can be adjusted to zero

- ac-excitation and detection:
  P_{heat} ~ [I sin(ωt)]^2
  ~ sin(2ωt) ($\omega/2\pi$ = 13 Hz)

First Experiments: Thermopower of a QPC

VOLUME 65, NUMBER 8 PHYSICAL REVIEW LETTERS 20 AUGUST 1990

Quantum Oscillations in the Transverse Voltage of a Channel in the Nonlinear Transport Regime

L. W. Molenkamp, H. van Houten, C. W. J. Beenakker, and R. Eppenga
Philips Research Laboratories, 5600 JA Eindhoven, The Netherlands

C. T. Foxon
Philips Research Laboratories, Redhill, Surrey RH1 5HA, England
(Received 5 March 1990)

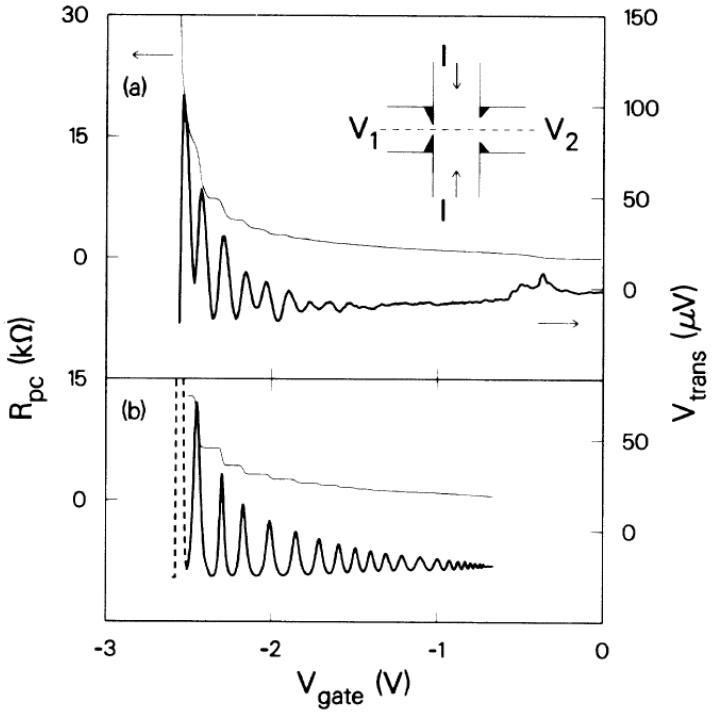

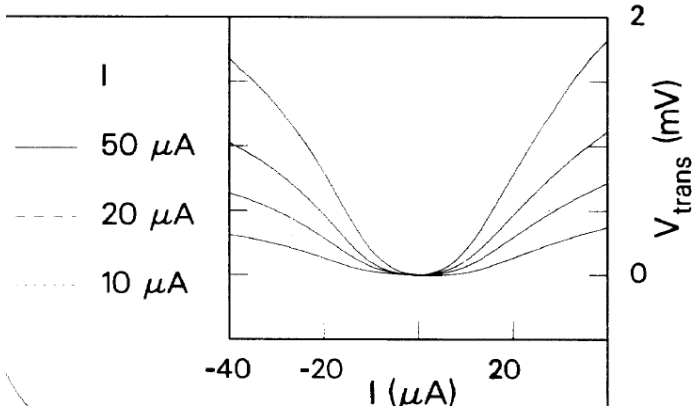

In semiconductors, at low T, $\tau_{e-p} \sim 100$ ps.

→ nearly thermalized hot electron distribution in the heating channel

Step-by-step Barrier

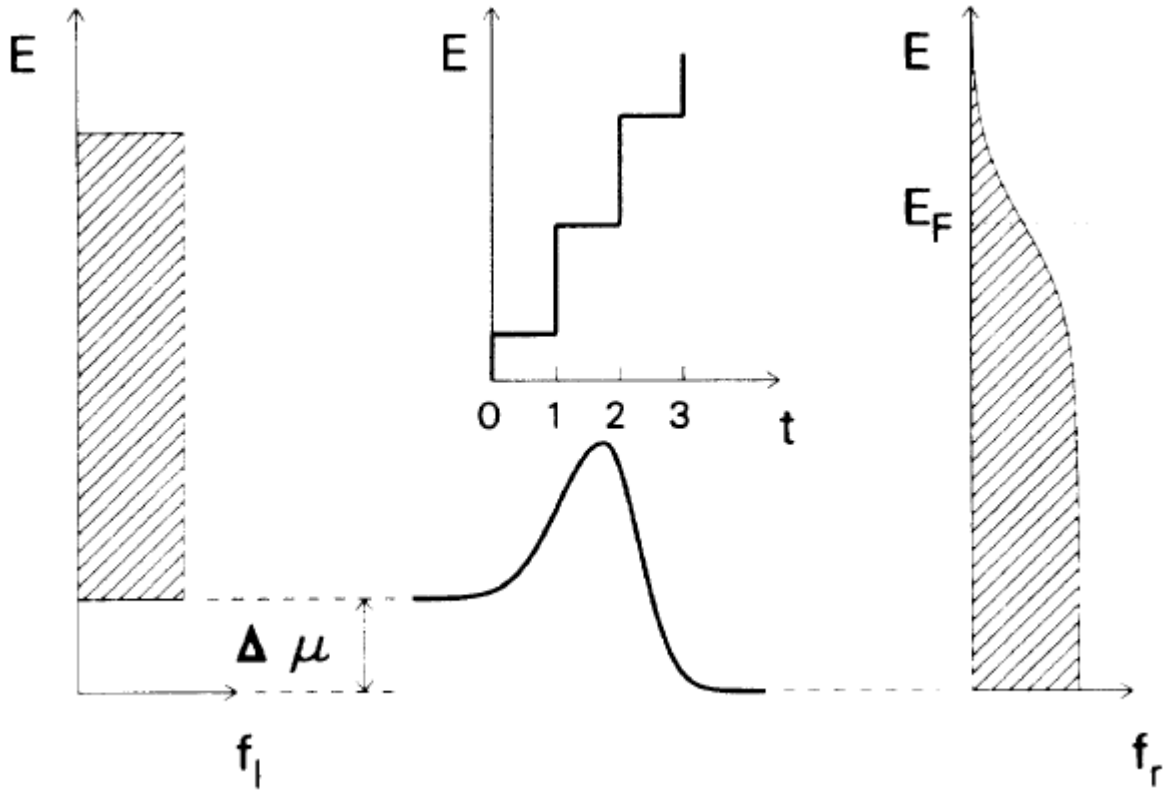

Each channel in the point contact acts as a potential barrier, hence the thermopower shows a series of peaks

L.W. Molenkamp et al., Phys. Rev. Lett. 65, 1052 (1990).

Thermopower of a QPC

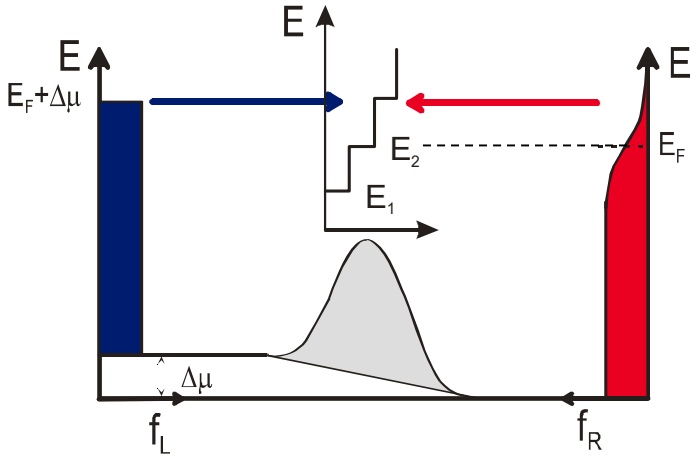

$$\int_0^\infty f dE = k_B T \ln\left[1+\exp\left(E_F / k_B T\right)\right]$$

$$\Rightarrow L = \frac{2e^2}{h}\frac{k_B}{e}\sum_{n=1}^{\infty}\left[\ln\left(1+e^{-\varepsilon_n}\right)+\ln\left(1+e^{\varepsilon_n}\right)^{-1}\right]$$

quantized thermopower

$$S = -\frac{k_B}{e}\frac{\ln 2}{N-\frac{1}{2}} \quad \text{if } E_F = E_N;\ N>1$$

$$S = -\frac{k_B}{e}\left(1+\varepsilon_1\right) \quad \text{if } N<1$$

H. van Houten et al., Semicond. Sci. Technol. **7**, B215 (1992)

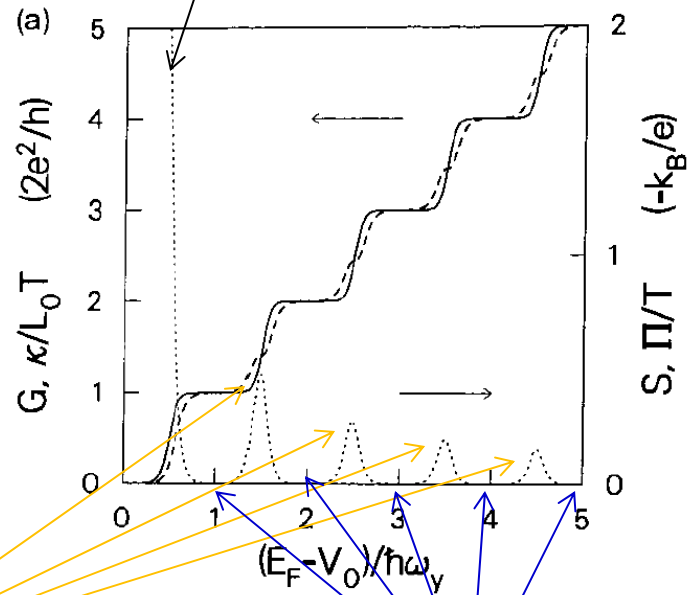

$$S = 0 \quad \text{if } E_F \neq E_N;\ N>1$$

Reference QPC

- Voltage Probes have to be at same temperature and of the same material
- QPC can be used as a reference since TP of QPC is known (can be adjusted to zero)
- G of QPC is quantized – and therefore, so is S. This can be used as a method of temperature calibration

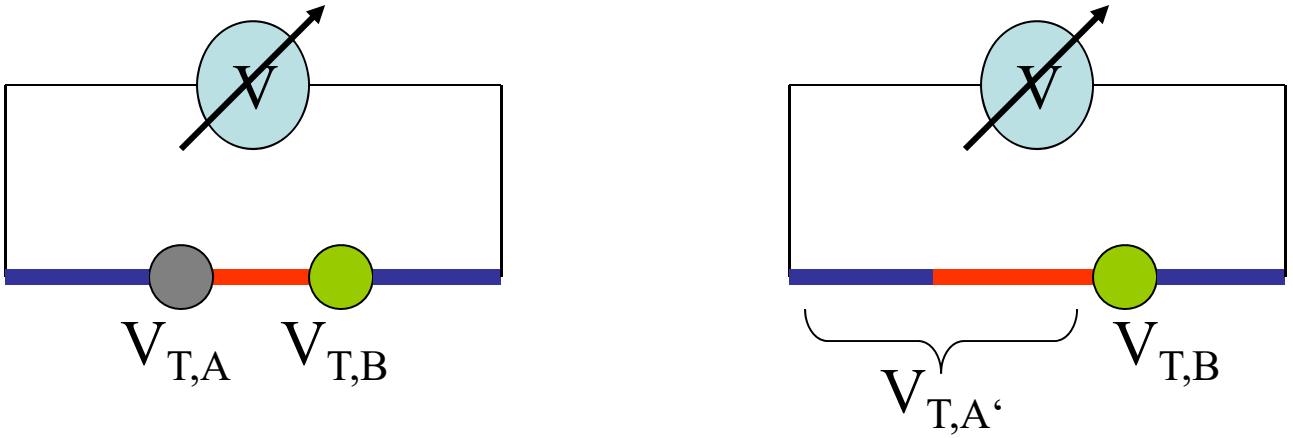

L.W. Molenkamp et al., Phys. Rev. Lett. 65, 1052 (1990).
L.W. Molenkamp et al., Phys. Rev. Lett. 68, 3765 (1992).
A.A.M. Staring et al., Europhys. Lett. 22, 57 (1993).
S. Möller et al., Phys. Rev. Lett. 81, 5197 (1998).
S.F. Godijn et al., Phys. Rev. Lett. 82, 2927 (1999).
R. Scheibner et al., Phys. Rev. Lett. 95, 176602 (2005).
R. Scheibner et al., Phys. Rev. B75, 041301(R) (2007).

Peltier Coefficient

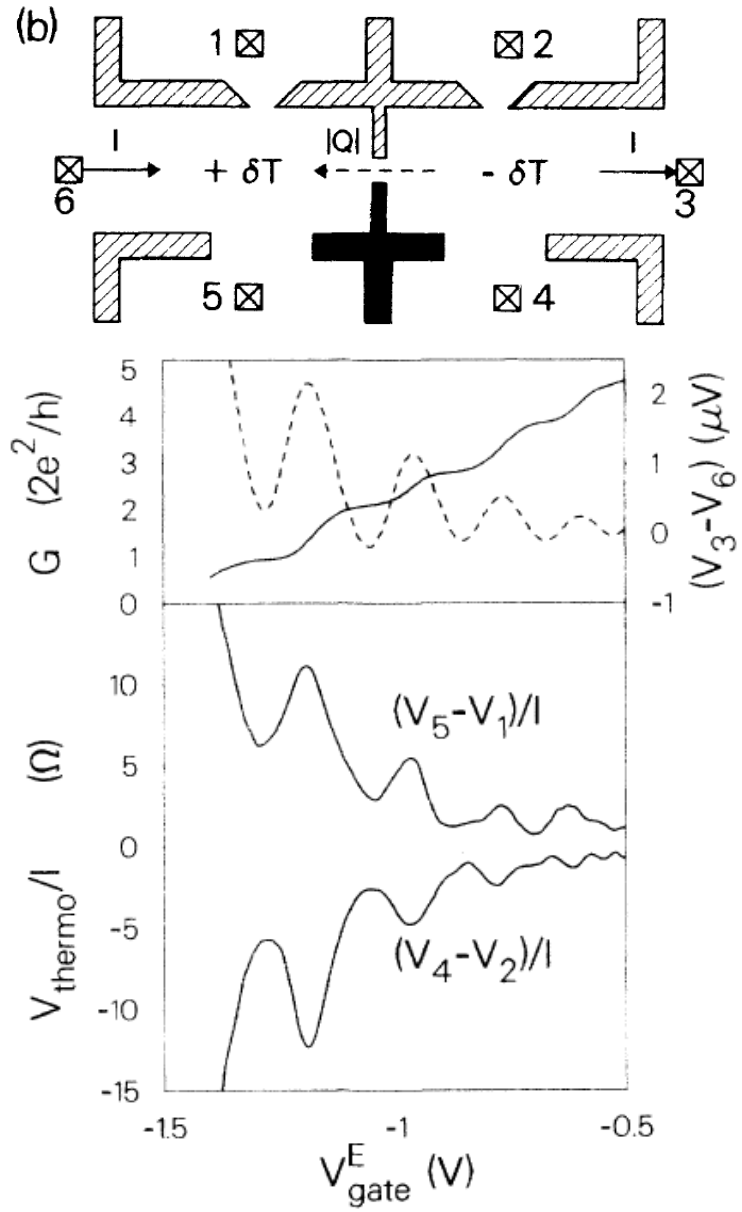

Kelvin-Onsager relation $\Pi = ST$

Theoretical estimate for Peltier coefficient

$$\Pi = ST = -(k_B T \ln 2)/(N + \tfrac{1}{2})e \approx -70\ \mu\mathrm{V}$$

is within factor of 2 from observed signal.

Peltier heating/cooling linear in current, detect only 1f signal!

L.W. Molenkamp et al., Phys. Rev. Lett. 68, 3765 (1992).

Thermal Conductance

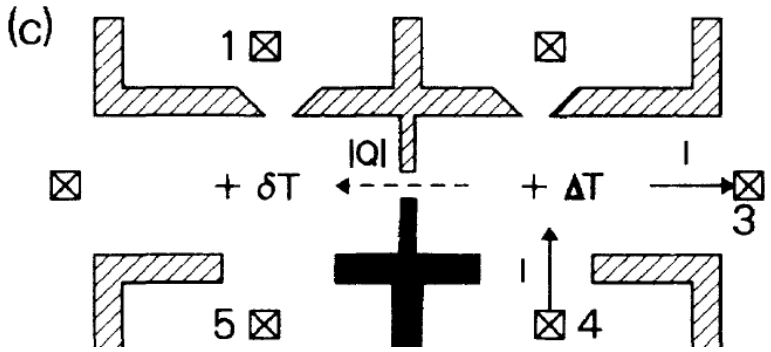

Wiedemann- Franz relation,

$$\kappa \approx L_0 T G ,$$

$L_0 \equiv k_B^2 \pi^2 / 3e^2$ is the Lorenz number.

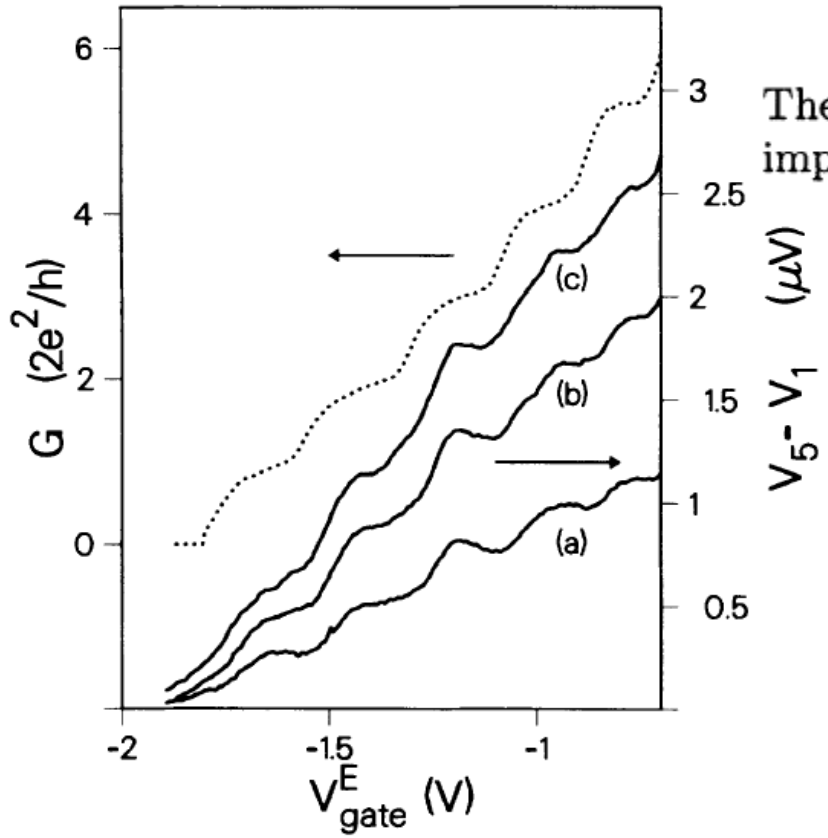

The Wiedemann-Franz relation (5), using $G = N(2e^2/h)$, implies $\kappa = 1.7 \times 10^{-11}$ W/K (for the $N = 5$ plateau).

again within factor of 2 from the observed signal.

Wiedemann-Franz yields thermal conductance quantum.

L.W. Molenkamp et al., Phys. Rev. Lett. 68, 3765 (1992).

What about the Channel Resistance?

PHYSICAL REVIEW B VOLUME 49, NUMBER 7 15 FEBRUARY 1994-I

Electron-electron-scattering-induced size effects in a two-dimensional wire

L. W. Molenkamp and M. J. M. de Jong*
Philips Research Laboratories, 5656 AA Eindhoven, The Netherlands
(Received 7 October 1993)

The differential resistance of wires defined in the two-dimensional electron gas in an (Al,Ga)As heterostructure is observed to first increase and then decrease with increasing current. It is demonstrated that this behavior results from the interplay of an enhanced electron-electron-scattering rate (due to current heating of the electron gas), and the partly diffusive nature of boundary scattering in the wire. The data are identified as an experimental observation of the Knudsen maximum and the Poiseuille flow regime in electron transport, and confirm an analogy between electron and gas flow that has been anticipated since the 1950s.

TABLE I. Length L, lithographic width W_{lith}, electrical width W, electron density n, mean free path l_b [at 1.5 K (sample I) and 1.8 K (samples II & III)], and specularity parameter α of the samples discussed in this paper.

Sample	L (μm)	W_{lith} (μm)	W (μm)	n (10^{11} cm^{-2})	l_b (μm)	α
I	20.2	3.9	3.5	2.2	12.4	0.6
II	63.7	4.0	3.6	2.7	19.7	0.7
III	127.3	4.0	3.6	2.7	19.7	0.7

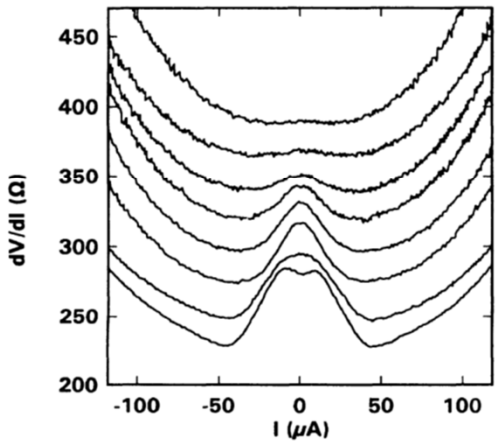

FIG. 1. Differential resistance dV/dI of wire I as a function of heating current I for lattice temperatures of (from top to bottom) 24.7, 20.4, 17.3, 13.6, 10.4, 8.7, 4.4, and 1.5 K.

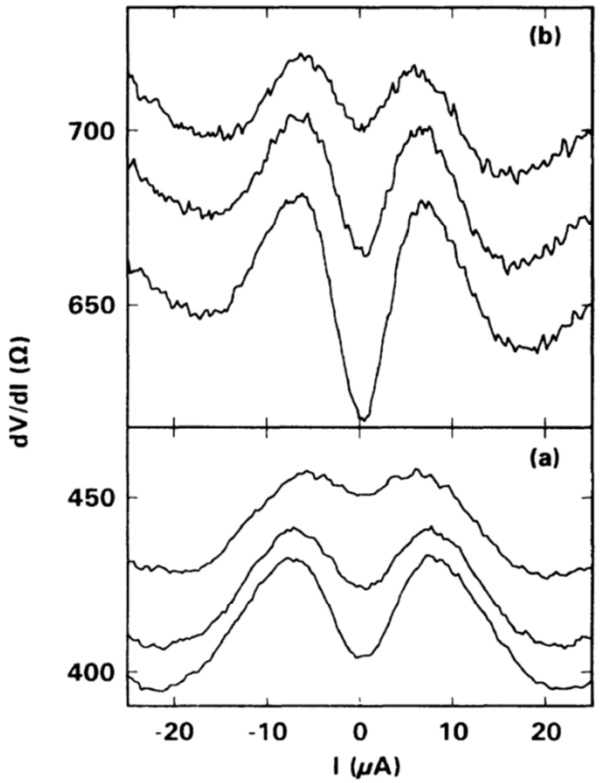

FIG. 2. Differential resistance dV/dI vs I for (a) wire II, and (b) wire III for lattice temperatures of (from top to bottom) 4.5, 3.1, and 1.8 K. At higher current levels, dV/dI exhibits a quasiquadratic increase with current, similar to that in Fig. 1.

Channel resistance reflects hydrodynamic Electron Flow

PHYSICAL REVIEW B VOLUME 51, NUMBER 19 15 MAY 1995-I

Hydrodynamic electron flow in high-mobility wires

M. J. M. de Jong* and L. W. Molenkamp†
Philips Research Laboratories, 5656 AA Eindhoven, The Netherlands
(Received 24 October 1994)

Hydrodynamic electron flow is experimentally observed in the differential resistance of electrostatically defined wires in the two-dimensional electron gas in (Al,Ga)As heterostructures. In these experiments current heating is used to induce a controlled increase in the number of electron-electron collisions in the wire. The interplay between the partly diffusive wire-boundary scattering and the electron-electron scattering leads first to an increase and then to a decrease of the resistance of the wire with increasing current. These effects are the electronic analog of Knudsen and Poiseuille flow in gas transport, respectively. The electron flow is studied theoretically through a Boltzmann transport equation, which includes impurity, electron-electron, and boundary scattering. A solution is obtained for arbitrary scattering parameters. By calculation of flow profiles inside the wire it is demonstrated how normal flow evolves into Poiseuille flow. The boundary-scattering parameters for the gate-defined wires can be deduced from the magnitude of the Knudsen effect. Good agreement between experiment and theory is obtained.

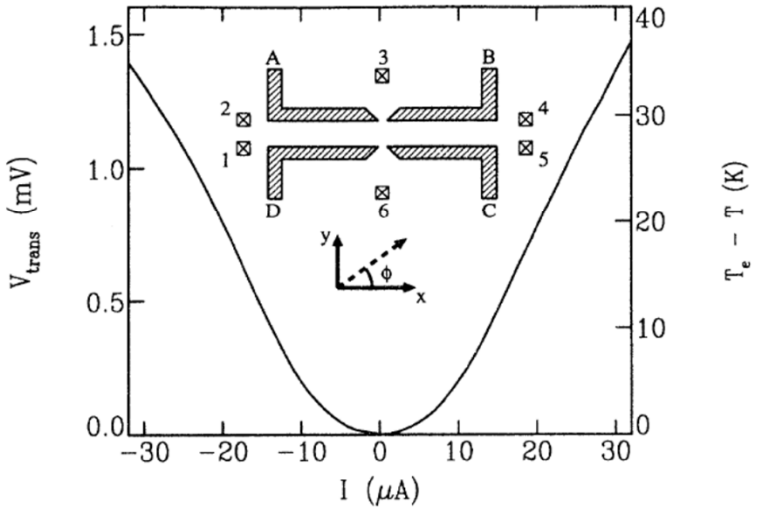

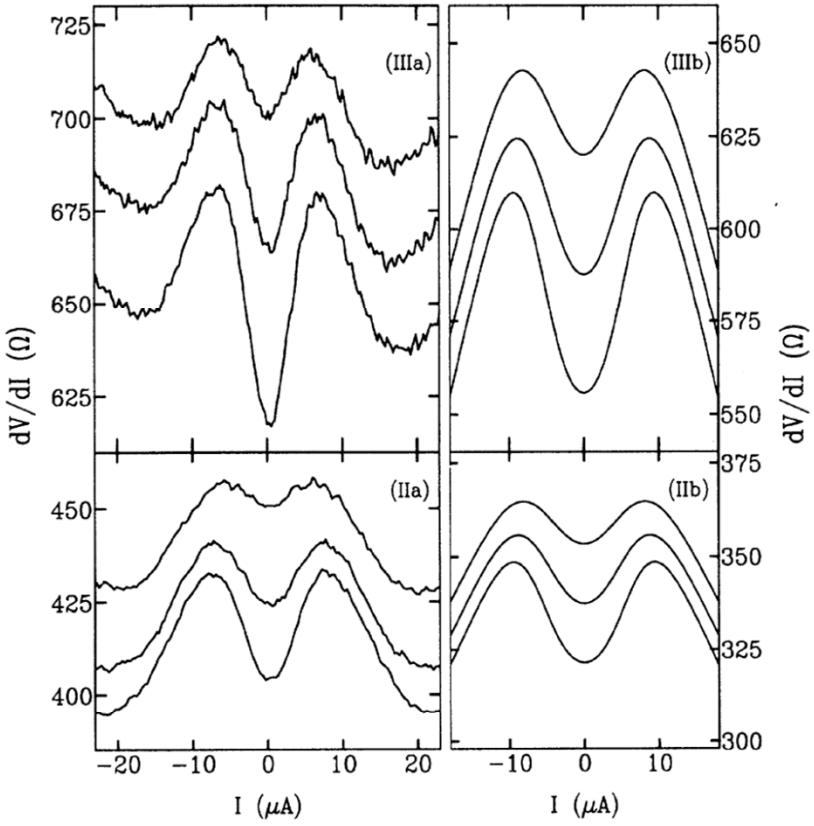

FIG. 3. Differential resistance dV/dI vs current I for wire II and III for lattice temperatures of (from top to bottom) T =4.5, 3.1, and 1.8 K. At higher current levels, dV/dI exhibits a quasiquadratic increase with current, similar to that in Fig. 2. Left panel (IIa) and (IIIa): experimental traces; right panel (IIb) and (IIIb): results of calculations, see Sec. V.

Knudsen- and Poiseuille Flow-Regime

$$n \leftrightarrow l_{ee}(T, n_e)$$

Gurzhi, Shevchenko, JETP (1968)

$$\frac{1}{l_{ee}} = \frac{E_F}{h v_F}\left(\frac{k_B T}{E_F}\right)^2\left[\ln\left(\frac{E_F}{k_B T}\right) + \ln\left(\frac{2q}{k_F}\right) + 1\right]$$

Guiliani and Quinn, PRB (1982)

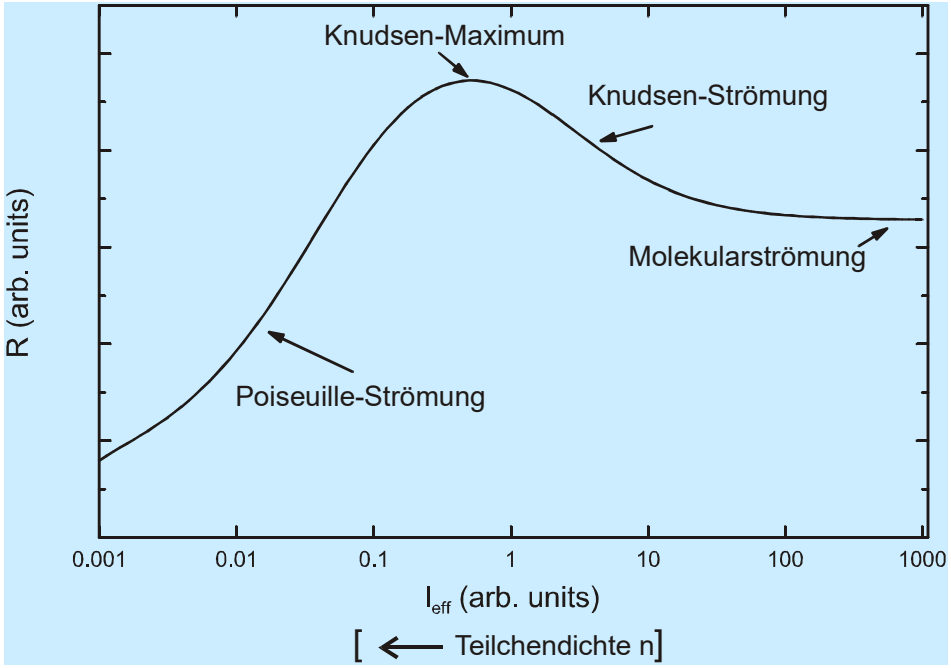

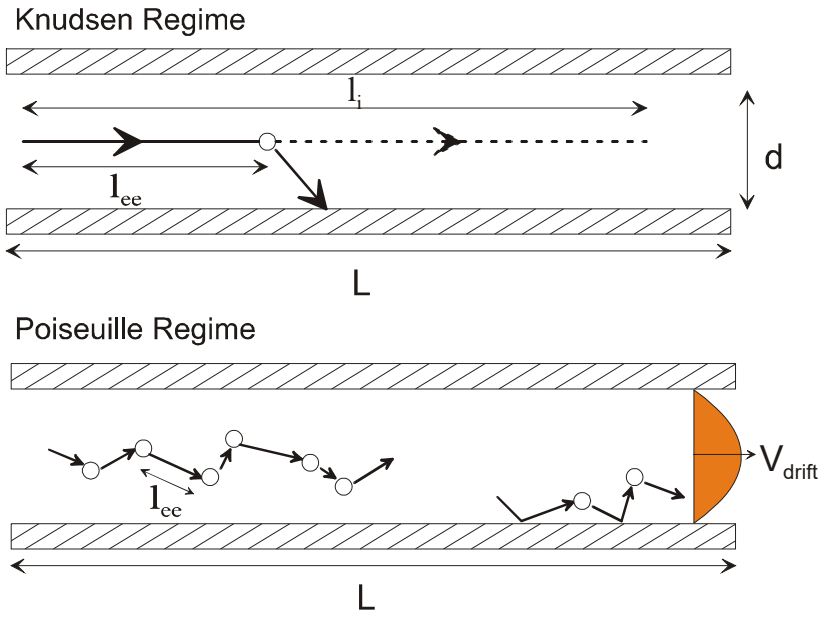

Electron-Electron Scattering Length in 2D

$$\frac{1}{l_{ee}} = \frac{E_F}{h v_F}\left(\frac{k_B T}{E_F}\right)^2\left[\ln\left(\frac{E_F}{k_B T}\right) + \ln\left(\frac{2q_F^{2D}}{k_F}\right) + 1\right]$$

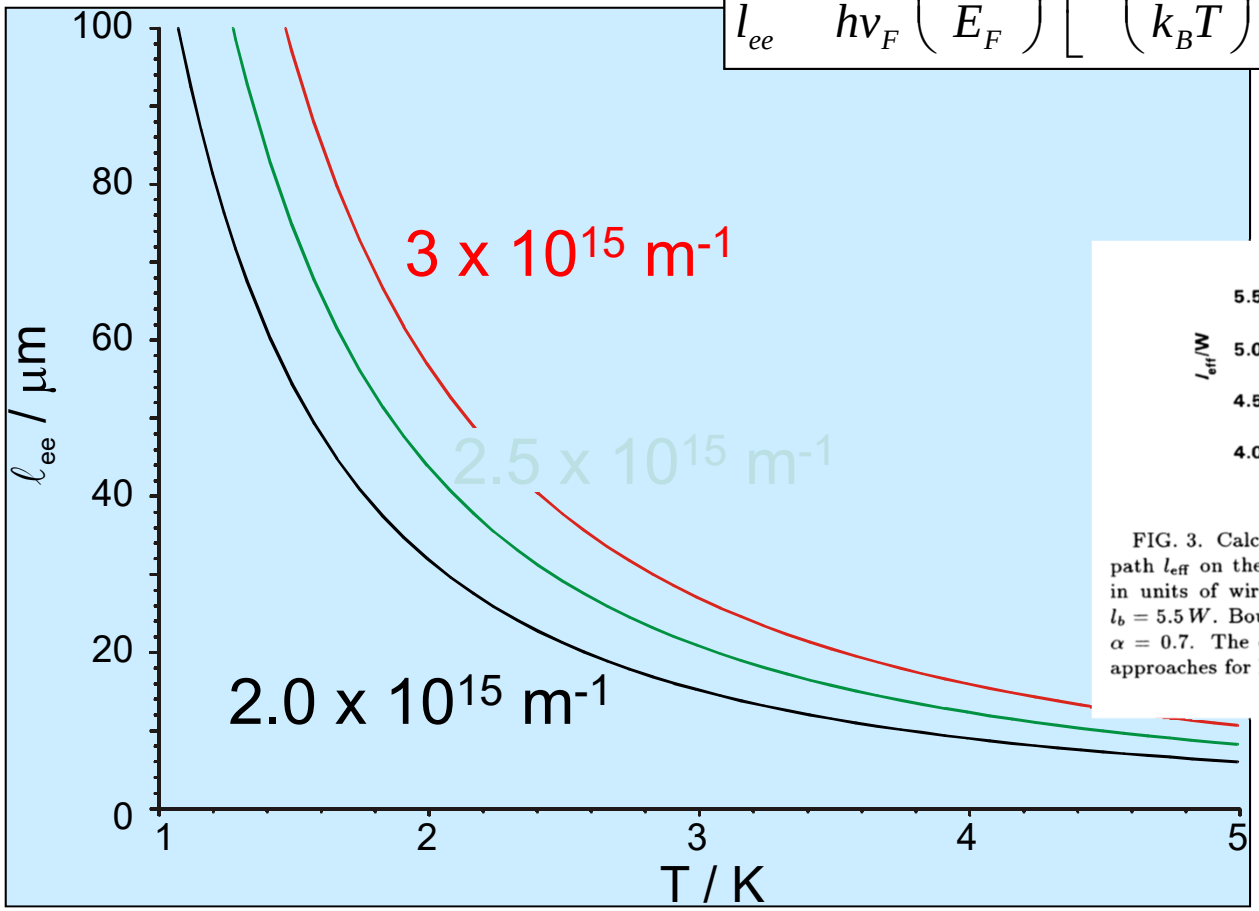

Guiliani and Quinn, PRB (1982)

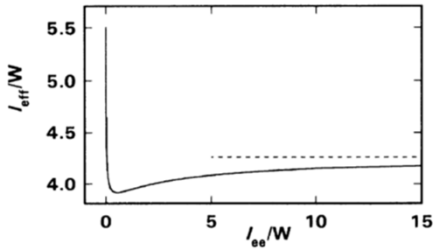

FIG. 3. Calculated dependence of the effective mean free path l_{eff} on the electron-electron-scattering length l_{ee} (both in units of wire width W), for fixed bulk mean free path $l_b = 5.5\,W$. Boundary scattering is modeled by Eq. (5), with $\alpha = 0.7$. The dashed line indicates the asymptote that l_{eff} approaches for large l_{ee}. Note that for $l_{ee} \to 0$, $l_{eff} \to l_b$.

Hydrodynamic Electron Flow

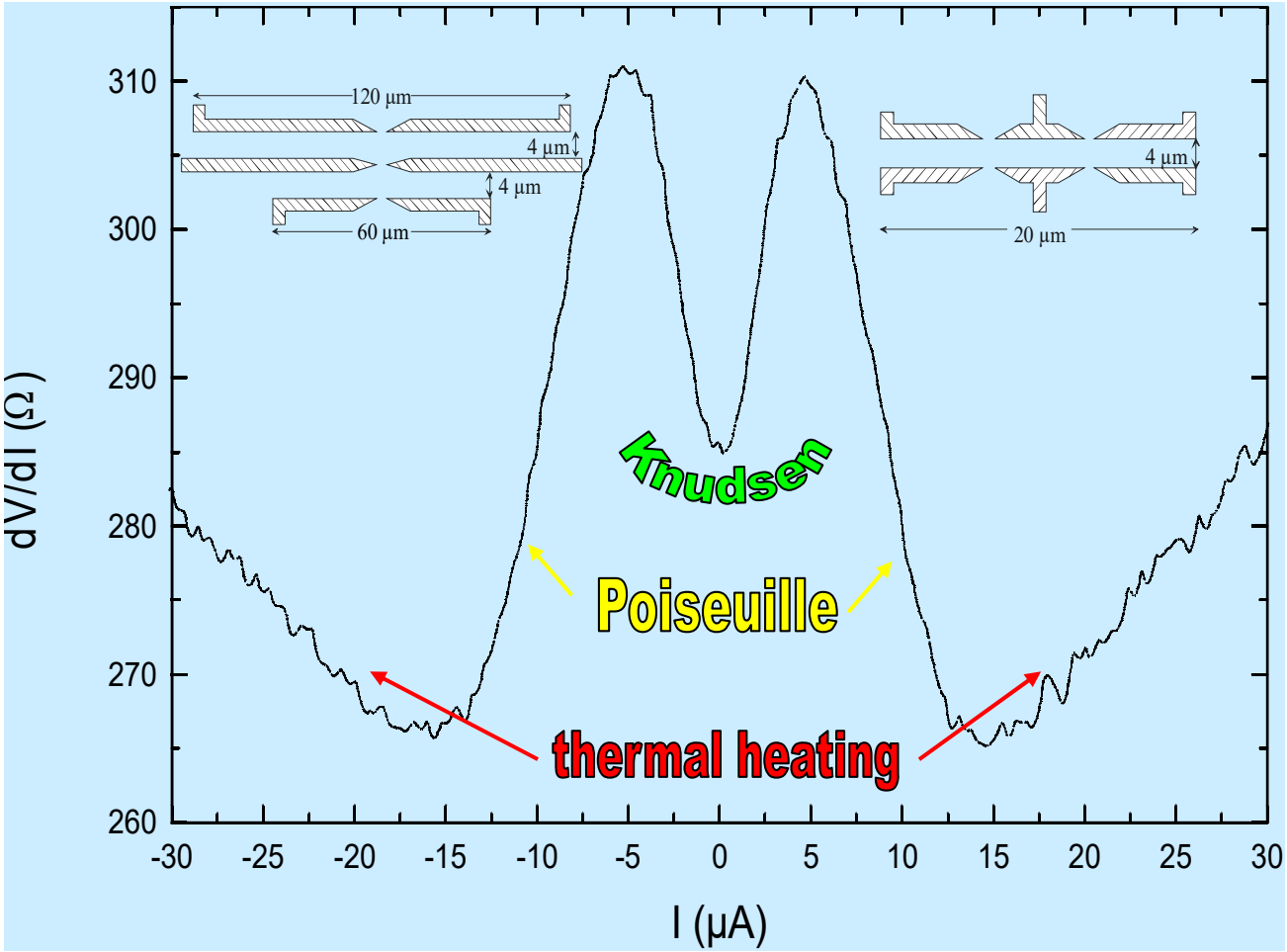

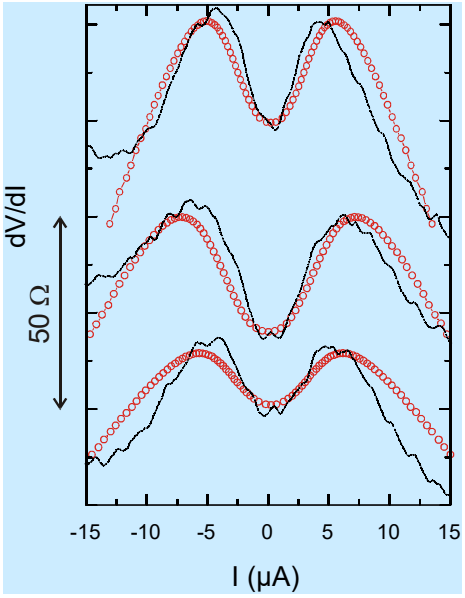

$$R = \frac{L}{W\sigma} + \frac{h\pi}{2e^2 k_F W} + R_0$$

$$\sigma = \frac{ne^2}{mv_F} L_{eff}$$

$$L_{eff} = \frac{ne^2}{mv_F} \int_0^W \frac{dy}{W} \tilde{l}_{eff}(y)$$

Hydrodynamic Electron Flow

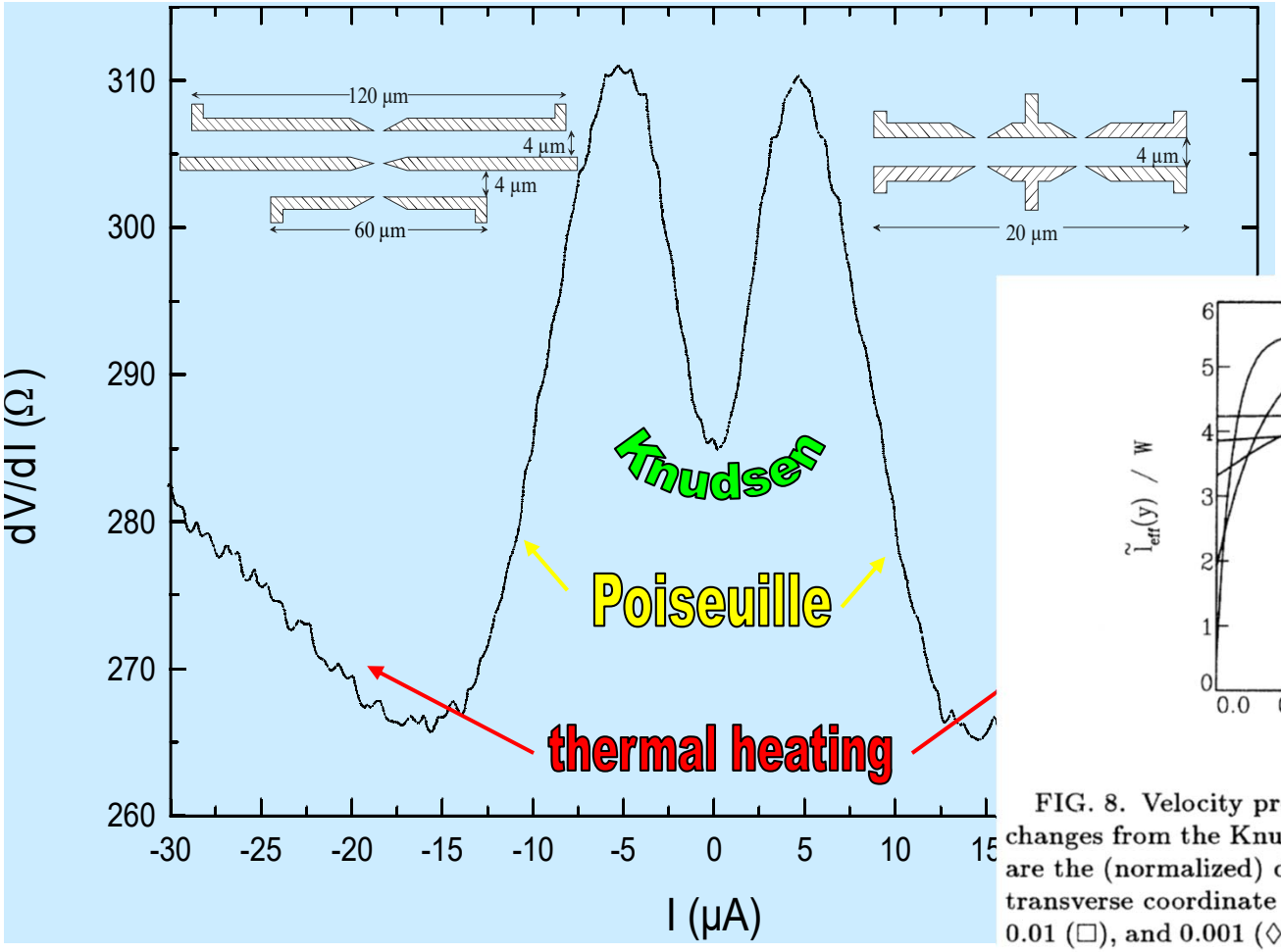

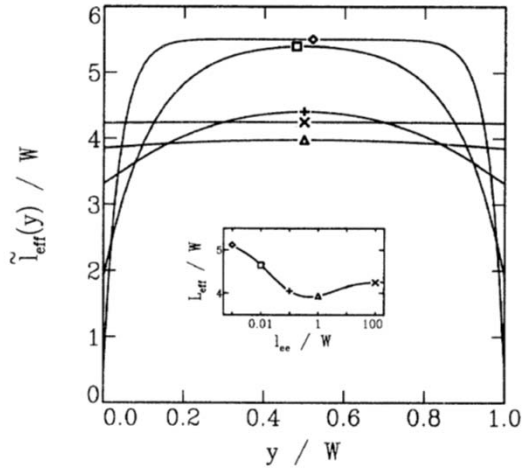

FIG. 8. Velocity profiles inside the wire show how the flow changes from the Knudsen upto the Gurzhi regime. Depicted are the (normalized) drift velocity $\tilde{l}_{\rm eff}(y)$, as a function of the transverse coordinate y for $l_{ee}/W = 100$ (×), 1 (△), 0.1 (+), 0.01 (□), and 0.001 (◊). The inset shows the conductivity $L_{\rm eff}$ as a function of the e-e scattering length l_{ee} and the symbols that indicate to which value each flow profile corresponds. Results are for the bulk mean free path $l_b = 5.5W$ and for angle-dependent boundary scattering with $\alpha = 0.7$.

ee-Scattering in 2D

1. small angle scattering

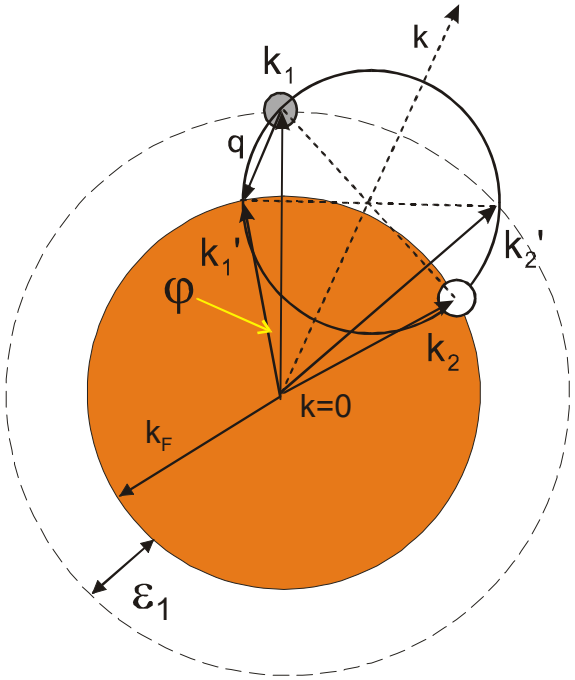

2. ee-scattering for $\vec{p} \approx -\vec{p}$

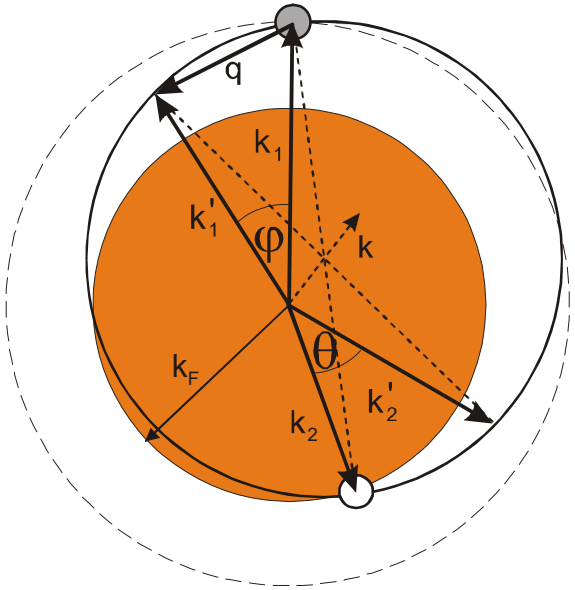

$$\frac{\delta\varphi}{\pi} \approx \frac{k_B T}{E_F} << 1$$

scattering angle

$$-\pi \le \delta\varphi \le \pi$$

Energy and Momentum-Relaxation

Due to the different scattering processes there exist two different relaxation times for symmetric and asymmetric processes:

Gurzhi et al., Adv. Phys. 1987

Momentum-Relaxation: $|\vec{q}| \approx k_B T / v_F$

$$\Longrightarrow \quad \tau_{ee}^{a} \approx \tau_{ee} \left(\frac{\varepsilon_F}{k_B T} \right)^2 \propto T^{-4}$$

Energy-Relaxation: $\left(\frac{|\vec{q}|}{k_F} \right) \cdot \left(\frac{|\vec{k}|}{k_F} \right) \leq \frac{k_B T}{\varepsilon_F}$

$$\Longrightarrow \quad \tau_{ee}^{s} \approx \tau_{ee} \propto T^{-2}$$

Additional hydrodynamic regime in 2D?

R.N. Gurzhi et al., Phys. Rev **B** 74, 3872 (1995)

Three transport regimes:

1. Knudsen: $d^2 / l_s << l_a$
2. 1d-Diffusion: $l_s k_B T / \varepsilon_F << d^2 / l_s << l_a$
3. Poiseuille: $l_a << d^2 / l_s$

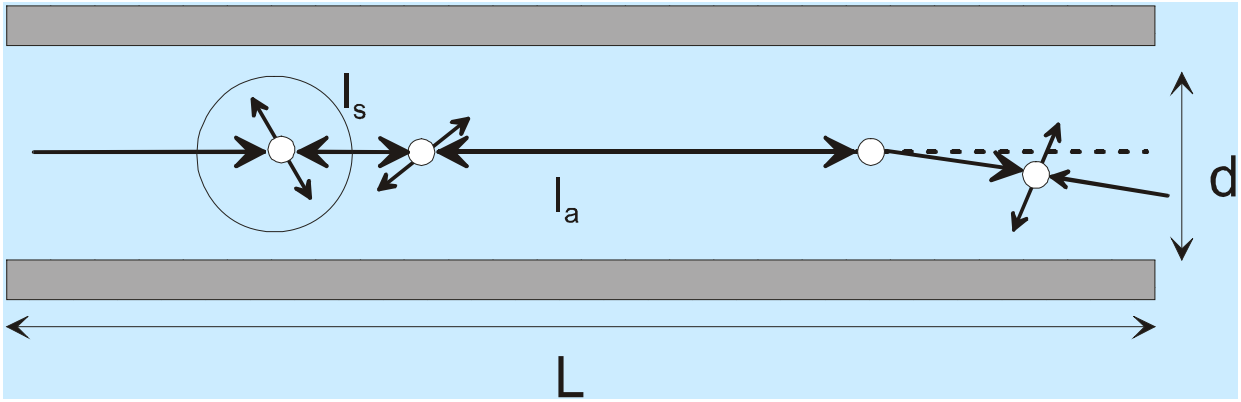

Not so easy to observe in heating experiment….

Electron Beam in a 2DEG

PHYSICAL REVIEW B VOLUME 41, NUMBER 2 15 JANUARY 1990-I

Electron-beam collimation with a quantum point contact

L. W. Molenkamp, A. A. M. Staring,* C. W. J. Beenakker, R. Eppenga, C. E. Timmering, and J. G. Williamson
Philips Research Laboratories, 5600 JA Eindhoven, The Netherlands

C. J. P. M. Harmans
Delft University of Technology, 2600 GA Delft, The Netherlands

C. T. Foxon
Philips Research Laboratories, Redhill, Surrey, RH1 5HA, England
(Received 12 July 1989)

Collimation of the electron beam injected by a point contact in a two-dimensional electron gas is demonstrated using a geometry with two opposite point contacts as injector and collector. The collimation is maintained over a distance of at least 4 μm, and is destroyed by a small magnetic field. The inferred collimation factor scales linearly with the point-contact resistance, as predicted by the semiclassical theory.

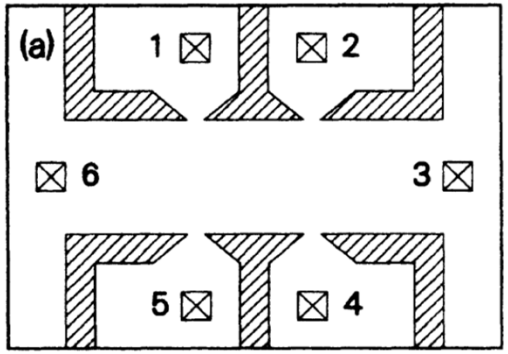

$$\Delta\alpha = 2\arcsin(1/f)$$

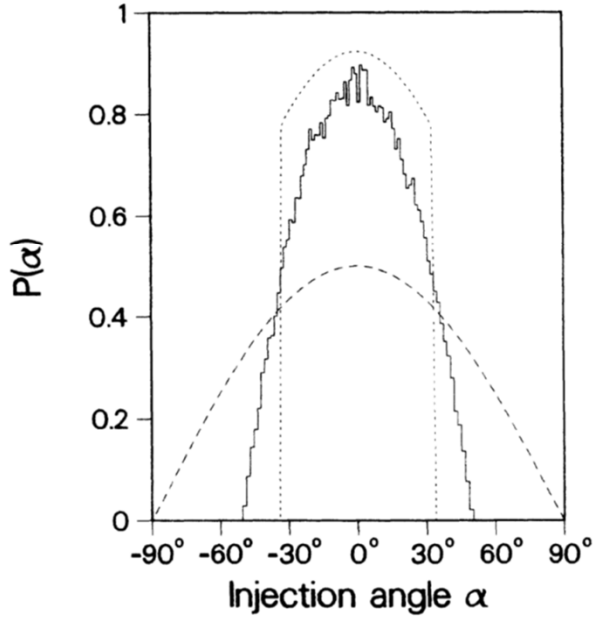

$$f = \frac{W_{max}}{W_{min}} \frac{k_F}{k_{pc}}$$

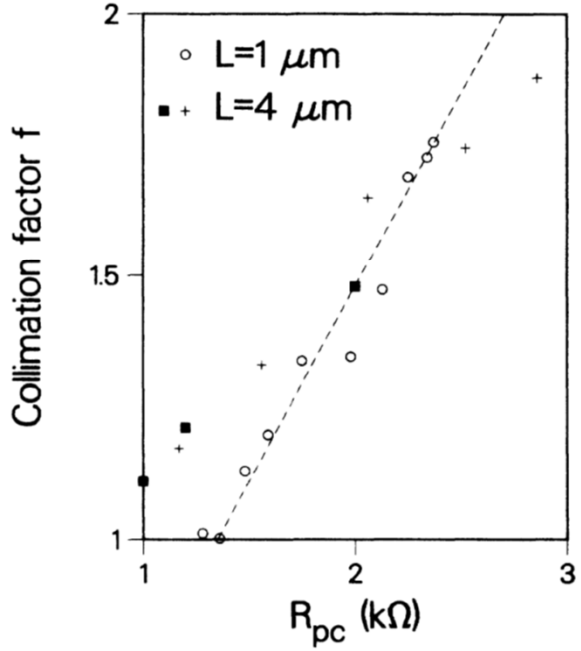

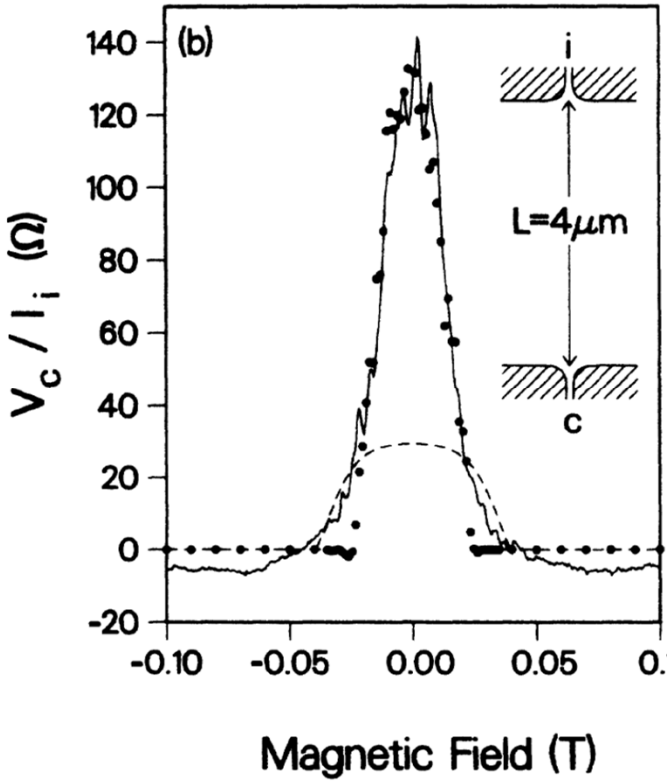

Semiclassical collimation mechanisms

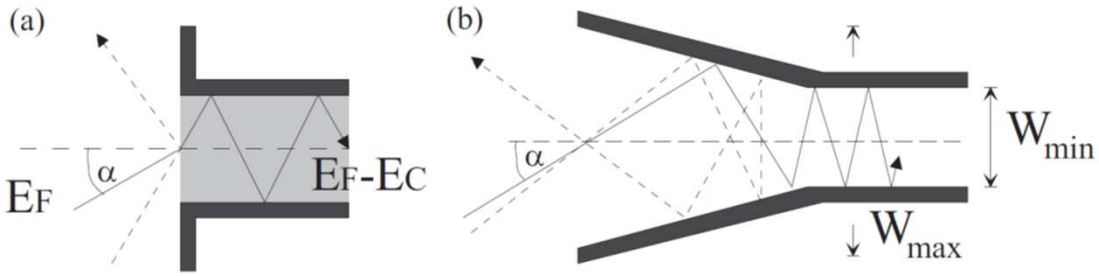

Abbildung 3.8: Schematische Darstellung der Kollimationsmechanismen. (a) Stufen-Effekt, (b) Horn-Effekt.

$$A = \hbar k_y W$$

(Semi-classical) action is constant of the motion.

Electron beam Propagation in a 2DEG

An anisotropic electron momentum distribution remains present over a long time, while the energy relaxation is fast.

e-beam injection

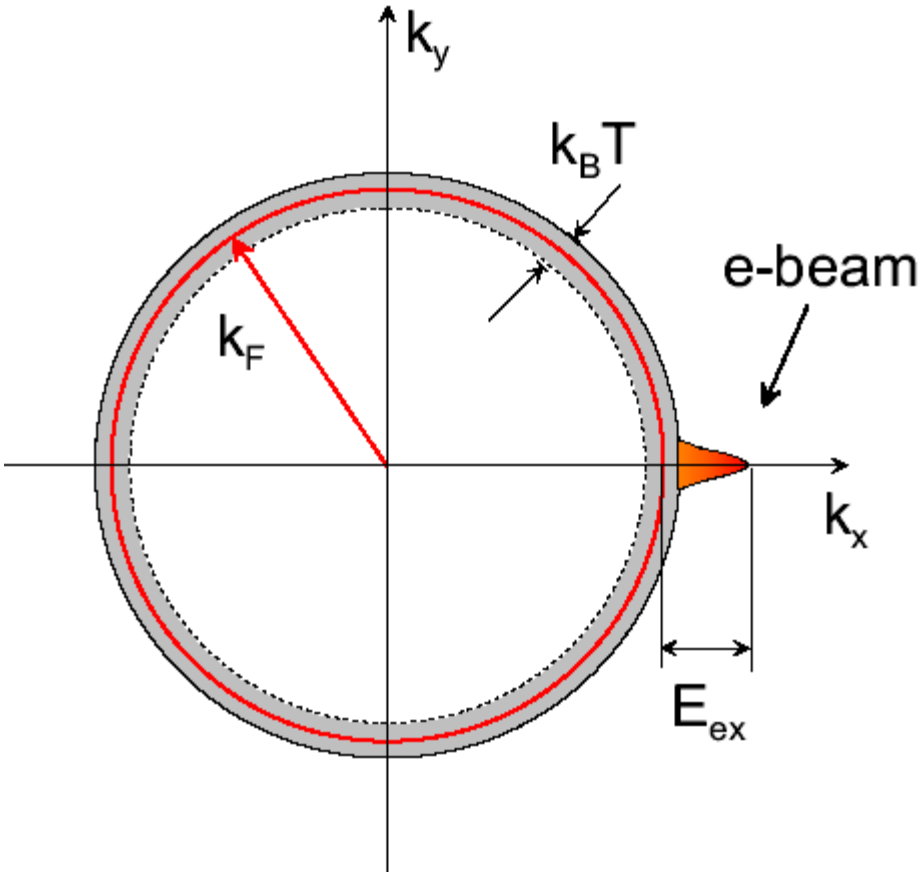

Electron Beam Propagation

kinetic equation:

$$v_x \frac{\partial f}{\partial v_x} + v_y \frac{\partial f}{\partial v_y} = \hat{I} f$$

I: Integral of electron-electron scattering

$$\hat{I} f = -\underbrace{\int d\mathbf{p}' \nu_{\mathbf{p}'\mathbf{p}} f_{\mathbf{p}}}_{\text{RTA}} + \underbrace{\int d\mathbf{p}' \nu_{\mathbf{p}\mathbf{p}'} f_{\mathbf{p}'}}_{\text{Feedback}} \equiv -\nu f + \hat{K} f$$

Considers all electron that scattered, but still preserve the momentum due to small angle scattering events.

$$\nu_{\mathrm{p}'\mathrm{p}} = \frac{1}{n(\varepsilon)} \int d\mathbf{p}_1 d\mathbf{p}_2 (2\ \Psi_{\mathrm{p}'\mathrm{p}_1\mathrm{p}\mathrm{p}_2} - \Psi_{\mathrm{p}'\mathrm{p}\mathrm{p}_1\mathrm{p}_2})$$

Integration over all $\nu_{p'p}$ results in the scattering angle distribution function: $g(\varphi)$

H. Buhmann et al., Fiz.Nizk. Temp. **24**, 978 (1998)

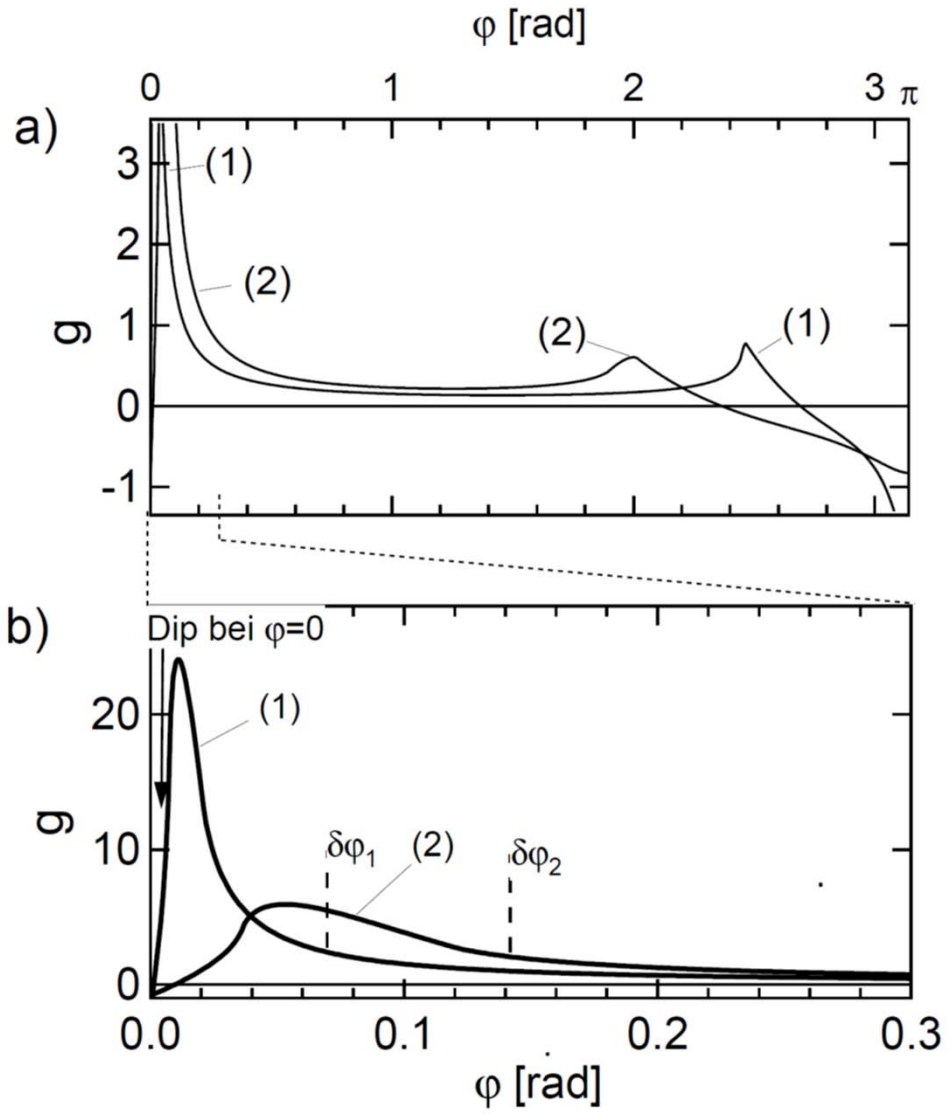
φ [rad]
0
1
2
3 π
a)
3
2
1
0
-1
g
(1)
(2)
(2)
(1)
b)
Dip bei φ=0
20
10
0
g
(1)
δφ1
(2)
δφ2
0.0
0.1
0.2
0.3
φ [rad]

Energy Dependent Scattering

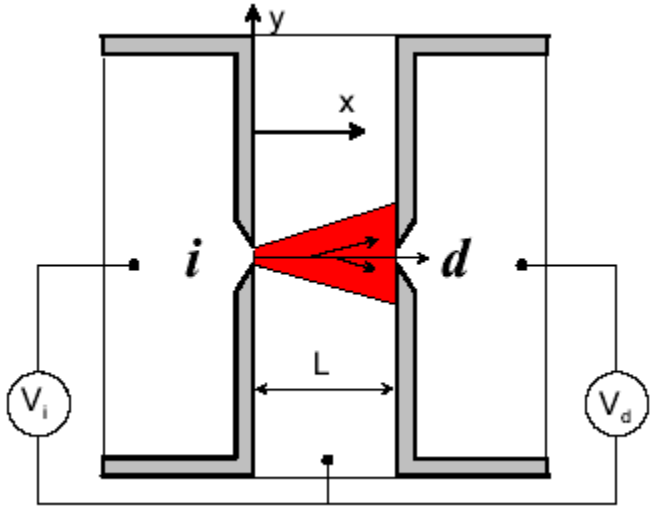

$$V_d = e \int d\varepsilon \int d\varphi \; \rho(\varphi)\, v_x \; f(L, y, \mathbf{p})$$

$\rho(\varphi)$: angle dependent detection

Model Calculation:

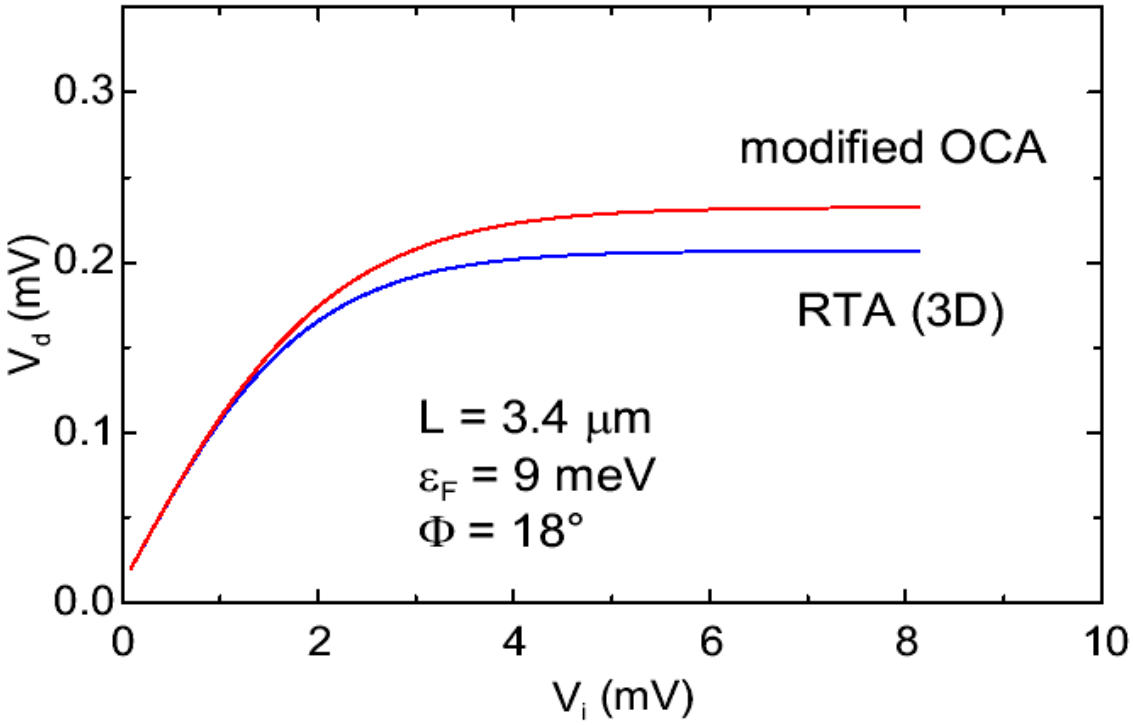

Experiment

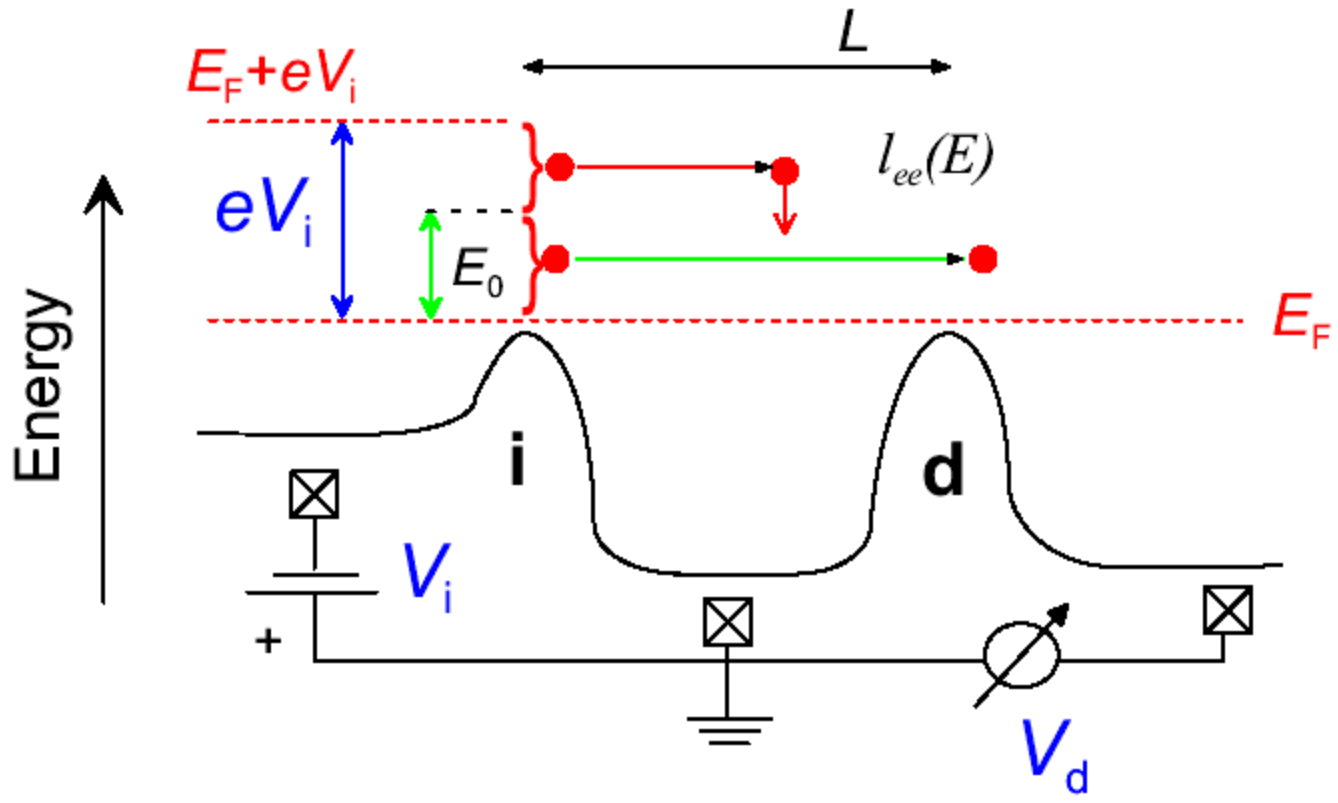

Sample Structure

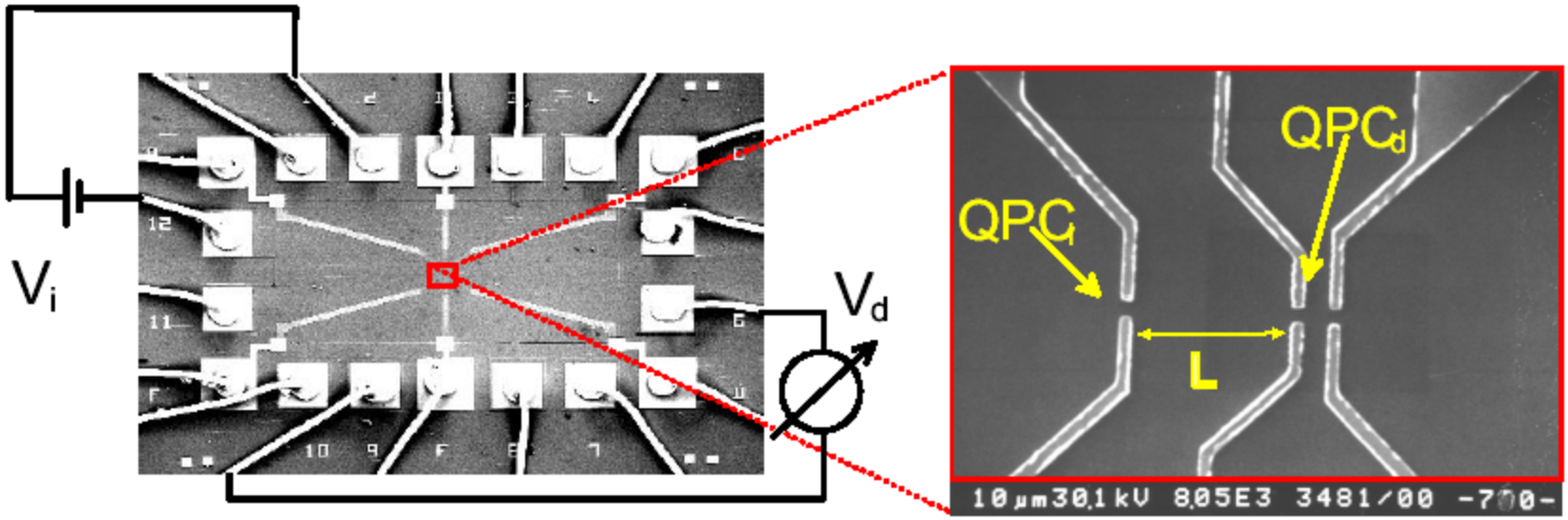

$L = 3.4\ \mu\text{m}$

$n_e = 2.45 \times 10^{11}\ \text{cm}^{-2} \Rightarrow E_F = 9\ \text{meV}$

$\mu \approx 1 \times 10^6\ \text{cm}^2(\text{Vs})^{-1} \Rightarrow l_{\text{imp}} \approx 20\ \mu\text{m}$

$G_{\text{QPC}} = 2e^2/h\ (N = 1)$

$T = 1.6\ \text{K}$

Experimental Result

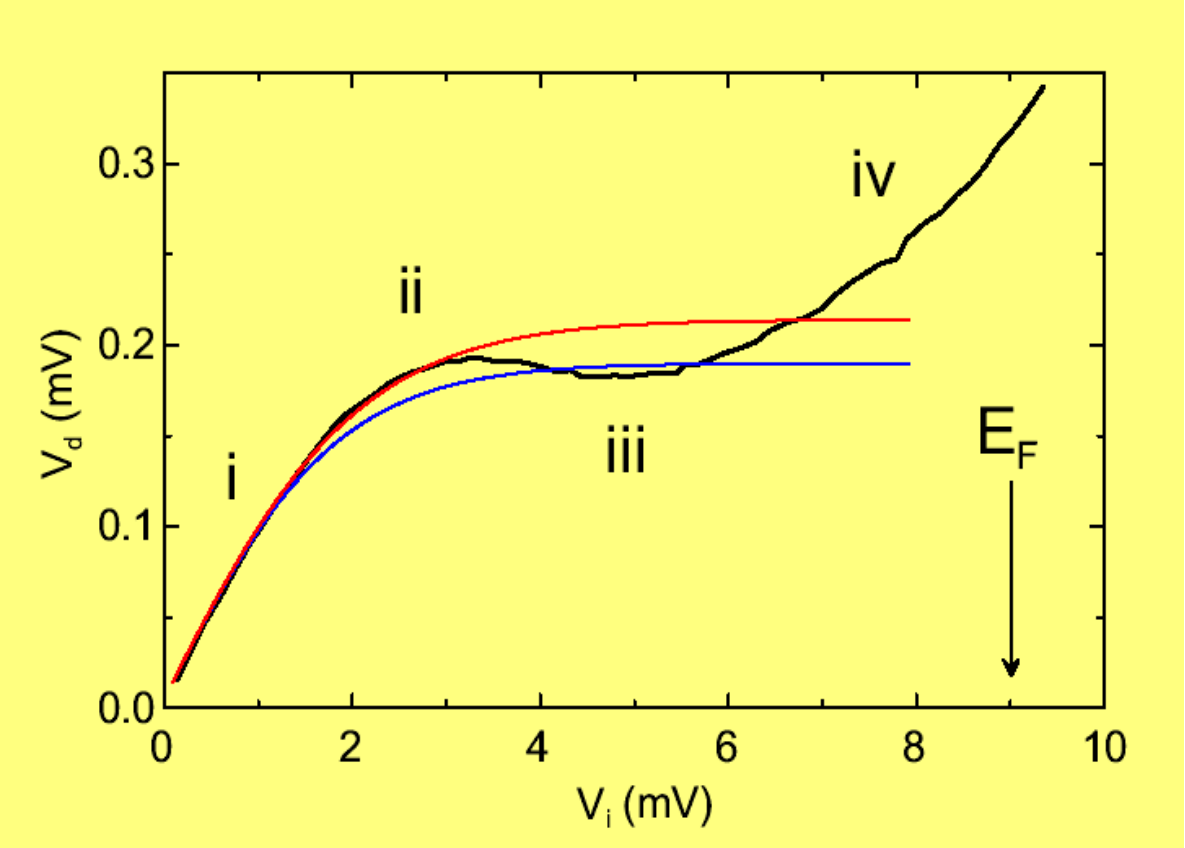

i. $l_{ee} > L$: $V_d \sim V_i$

i. $l_{ee} \approx L$: electron with $\varepsilon > \varepsilon_0$ before reaching d

ii. $l_{ee} < L$: increased ee-scattering causes heating of the 2DEG

iii. increasing heating results in a thermovoltage

Thermoelectric Effect

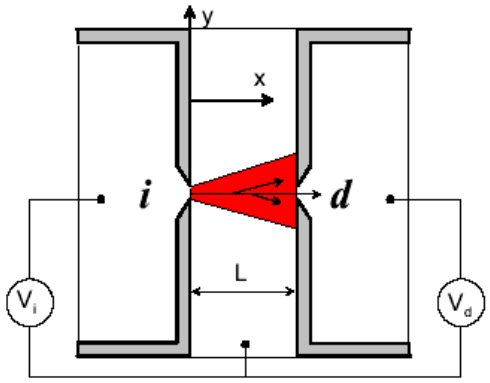

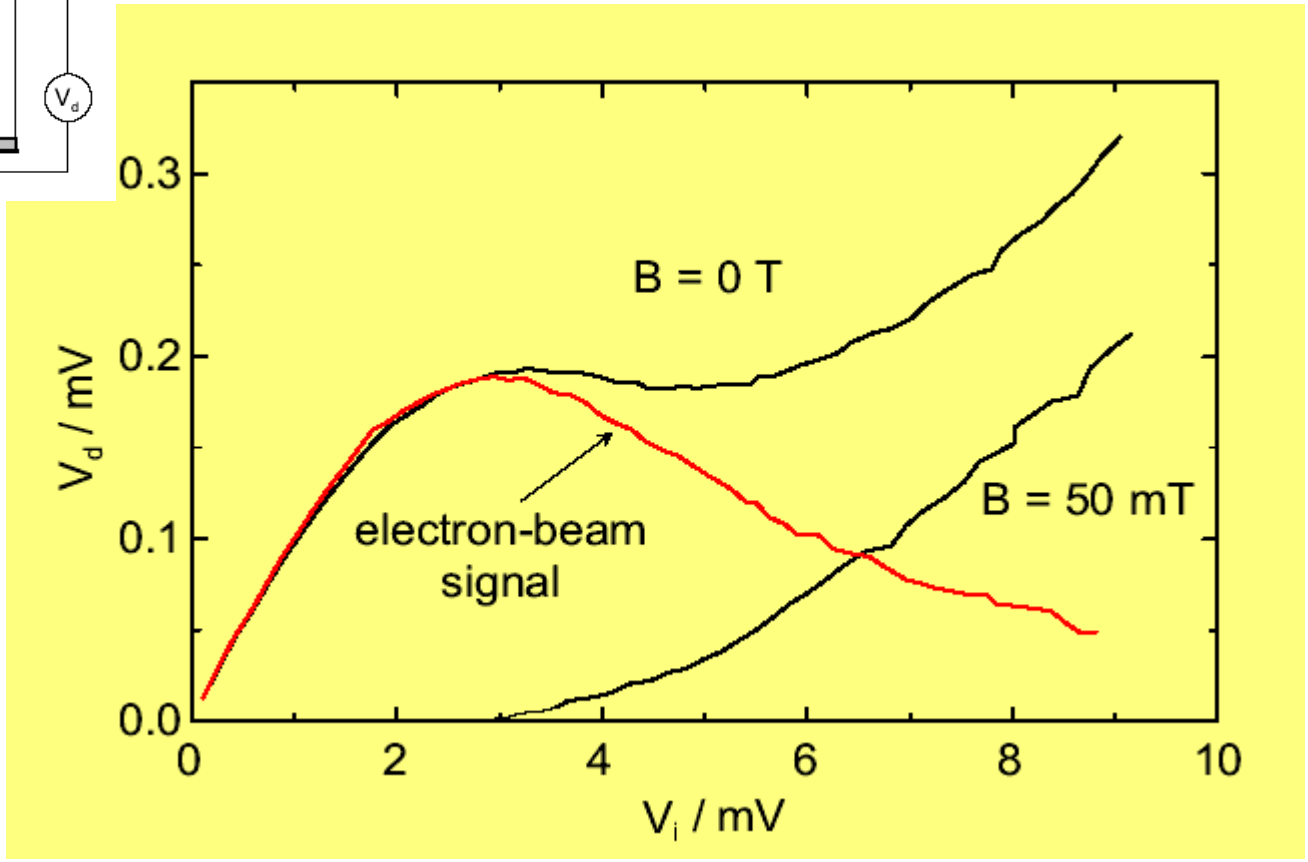

Thermoelectric Effect

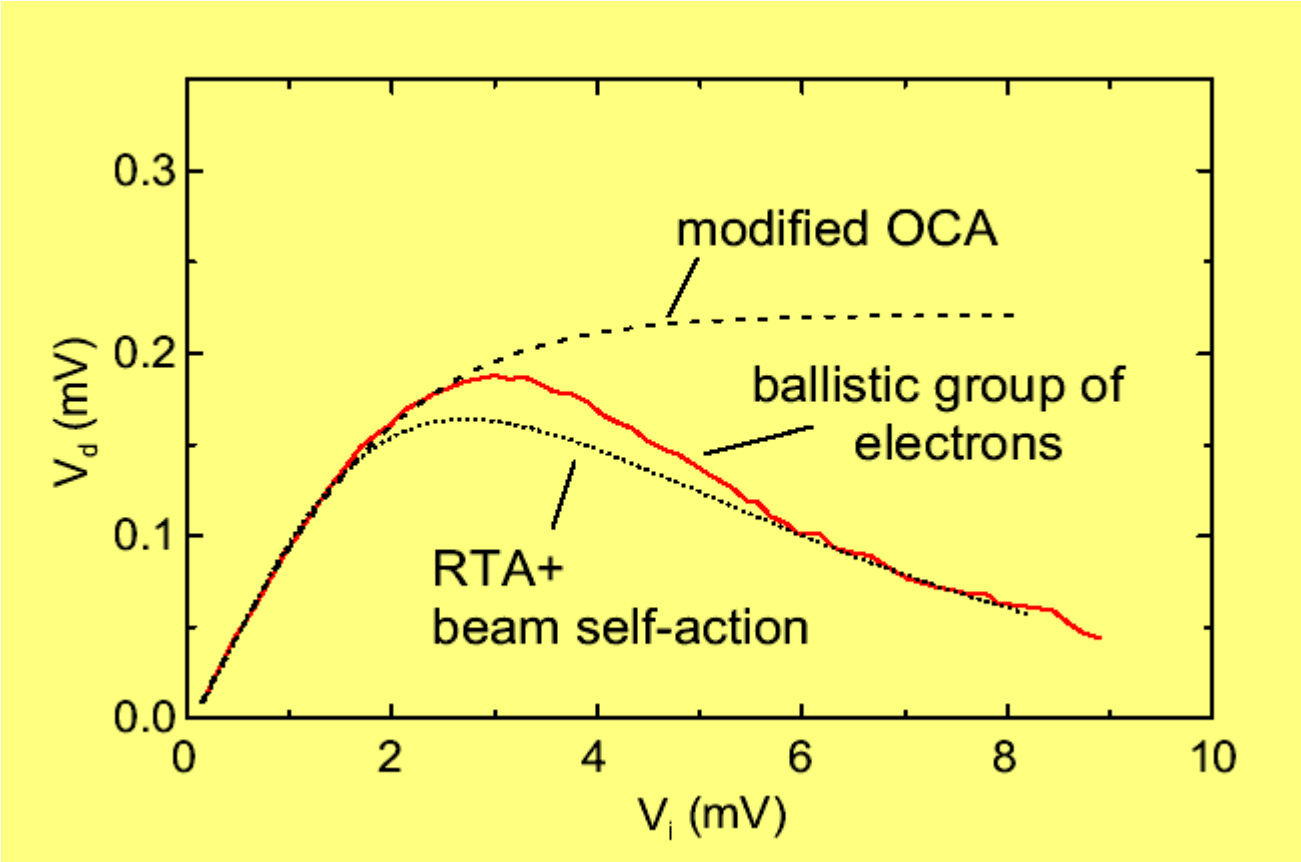

H. Predel et al., Phys. Rev. B **62**, 2057 (2000)

Angle resolved ee-scattering in a 2D system

Europhys. Lett., **56** (5), pp. 709–715 (2001)

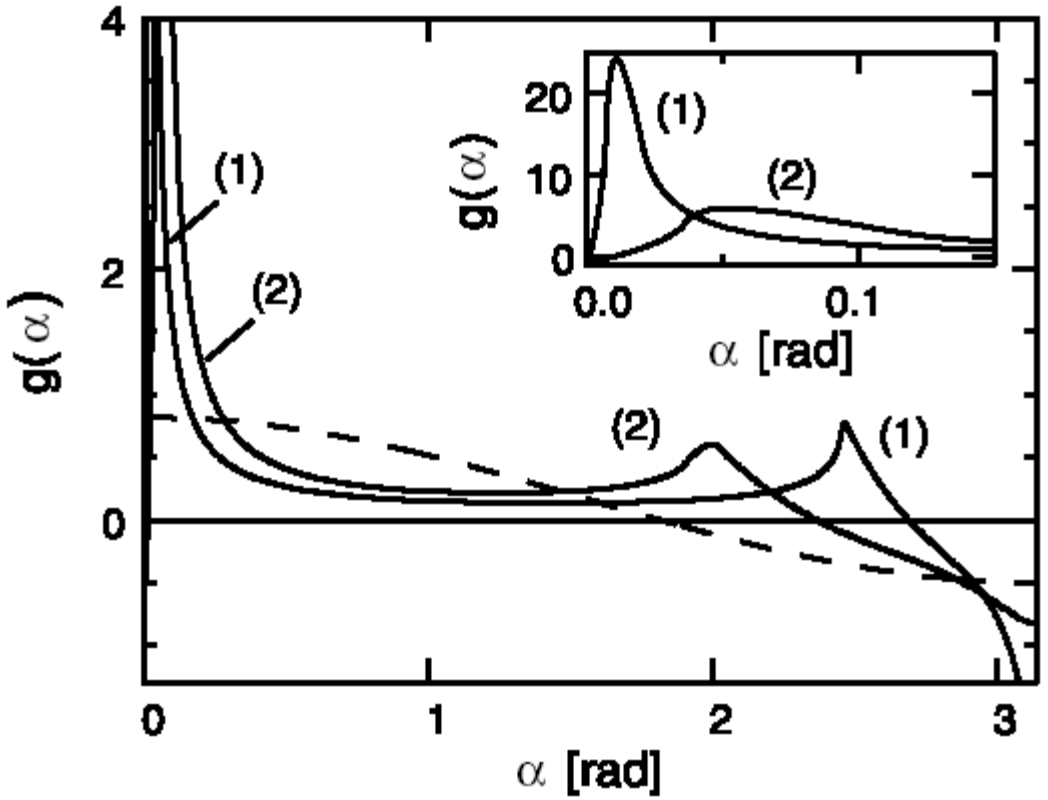

Fig. 1 – ee-scattering angular distribution function $g(\alpha)$ in a 2D system, 2DEG temperature $T = 0$, (1) $\varepsilon = 0.12\varepsilon_F$, (2) $\varepsilon = 0.4\varepsilon_F$, dashed line: 3D case (Callaway's Ansatz). Here angle α is measured with respect to the momentum of scattering electron, p [8]. By definition, $|g(\alpha)|d\alpha$ characterizes the probability that a non-equilibrium electron, $g(\alpha) > 0$ (or hole for $g(\alpha) < 0$), emerges in an interval $d\alpha$ after scattering. The function $g(\alpha)$ is normalized to the unity (this corresponds to the scattering of one electron).

Angle resolved ee-scattering in a 2D system

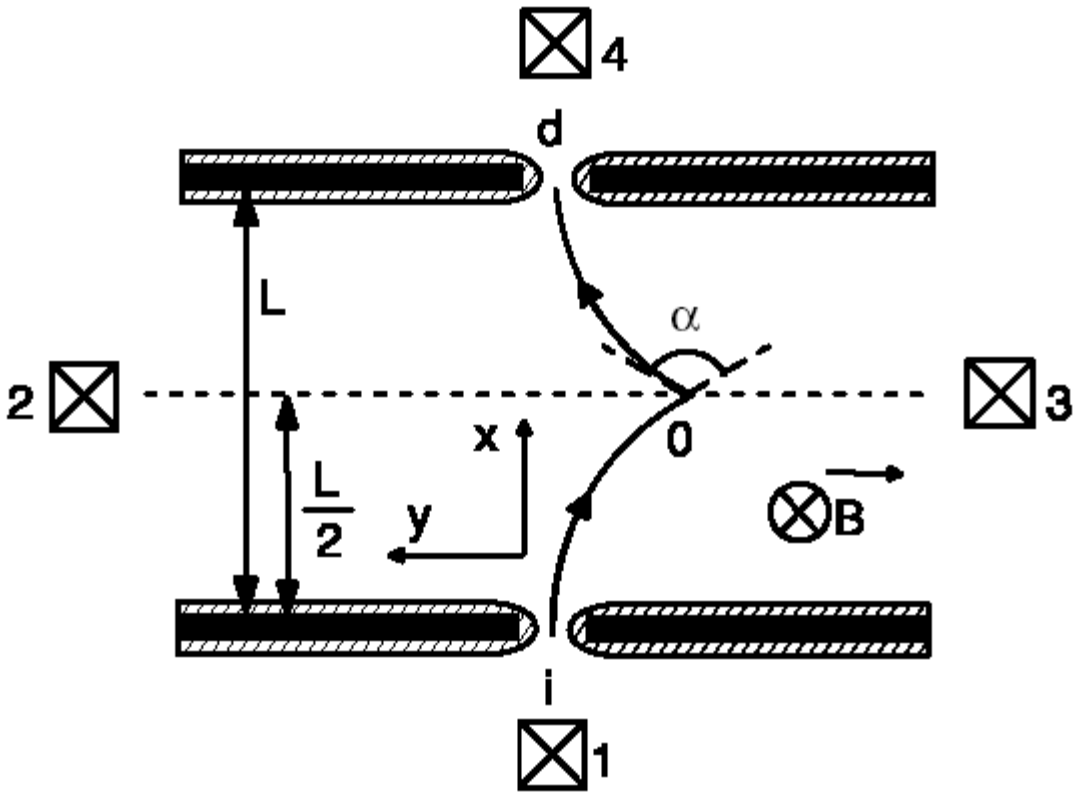

Angle resolved ee-scattering in a 2D system

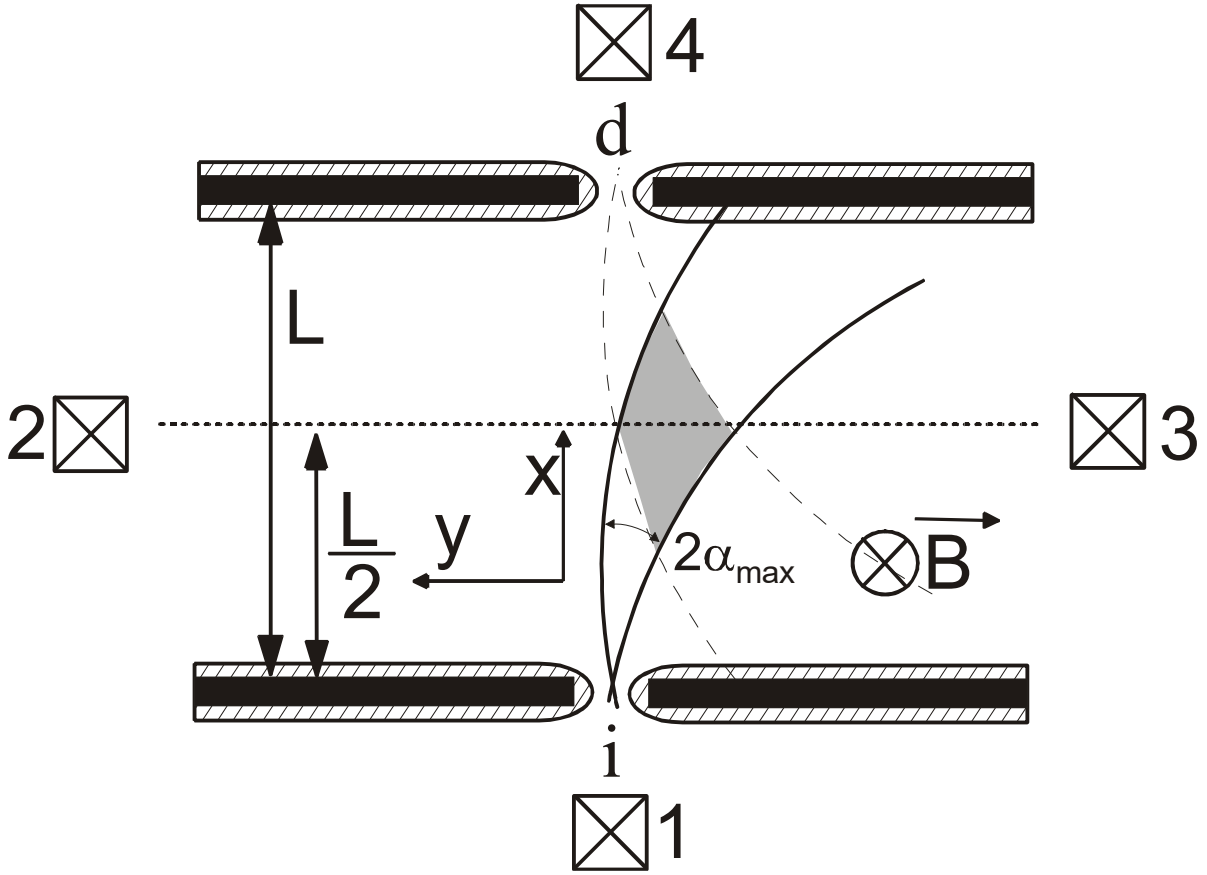

Measurement

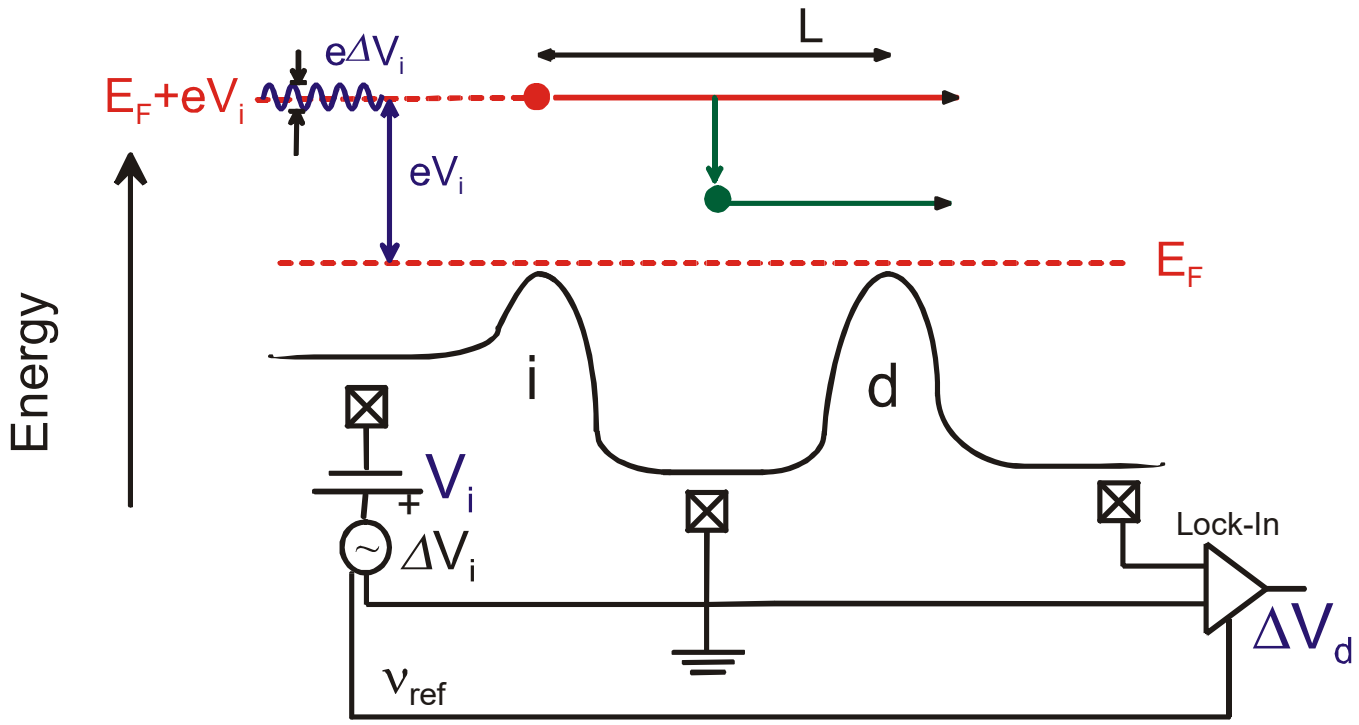

Measurement

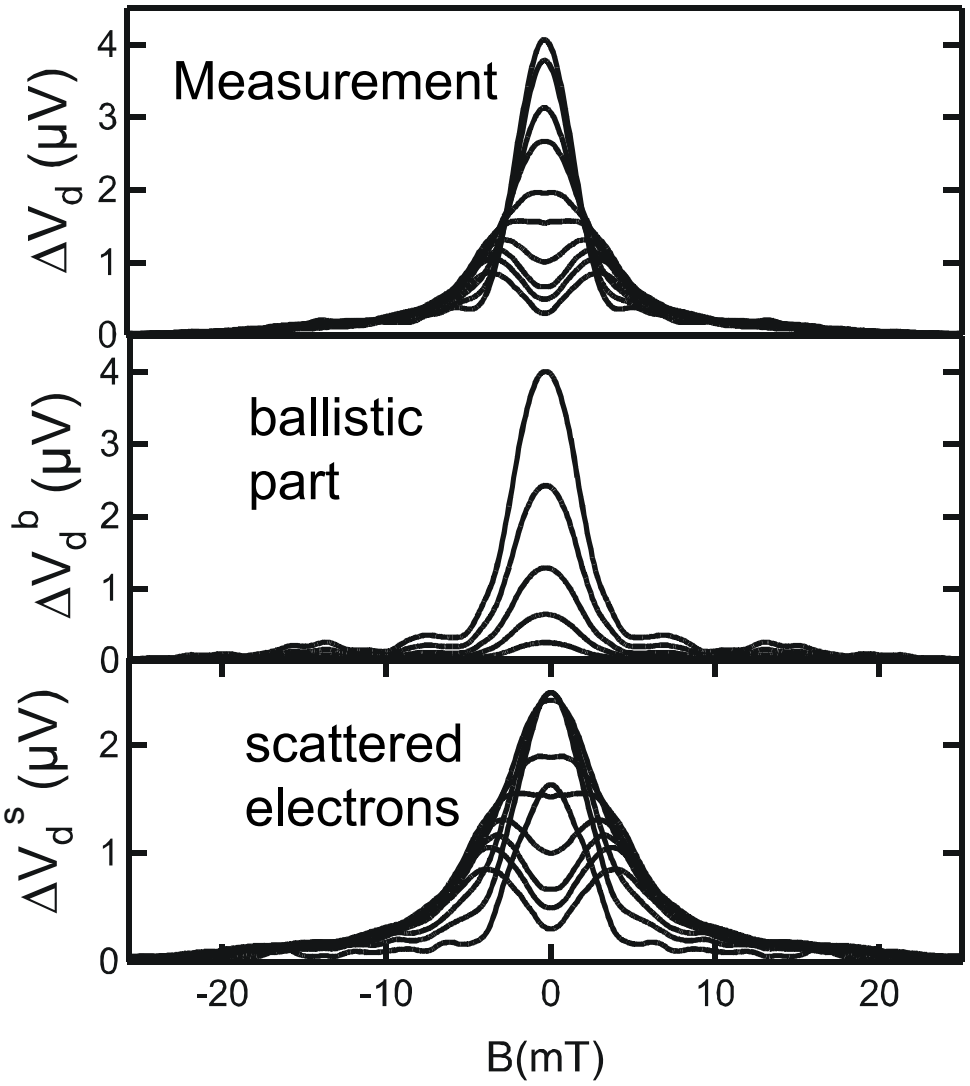

From experiment at zero excess energy, corrected for l_{ee}

$$\Delta V_d^b(r_c, V_i) = exp\left(-\frac{2r_c}{l_{ee}(eV_i)}\arcsin\frac{L}{2r_c}\right)\Delta V_d^0(r_c).$$

Simply by subtracting the ballistic part

Result

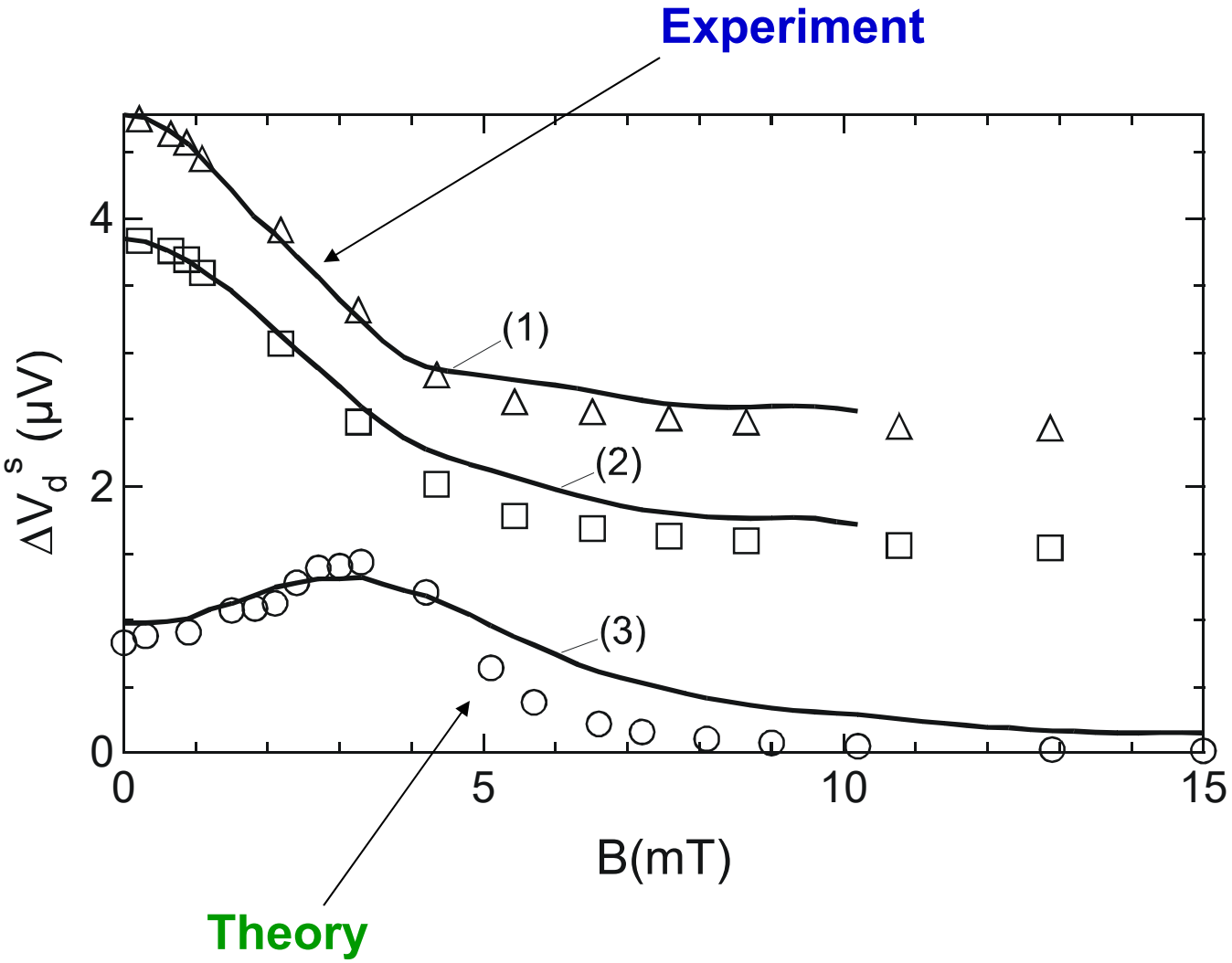

Opening Angle Distribution

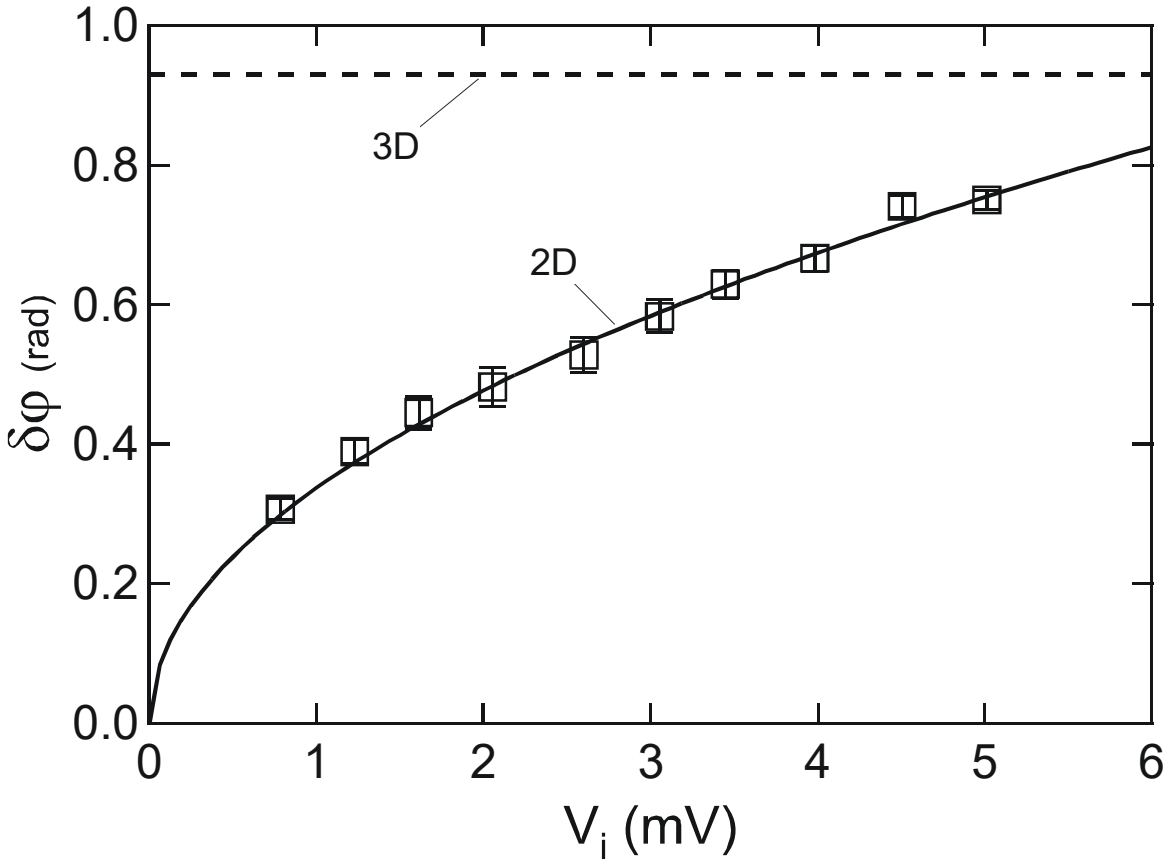

Model allows for extraction of opening angle from experiment
(Note: „3D“ Model does not include collimation effects)

H. Predel, PhD Thesis 2001
Yanovski *et al*., *Europhys. Lett.*, **56**, 709 (2001)

Negative beam Signal – Vortices? Uuumh…

PHYSICAL REVIEW B VOLUME 57, NUMBER 7 15 FEBRUARY 1998-I

Classical rebound trajectories in nonlocal ballistic electron transport

A. S. D. Heindrichs, H. Buhmann, S. F. Godijn, and L. W. Molenkamp
2. Physikalisches Institut, RWTH-Aachen, D-52056 Aachen, Germany
(Received 15 August 1997)

We demonstrate experimentally and by Monte Carlo simulation that the negative dips which occur at low magnetic fields on both sides of the main signal in nonlocal electron-beam measurements in semiconductor nanostructures result from electrons following classical rebound trajectories. We propose an alternative measurement geometry that eliminates these effects.

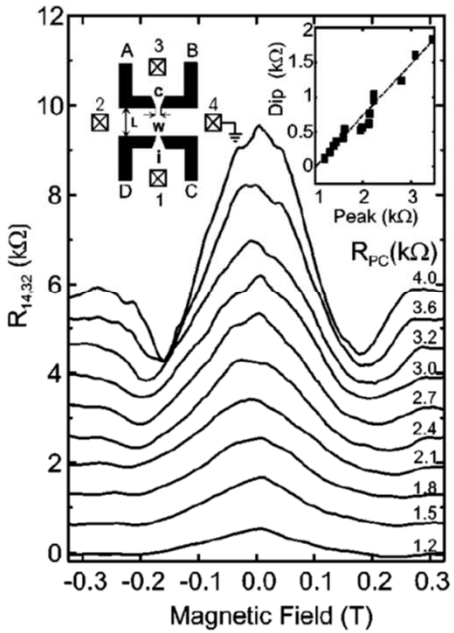

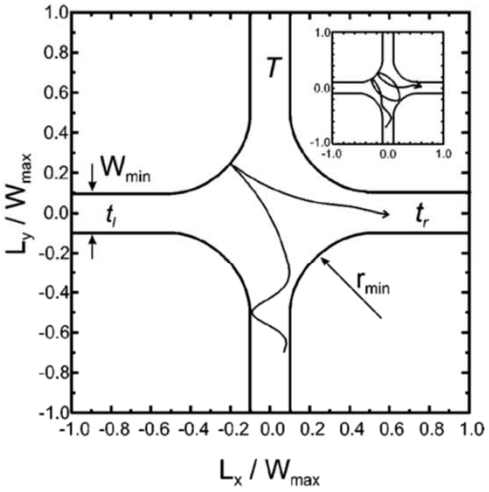

FIG. 1. Measured signal $V_c/I_i = R_{14,32}$ vs magnetic field for different point-contact resistances R_{PC}. The channel width is $L = 0.5\ \mu$m. All curves are plotted with a constant offset. The left inset displays the contact geometry of the device, and the right inset shows the dependence of the dip value on the collimation peak, only for those measurements where dips are clearly resolved, i.e., $R_{PC} > 1\ \text{k}\Omega$.

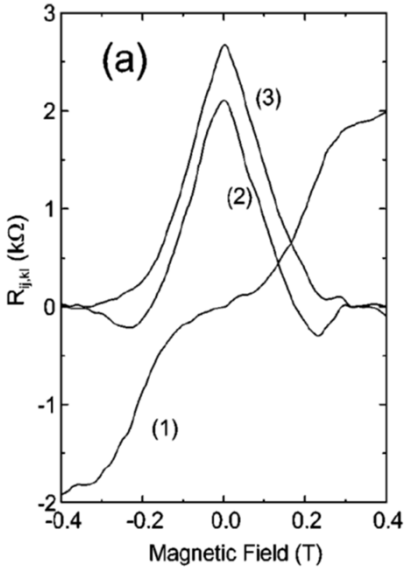

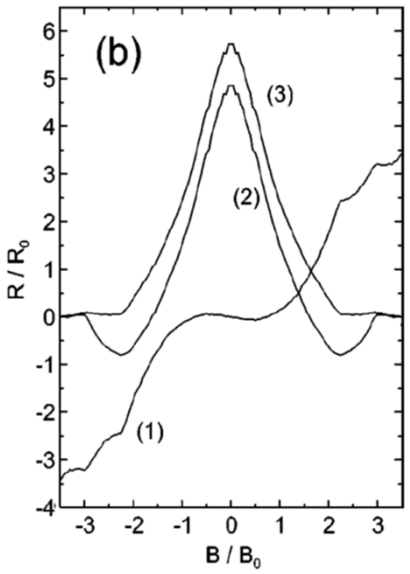

Julius-Maximilians-
UNIVERSITÄT
WÜRZBURG

Thermopower of quantum dots

EP 3

- GaAs/AlGaAs - 2DEG
- n = 2.3 10^{11} cm^{-2}, μ = 10^6 cm^2/Vs
- Ti/Au-surface electrodes
- (opt. and e-beam lithography)
- Au/AuGe - ohmic contacts

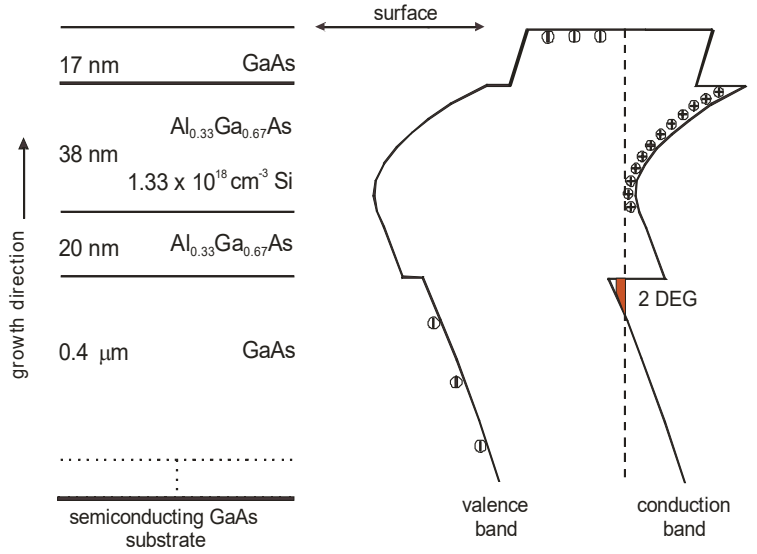

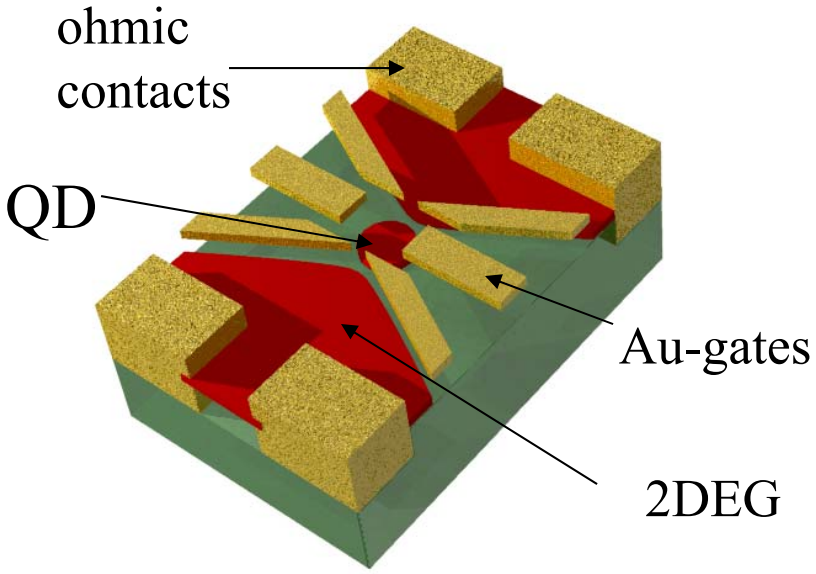

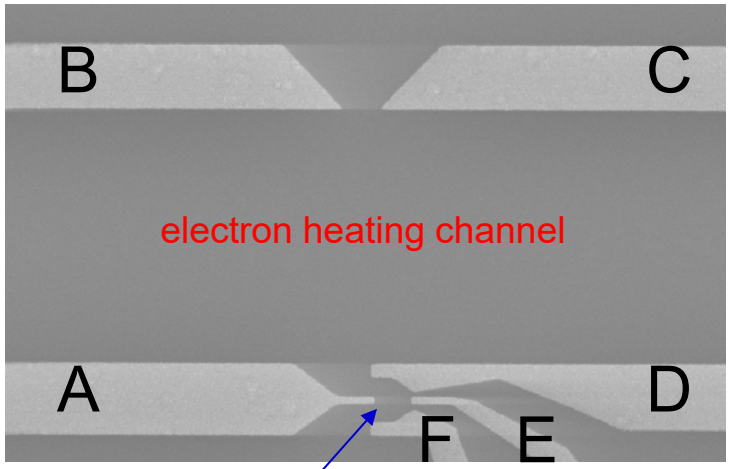

Quantum Dot (QD)

- Constant Interaction model:
  - QD = small capacitor
  - energies depend linearly on V_{gate}
  - coefficients do not depend on N (number of electrons)

- Energy needed to add one electron:
  - qm. Energy E_{qm} ~ 100 µeV
  - Coulomb Interaction $E_C = ½ e^2/C$ ~ 2 meV
  - $E_C = E_{qm} + E_C$

- Parameters accessible in conventional transport experiments

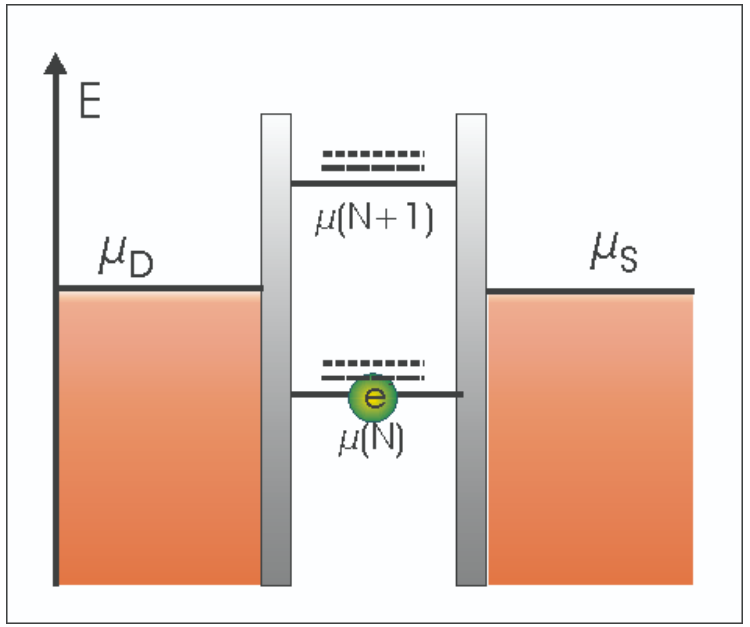

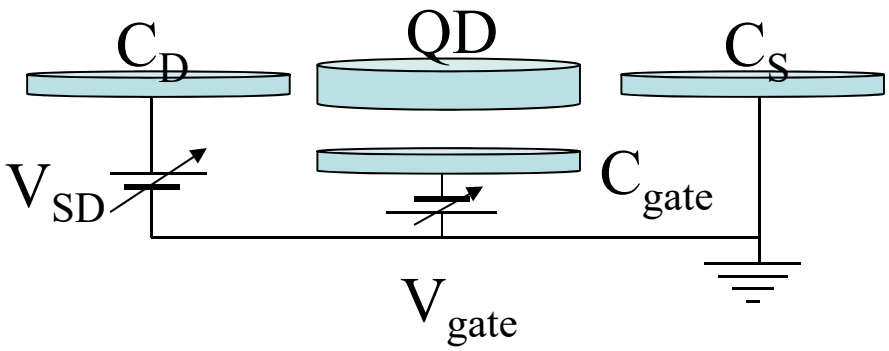

Transport Properties

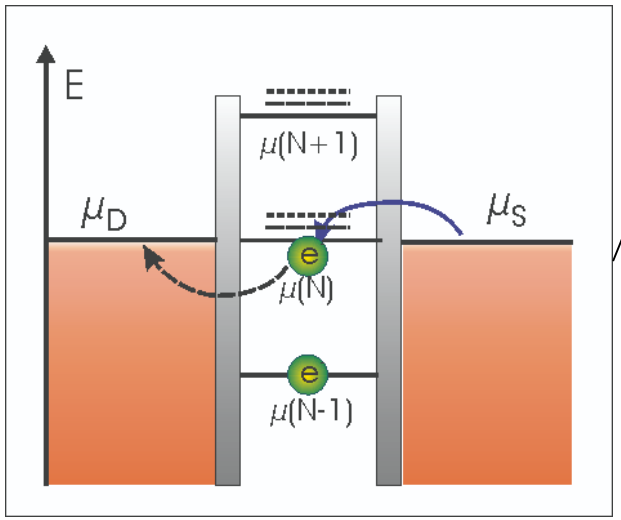

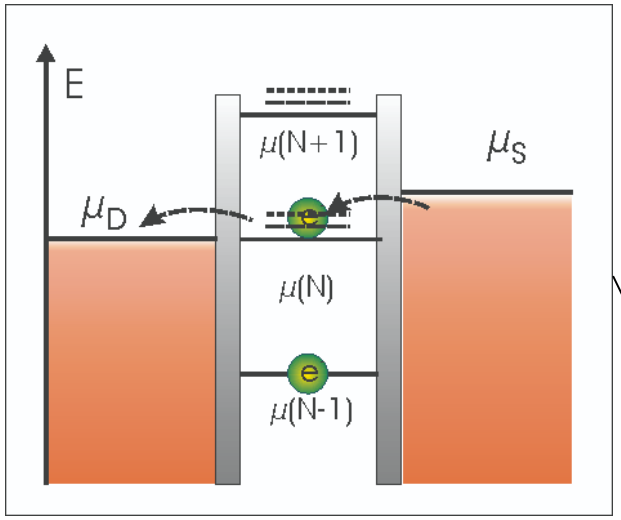

linear transport

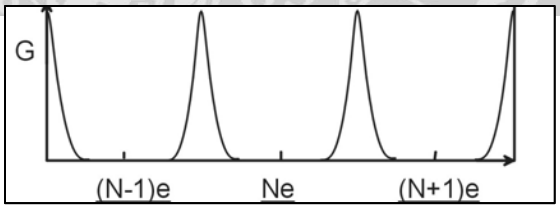

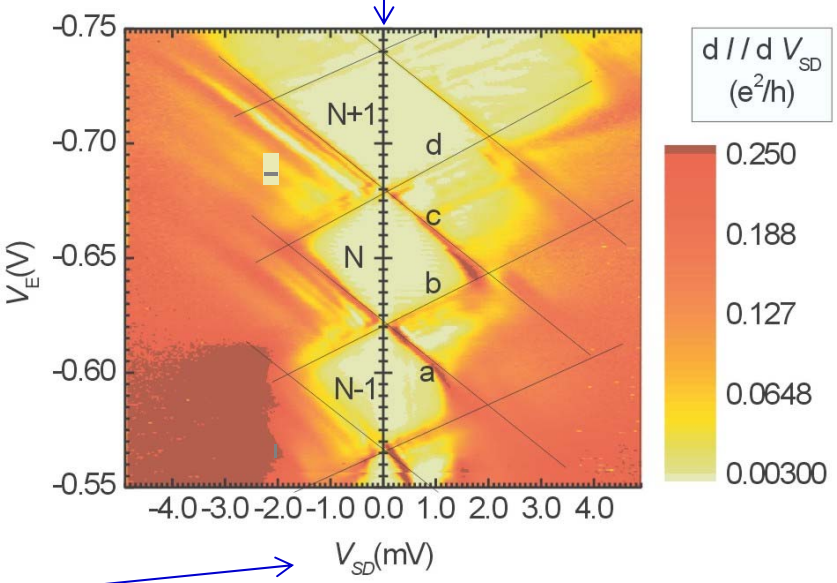

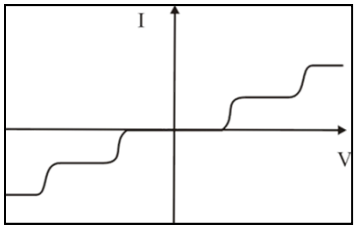

non-linear transport:

- capacitive coupling of leads and QD
- strong influence on hybridization of leads and QD

Thermopower of a QD

e - like

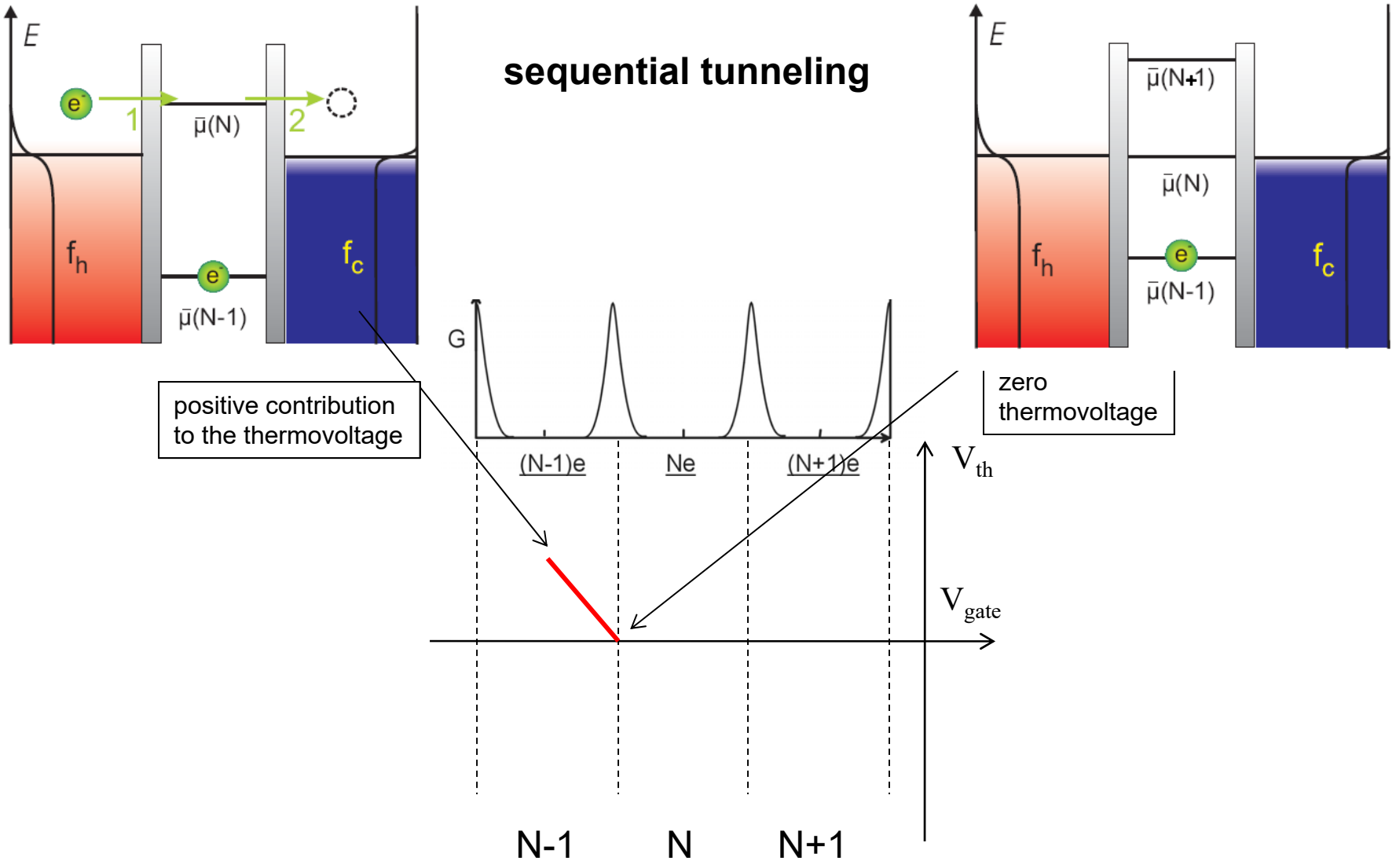

Thermopower of a QD

e - like

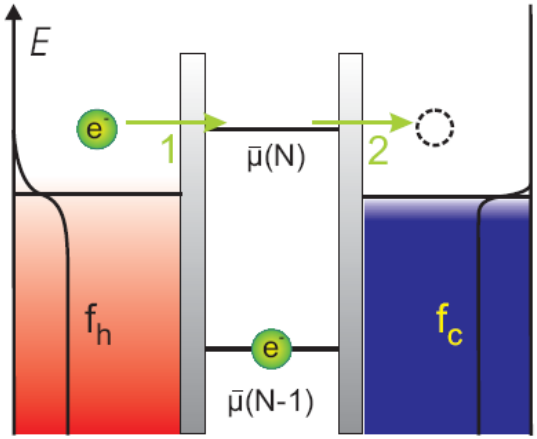

positive contribution to the thermovoltage

sequential tunneling

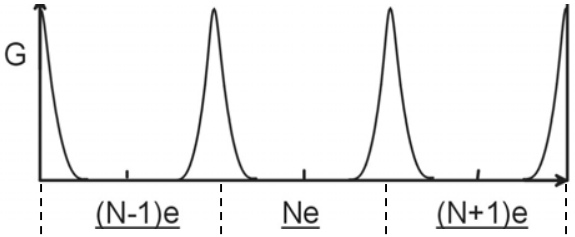

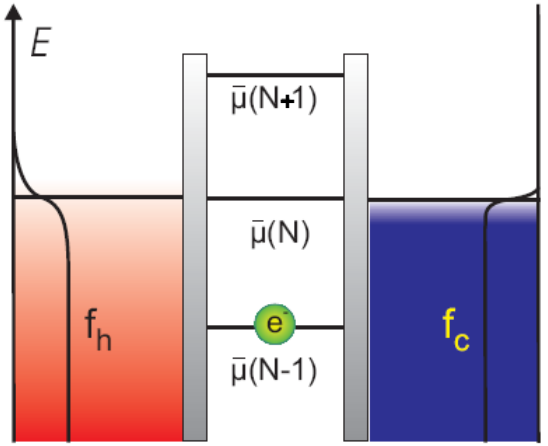

zero thermovoltage

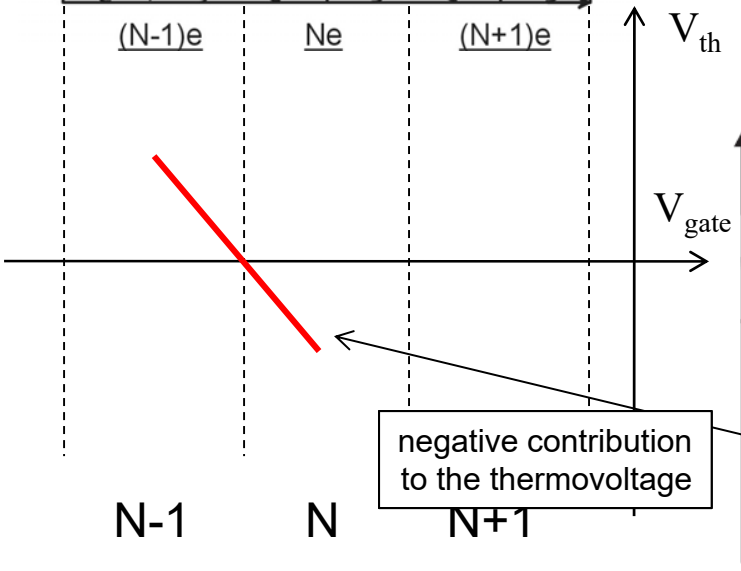

negative contribution to the thermovoltage

h - like

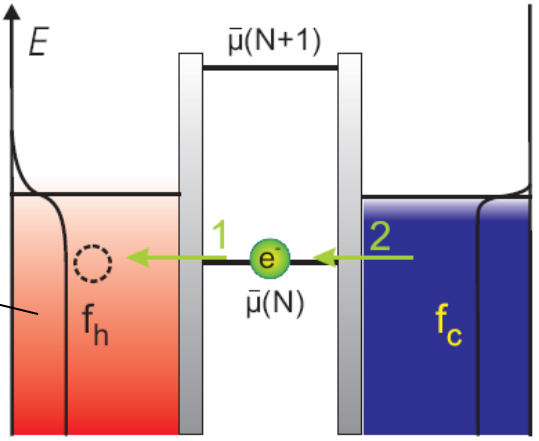

Thermopower of a QD

e - like

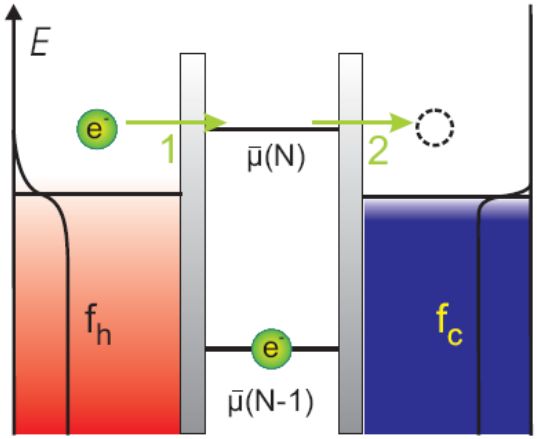

positive contribution to the thermovoltage

sequential tunneling

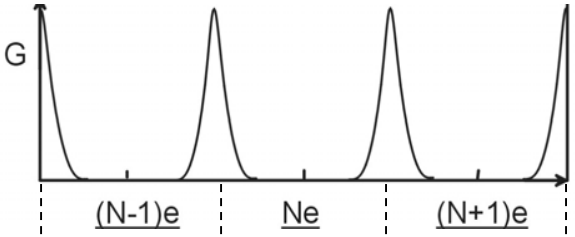

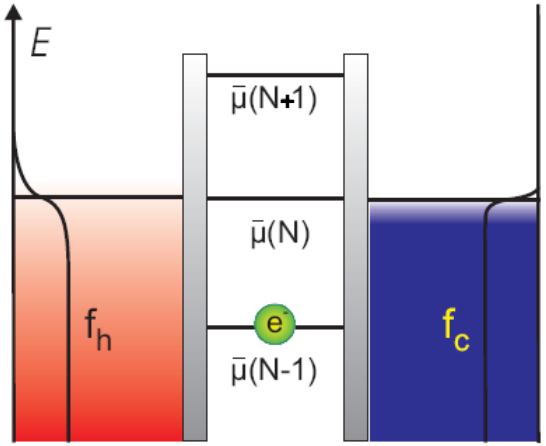

zero thermovoltage

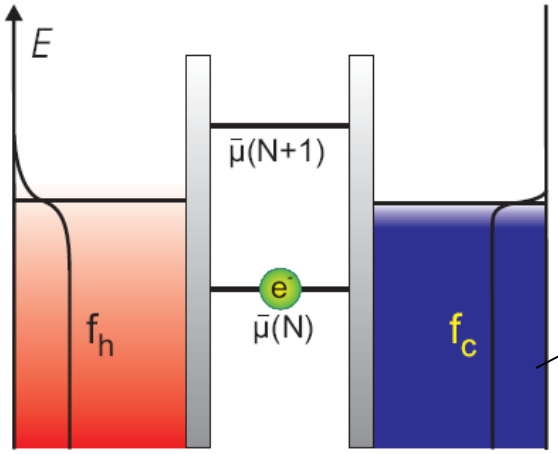

zero thermovoltage

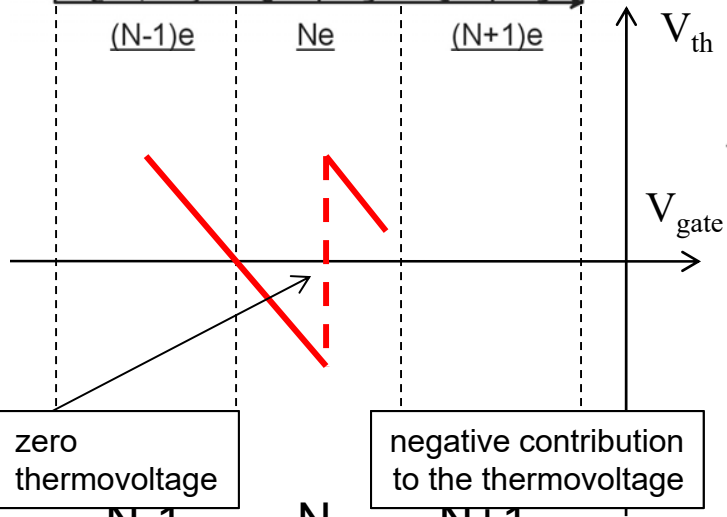

negative contribution to the thermovoltage

h - like

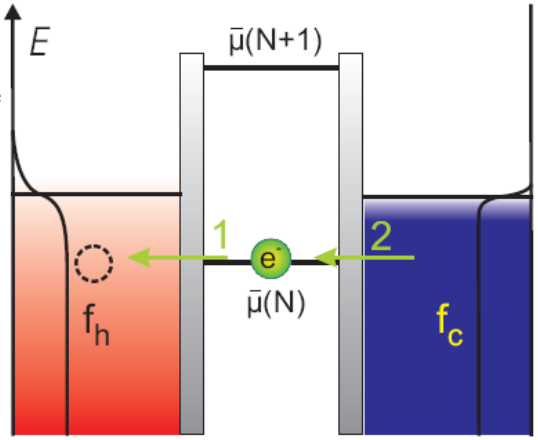

Thermopower of a QD

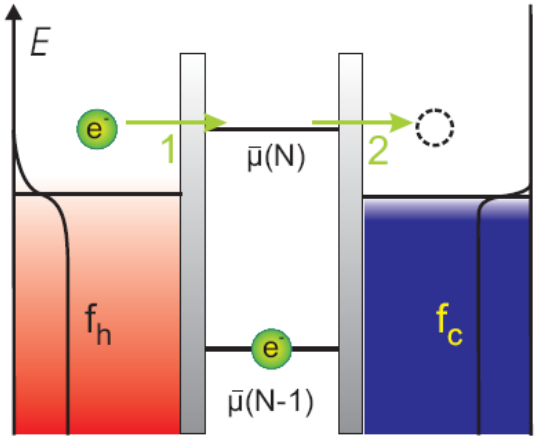

sequential tunneling

$$V_T \propto \frac{E_{gap}}{T}$$

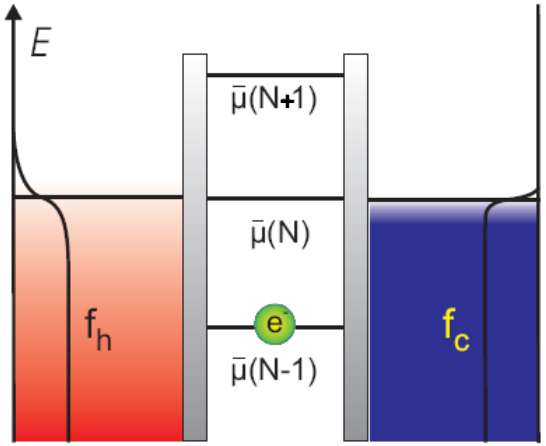

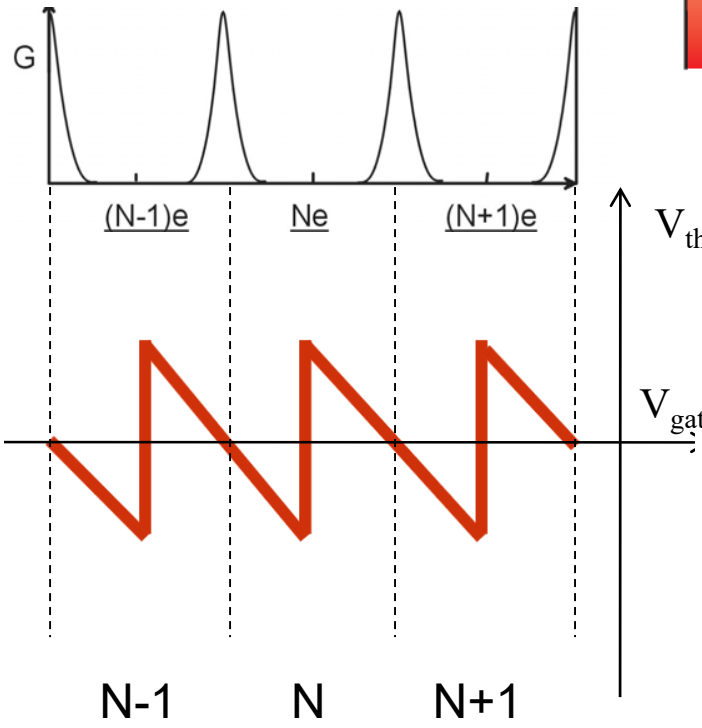

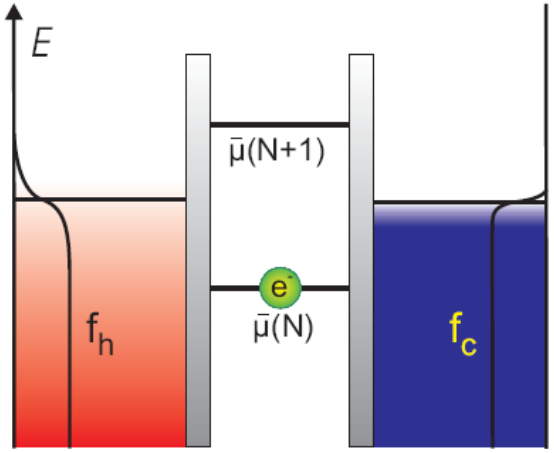

h - like

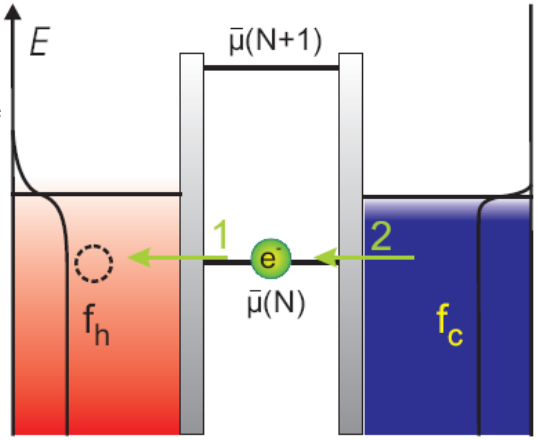

Thermopower of a QD

sequential tunneling

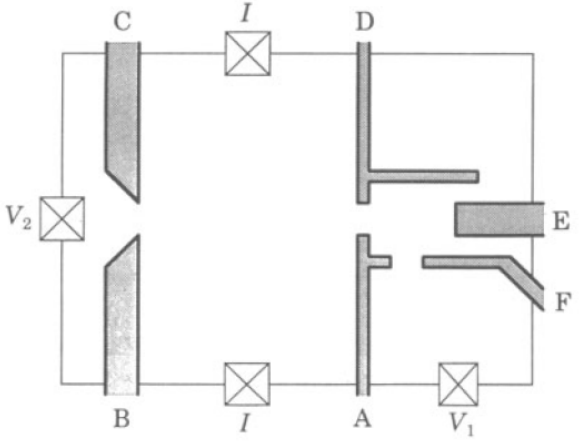

Large, metallic-like QD
N ~ 300
T ~ 230 mK
E_C ~ 0.3 meV
E_C / k_BT ~ 15

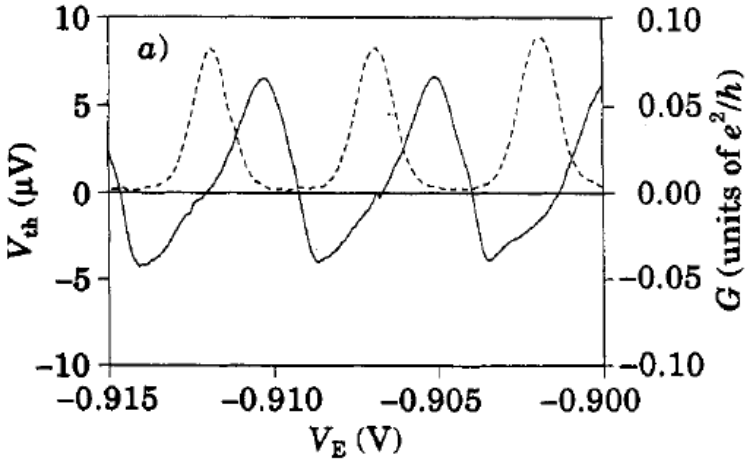

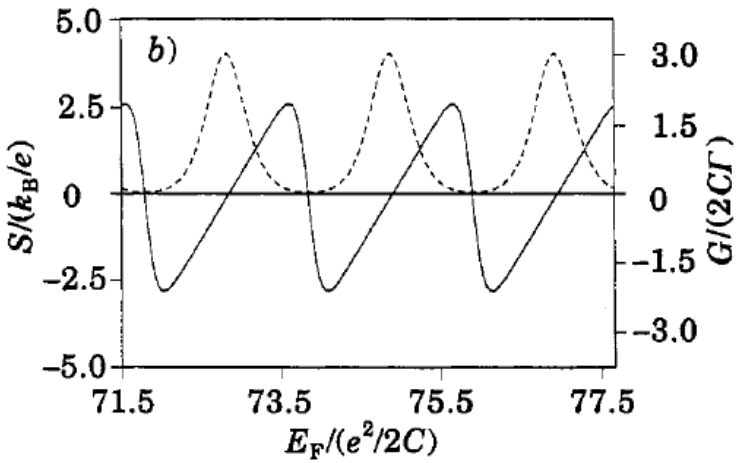

A.A.M. Staring et al., Europhys. Lett. 22, 57 (1993).

Thermopower of a QD

sequential tunneling

$\propto S$

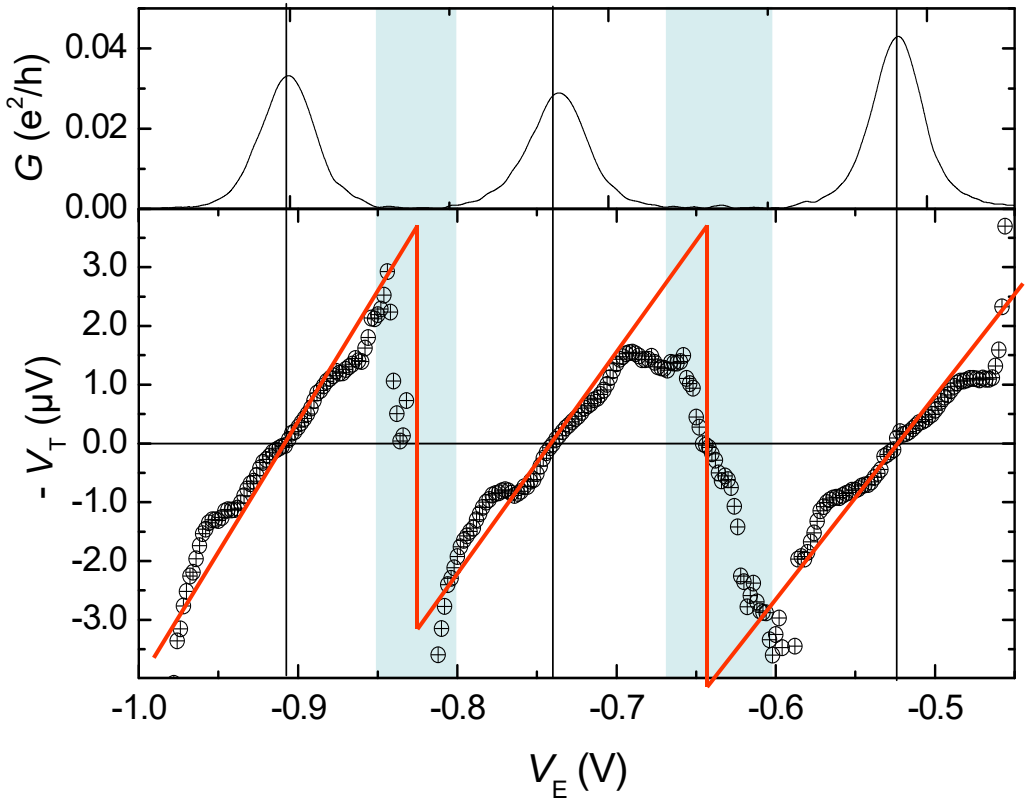

small QD
N ~ 15
T ~ 1.5 K
E_C ~ 2 meV
$E_C / k_B T \sim 15$

Sample:
Bo_I13C

Thermopower of a QD

cotunneling contribution

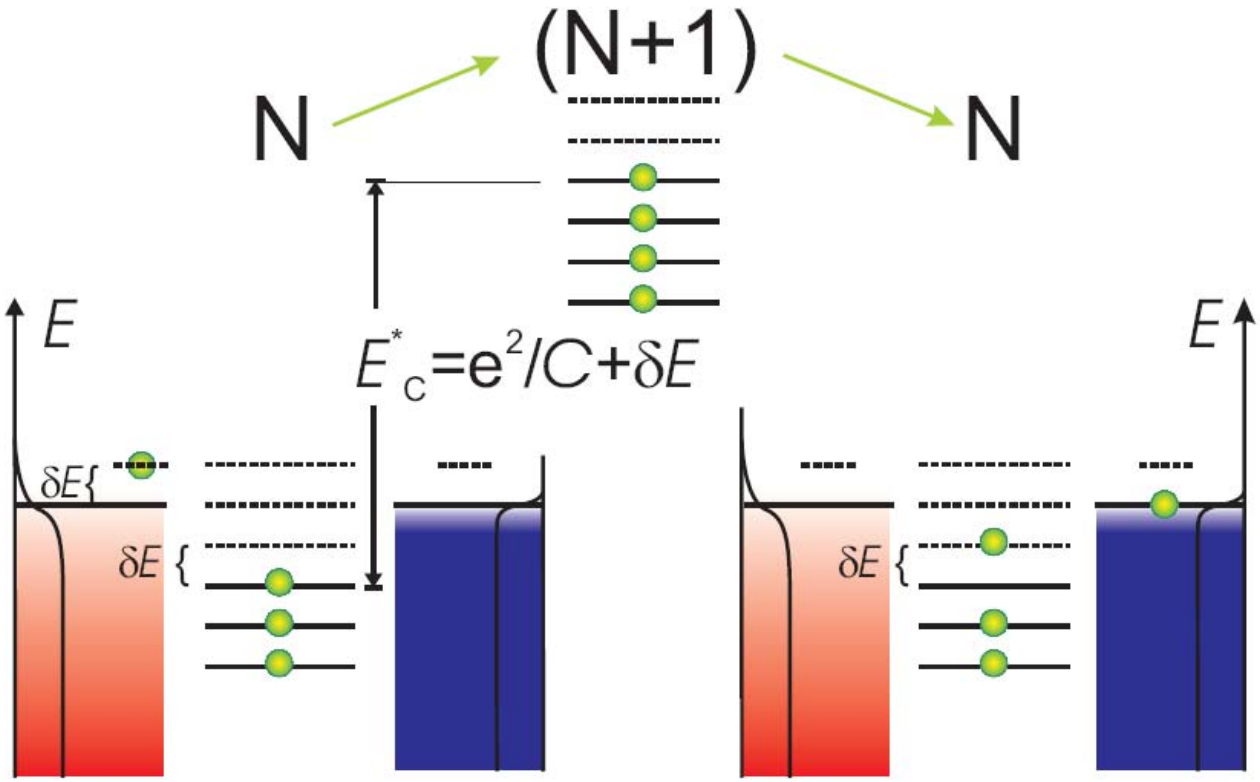

suppression of thermovoltage

Thermopower of a QD

cotunneling contribution

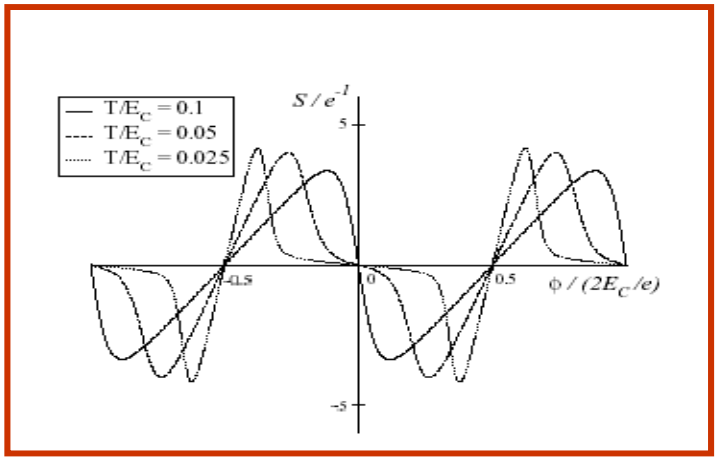

[M. Turek and K.A. Matveev, PRB, **65**, 115332 (2001)]

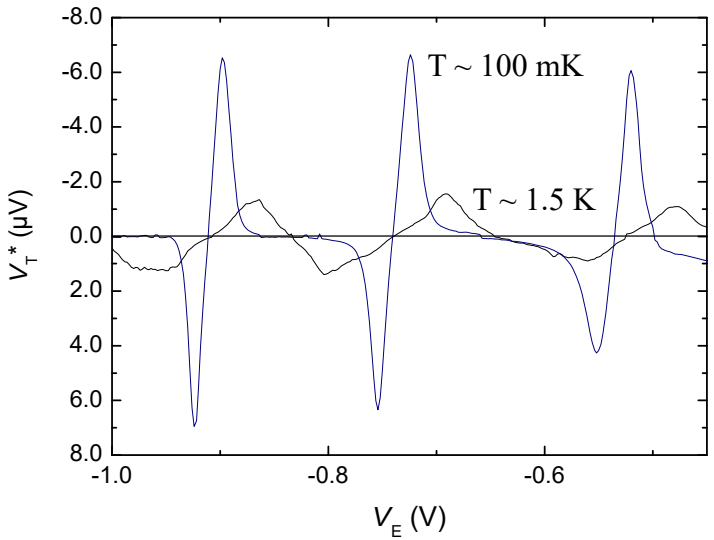

N ~ 15
$E_C \sim 2$ meV
$E_C / k_B T \sim 230$

R. Scheibner et al., PRB **75**, 041301 (2007)

Thermopower of a QD

cotunneling contribution

no signatures of cotunneling processes in the CB regime

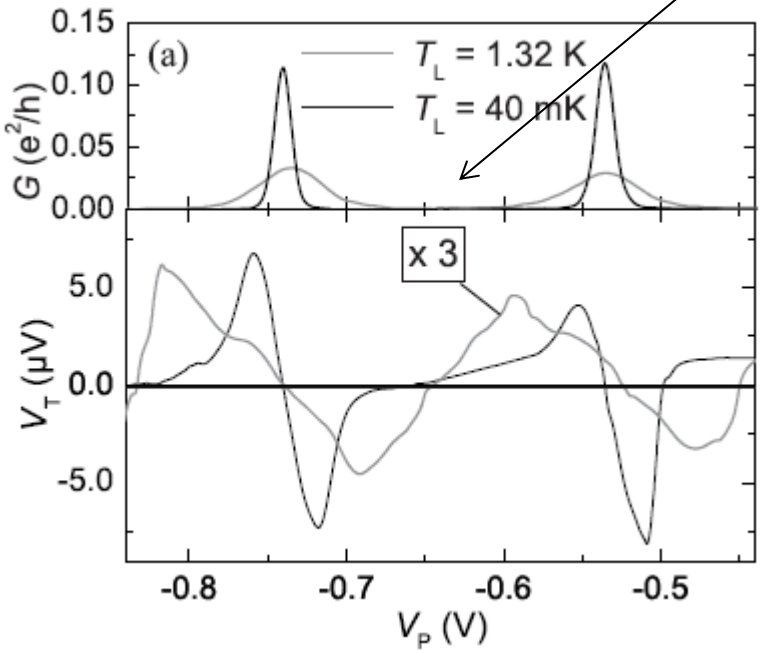

R. Scheibner et al., PRB **75**, 041301 (2007)

Chaotic Quantum Dot

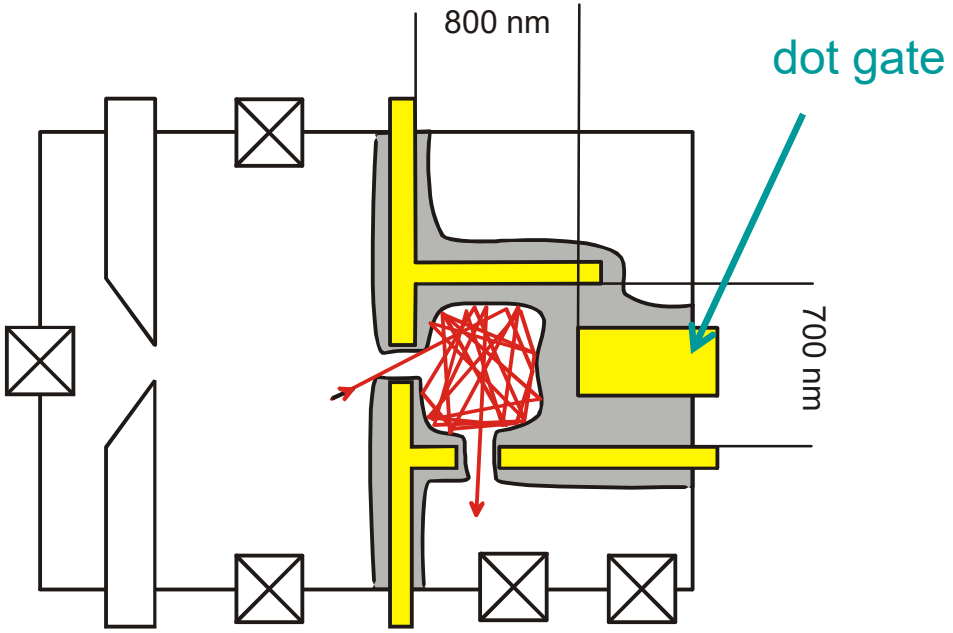

n_s = 3.4 x 10^{11} cm^{-2}

μ = 1 x 10^6 cm^2 / (V sec)

$G_{qpc} = 4\, e^2 / h$

$(N_{qpc} = 2\ )$

Conductance Fluctuations

T = 20 mK

statistical ensemble

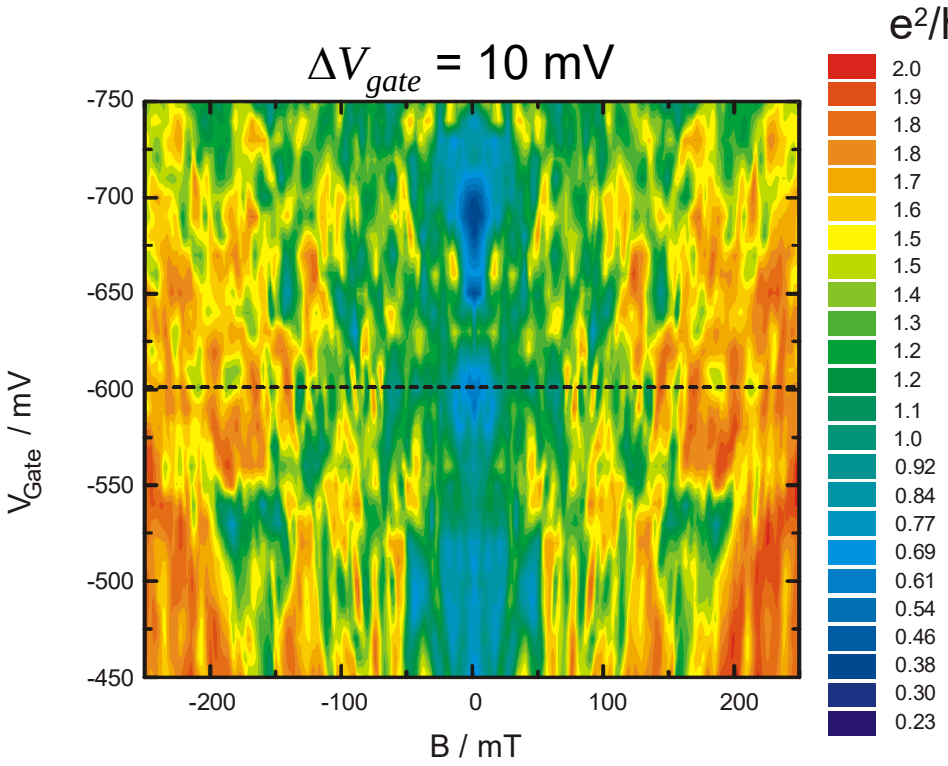

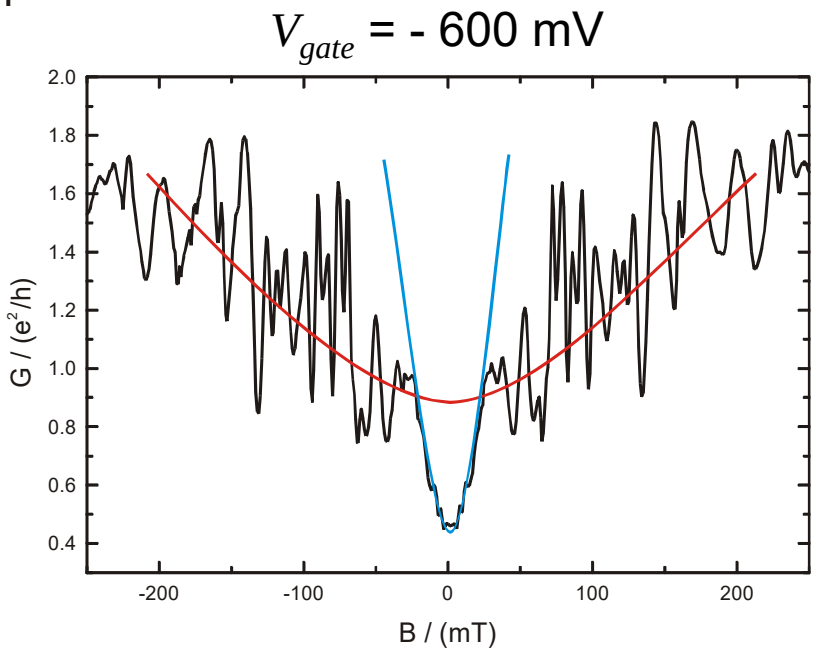

⇒ weak localization and short trajectories

Conductance Fluctuation Distribution

transmission probability distribution:

$$p(t) = \frac{1}{2}\beta\, t^{-1+\beta/2}, \quad 0 < t < 1$$

$\beta = 2$: equal distribution

only for $N_1 = N_2 >> 1$: gaussian distribution

here: $N_1 = 1, N_2 = 2$

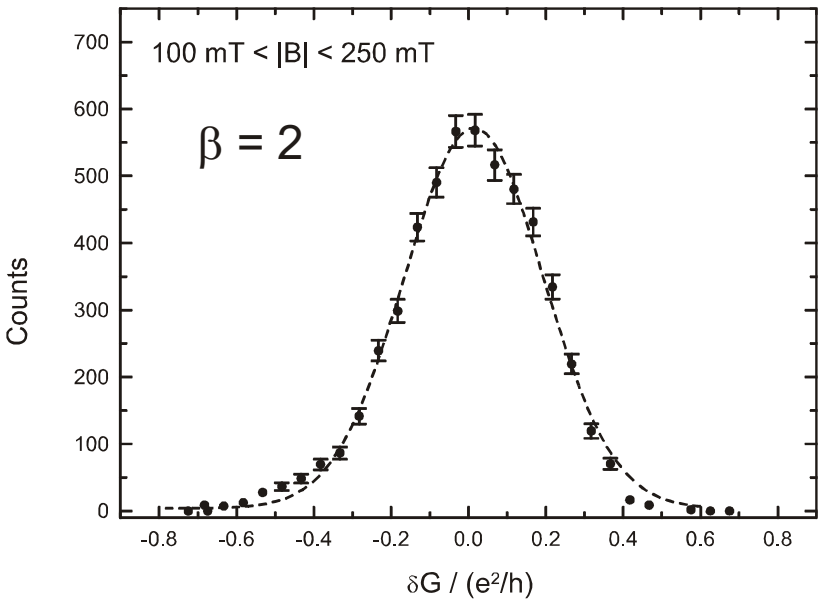

Problems:

- current transport in a QD is accompanied by dephasing
- weak localisation and short trajectories obscure effects of chaotic transport

Weak Localization

$$\Rightarrow \langle G(B) \rangle = \langle G \rangle_{\beta=2} - \frac{\delta \langle G \rangle_{\beta=1}}{1 + (\Phi / \Phi_c)}$$

with $\Phi = BA$

and $\Phi_c = \frac{h}{e} \left(\frac{\tau_{ergodic}}{\tau_{dwell}} \right)^{1/2}$

averaged conductance

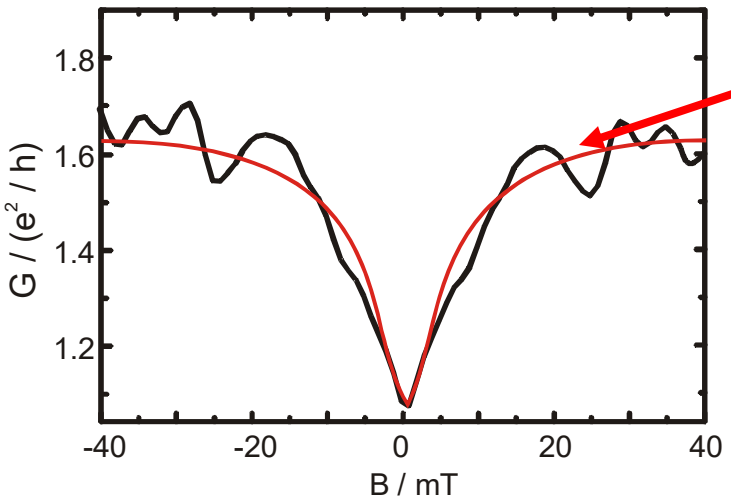

Fit:

$\langle G \rangle_{\beta=2} = 1.3\ e^2/h$

$\delta \langle G \rangle_{\beta=1} = 0.3\ e^2/h$

$\Phi_c / A = 6$ mT

$A = 0.3\ \mu m^2$

$(\Rightarrow A_{eff} = 1.15\ A)$

$$\Rightarrow \frac{\tau_{dwell}}{\tau_{ergodic}} = \left(\frac{h/e}{\Phi_c} \right)^2 \approx 5.3 > 1$$

i.e. the QD is chaotic!

Thermovoltage Fluctuations

T = 20 mK

statistical ensemble

ΔV_{gate} = 10 mV

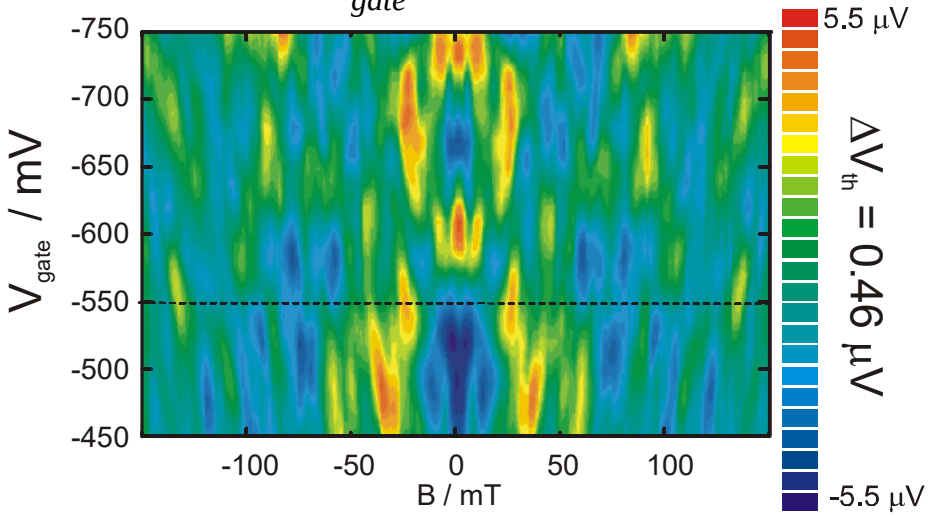

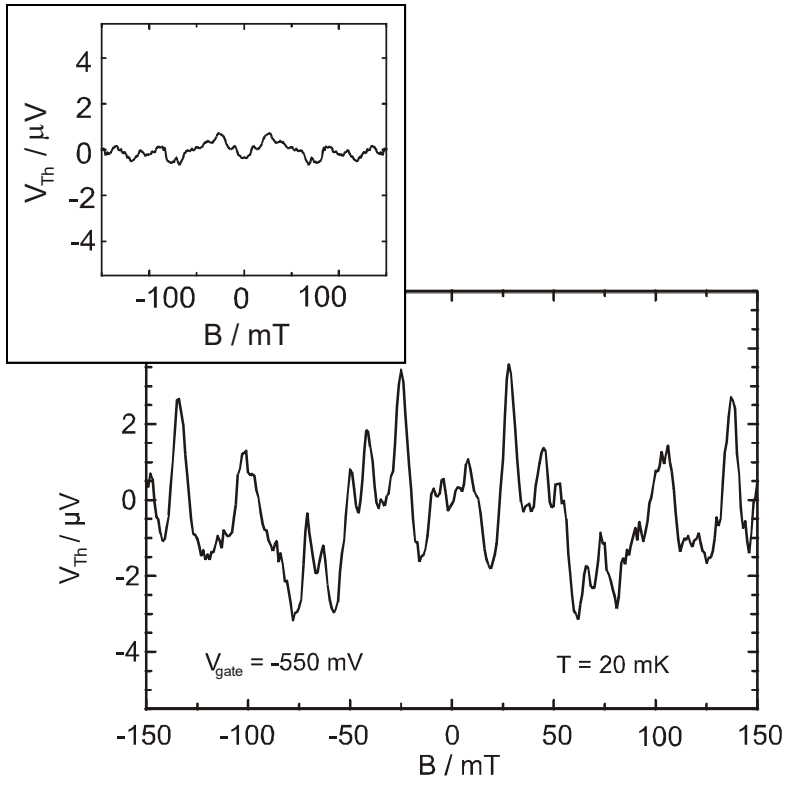

V_{gate} = - 550 mV

$I_{heating} = 40$ nA

$\Delta T \approx 235$ mK

Thermopower Fluctuation Distribution

$$\frac{\partial G}{\partial E} = c(\tau_1 - \tau_2)\sqrt{G(1-G)}$$

RMT:

analytic form for $N_1 = N_2 = 1$

here: $N_1 = N_2 = 2$

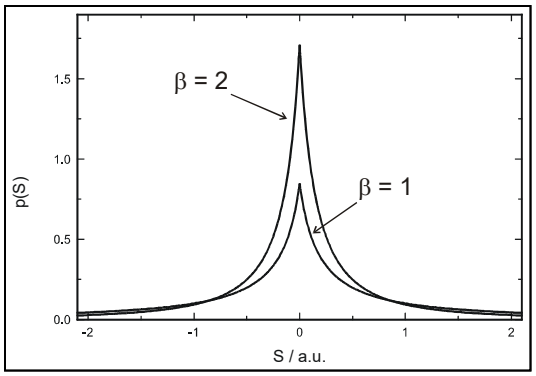

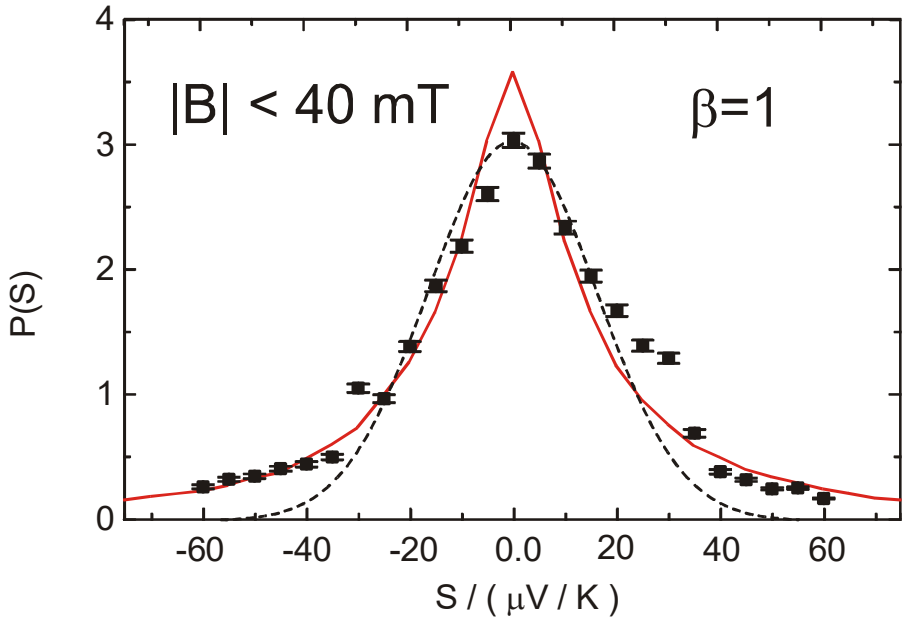

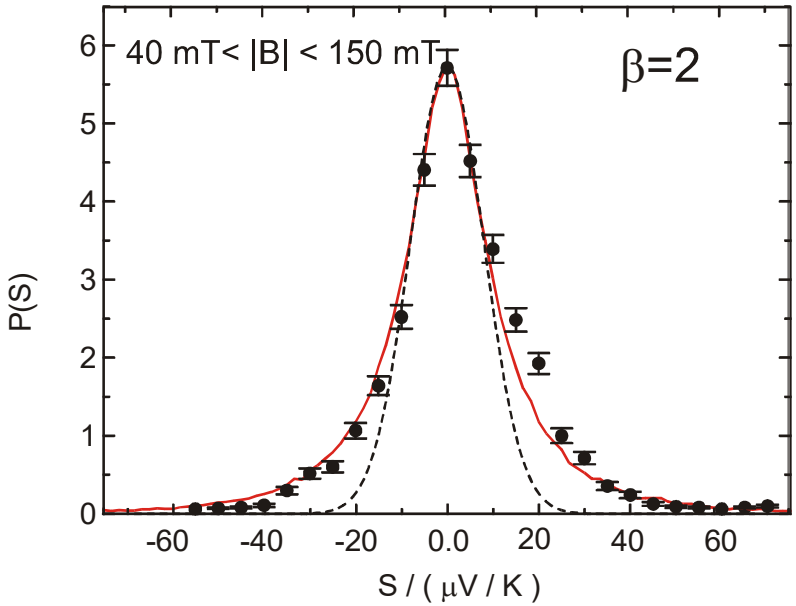

S. Godijn et al., PRL **82**, 2927 (1999)

Residual Charging Energy

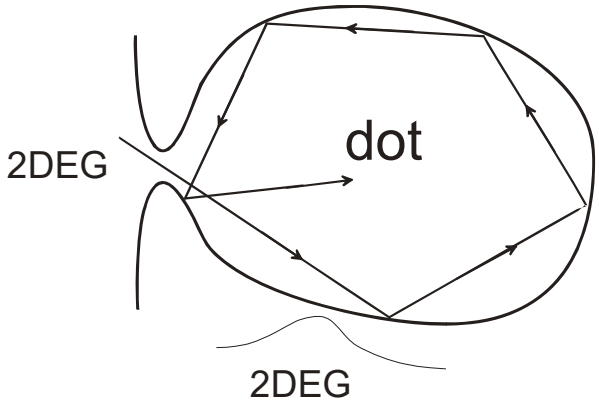

characteristic time scale:

$$\tau_{erg} = \Delta E / h$$

$$\tau_{dwell} = U^* / h$$

Luttinger liquid theory:

$$U^* = U_0 (1-t)^N$$

(Flensberg, 1993, 1994)

chaotic QD: $t \to 1 \Rightarrow$

(Aleiner and Glazman, 1998)

$$(1-t) \to \frac{\Delta E}{U_0} \ln^2\left(\frac{U_0}{\Delta E}\right)$$

Thermopower in the Coulomb-Blockade Regime

$$\Delta E << k_B T << e^2 / C \quad \text{(classical limit)}$$

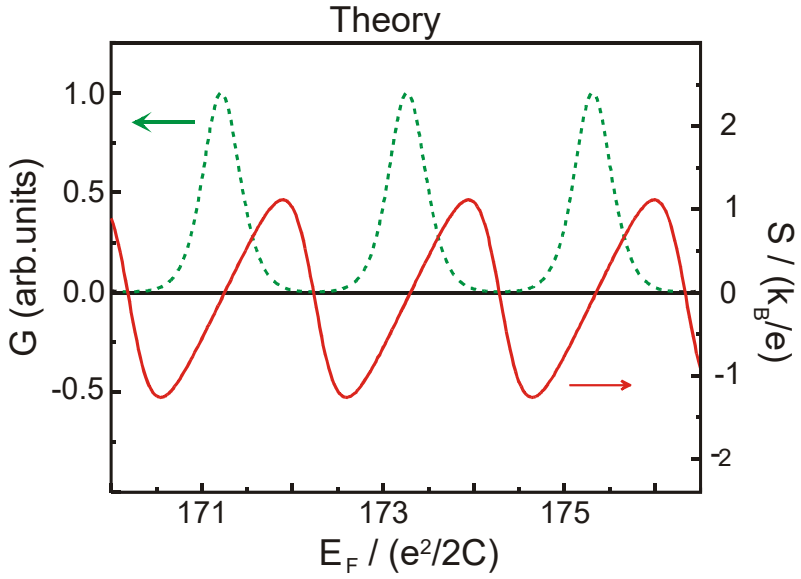

Beenakker *et al.*, PRB **46**, 9667 (92)

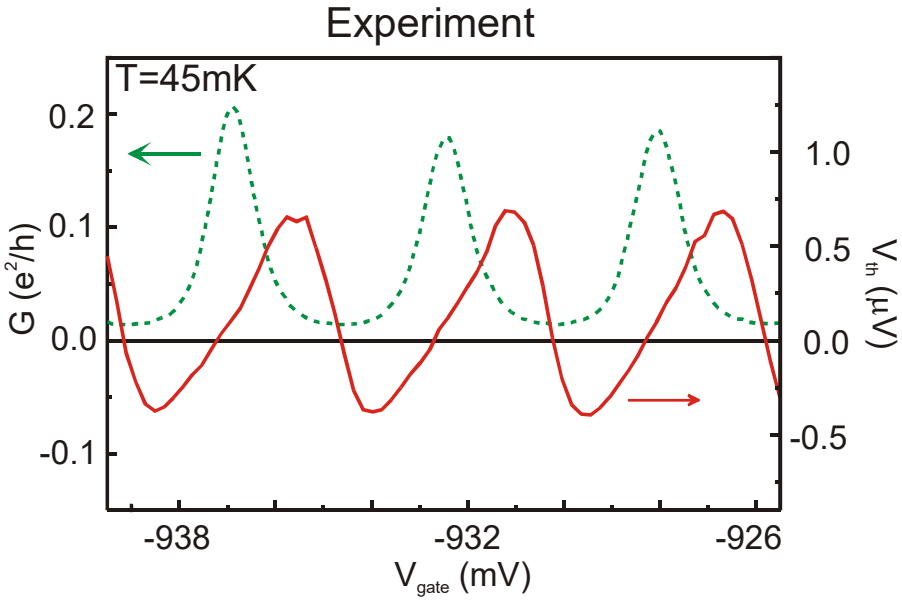

Staring *et al.*, Europhys. Lett. **22**, 57 (93)

Molenkamp *et al.*, Semicond. Sci. Technol. **9**, 903 (94)

$$S = -\frac{1}{2eT}\left[\left(N-\tfrac{1}{2}\right)\frac{e^2}{C} + \overline{\mu} - e\Phi_{ext} - E_F\right] = -\frac{U^*}{2eT}$$

Scaling Experiment

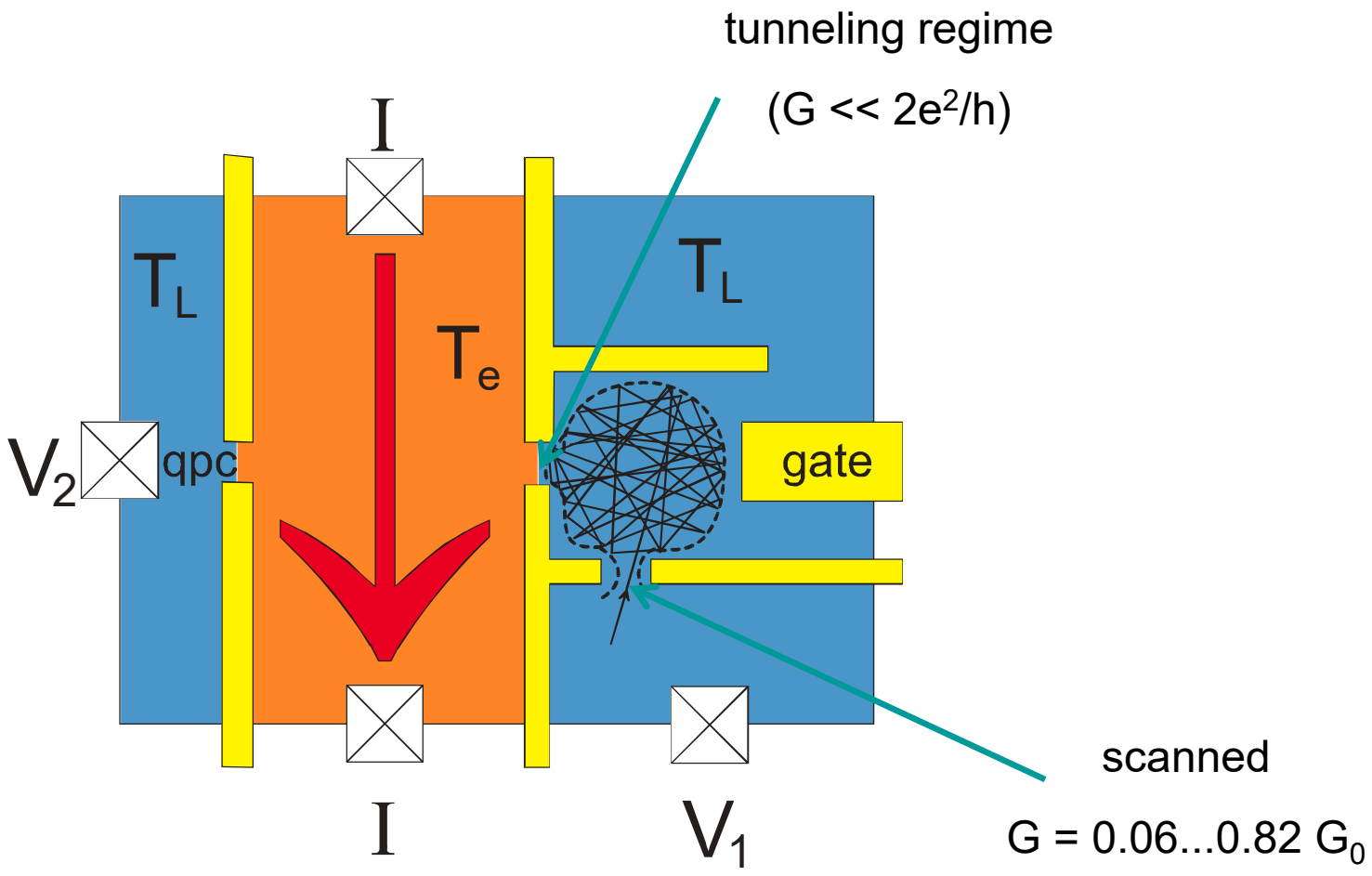

Scaling Results

Thermovoltage

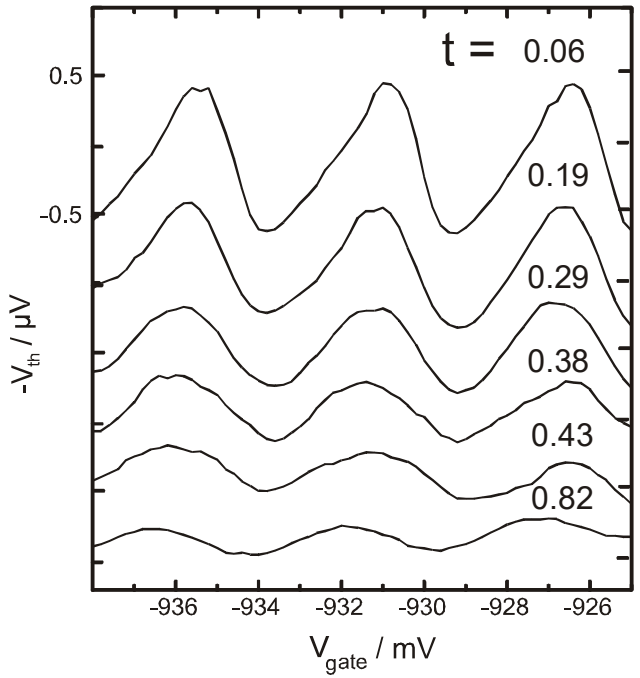

Thermopower

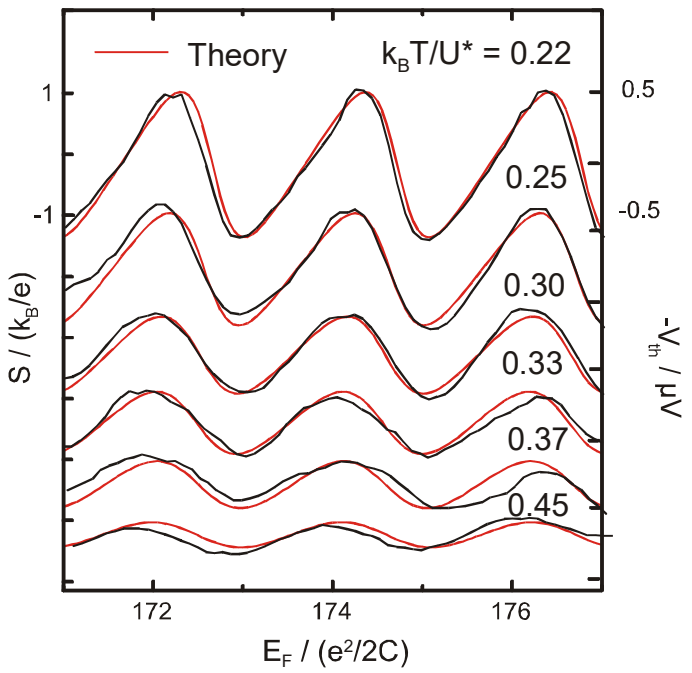

$$I_{heating} = 40 \text{ nA}$$

$$T_e = 255 \text{ mK}, T_L = 40 \text{ mK}$$

Scaling

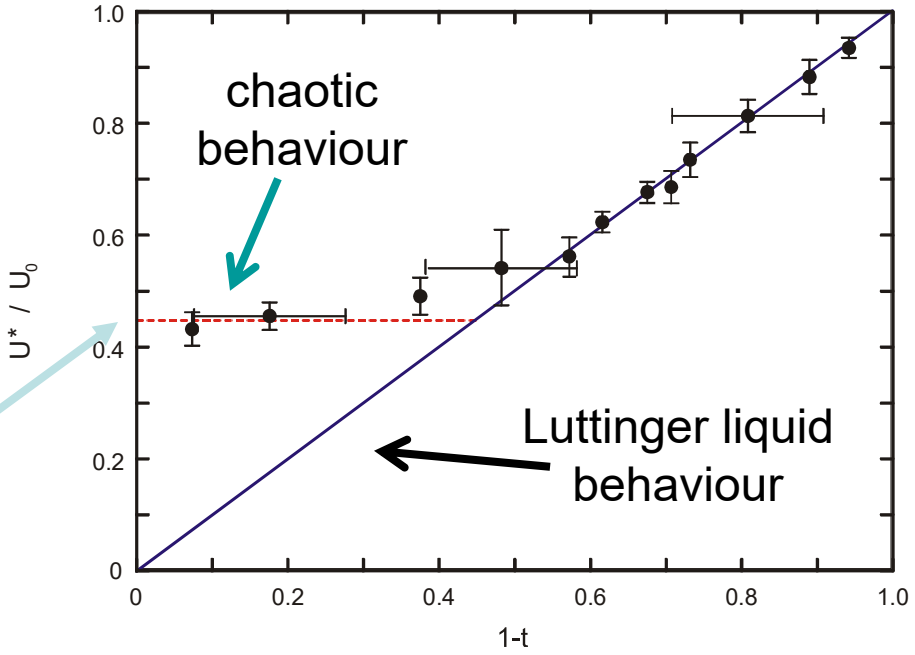

extrapolation

$t \to 1$

$$U^*_{\mathrm{exp}}(t \to 1) \approx 0.45 U_0$$

theory

$\Delta E = 23\ \mu\mathrm{eV}$

$U_0 = 100\ \mu\mathrm{eV}$

$$U^* = U_0 \frac{\Delta E}{U_0} \ln^2\left(\frac{U_0}{\Delta E}\right) = 0.49 U_0$$

S. Möller et al., PRL **81**, 5197 (1998)

Spin-Correlated QD

- existence of a magnetic moment on the QD can lift the CB
- transport mechanism: spin scattering
- hybridization of free electrons in the leads with localized magnetic moment leads to resonance at the Fermi edge

Kondo Resonance

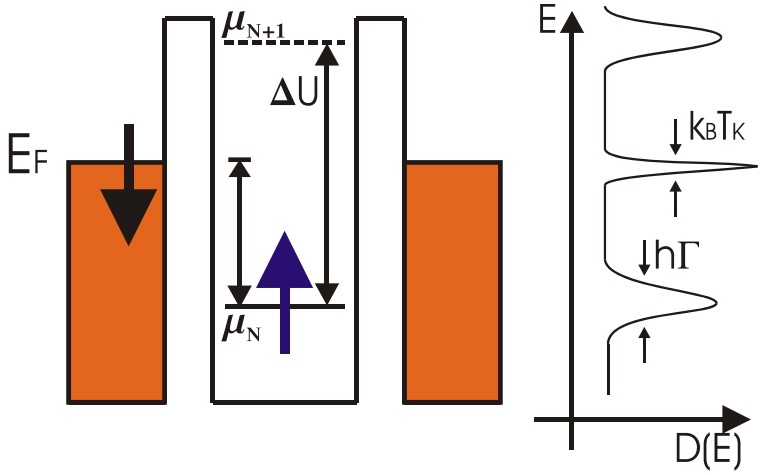

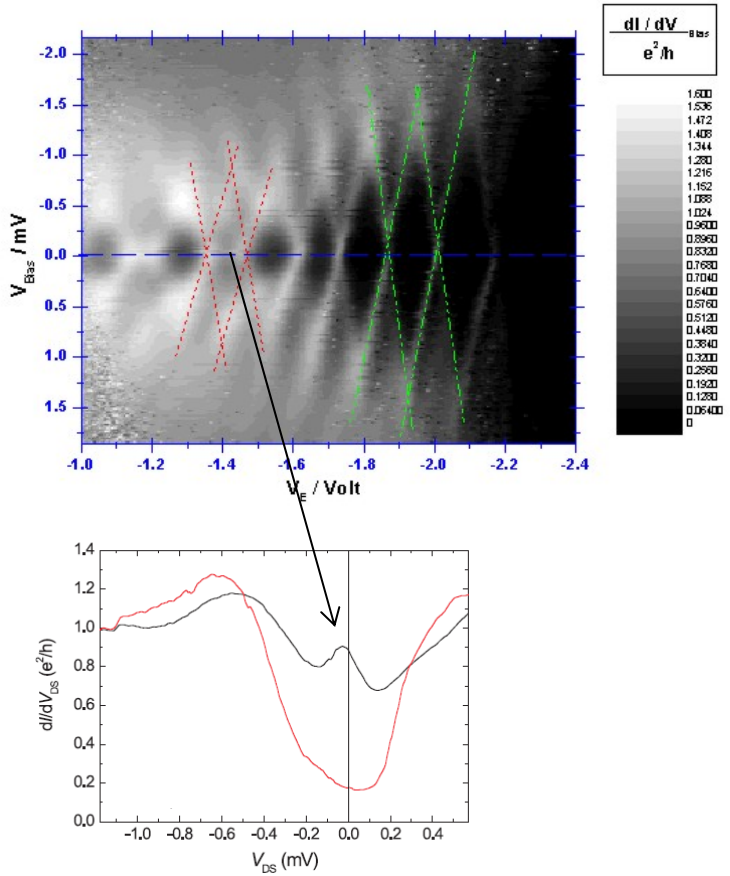

Spin-Correlated QD

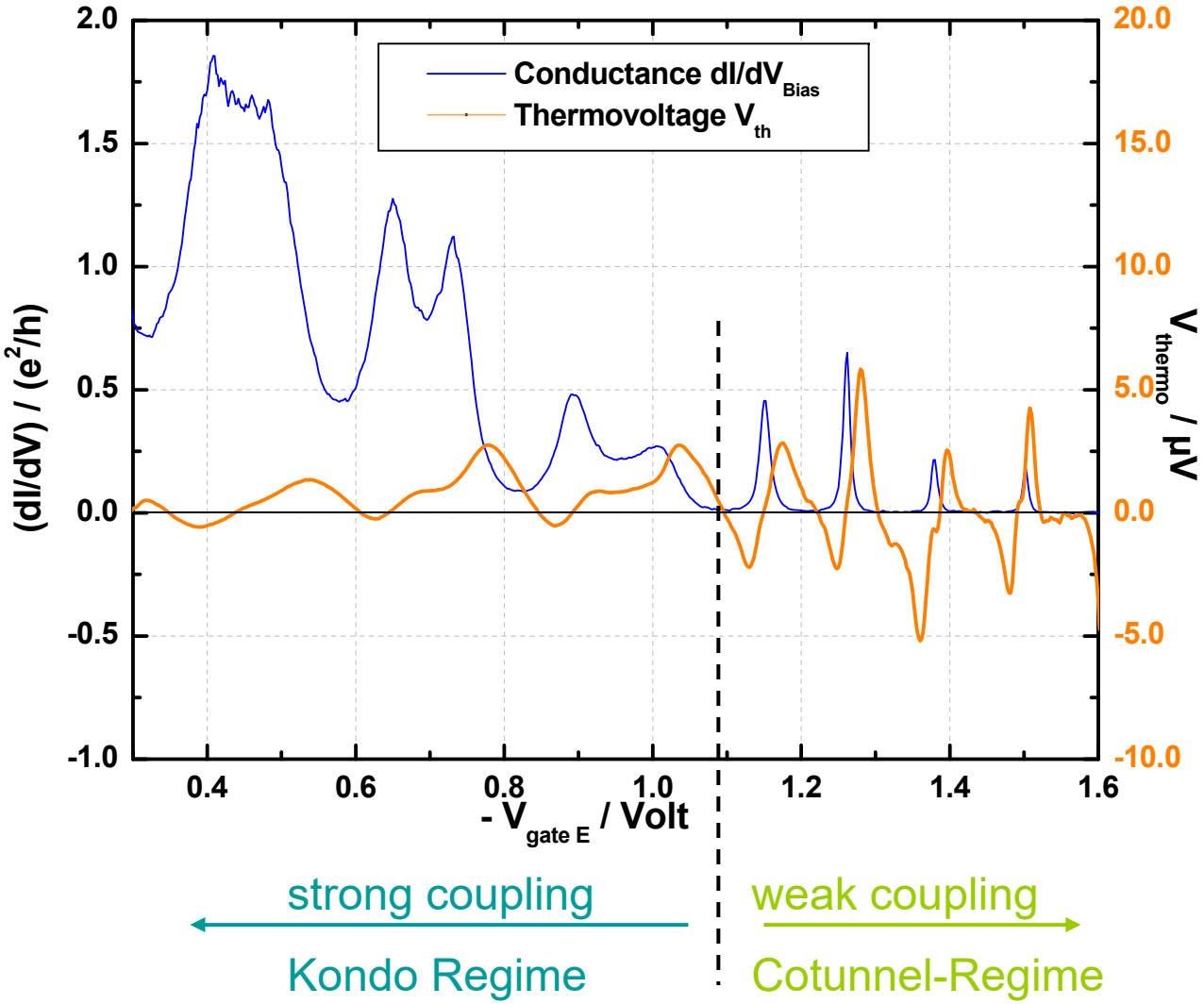

Spin-Correlated QD

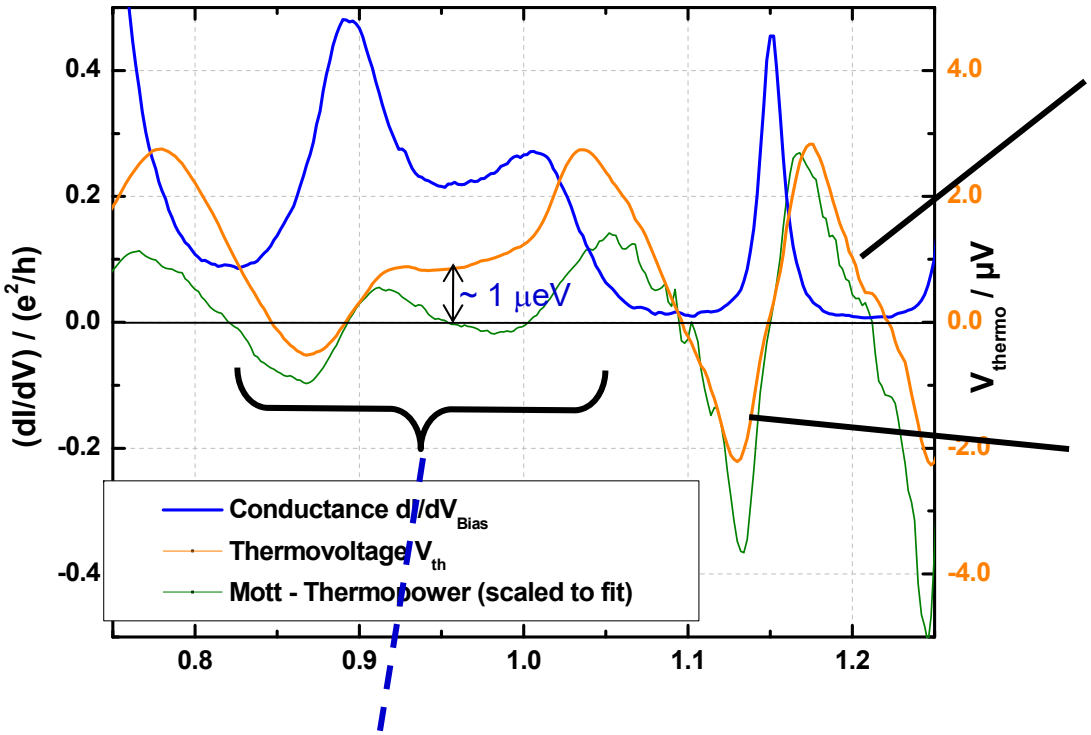

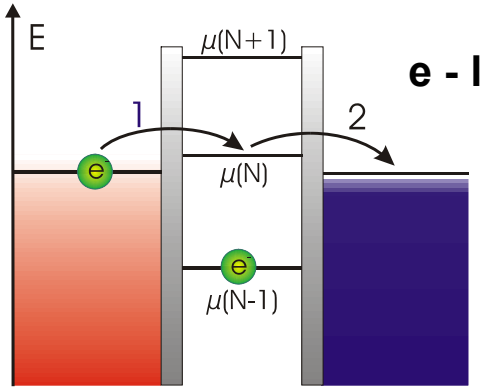

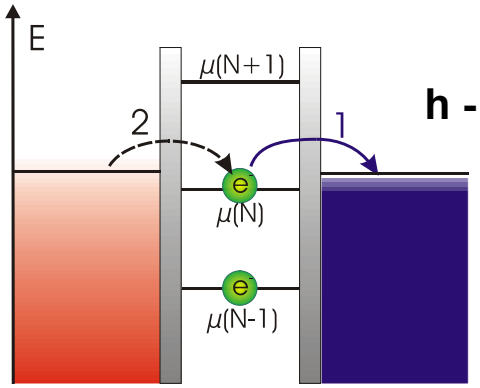

Asymmetry between
electron- and hole-like transport:
Mixed-valence regime

Scheibner *et al*. PRL **95**, 176602 (2005)

Spin-Entropy Transport

Entropy change ΔS

adding one electron to an empty site: $\Delta S = k_B(\ln g_f - \ln g_i) = k_B(\ln 2 - \ln 1) = k_B \ln 2$

$-V_g$ ←

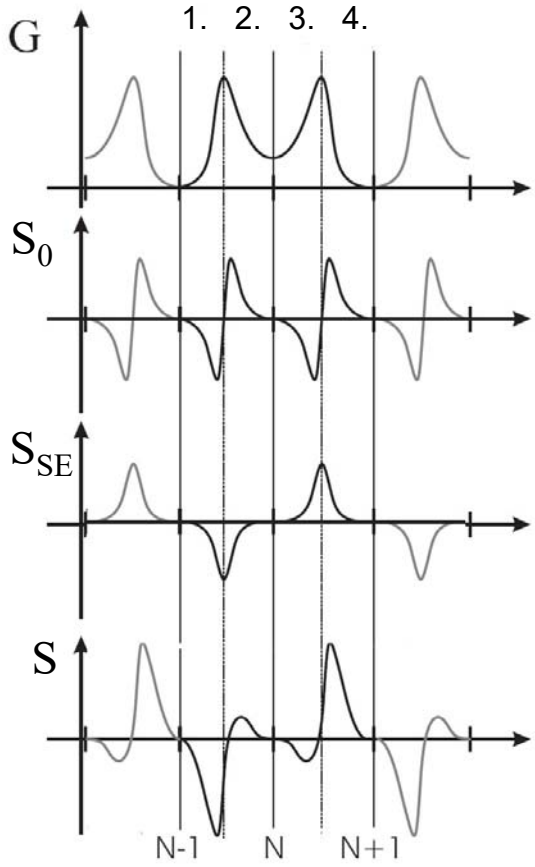

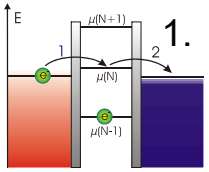

1. e-like transport from the hot to the cold reservoir
   $\Delta S = k_B(\ln g_f - \ln g_i) = k_B(\ln 2 - \ln 1) = k_B \ln 2$

   ➔ $S_{SE}=-k_B/e \ln 2$

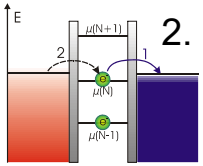

2. h-like transport from the cold to the hot reservoir
   $\Delta S = k_B(\ln g_f - \ln g_i) = k_B(\ln 1 - \ln 2) = -k_B \ln 2$

   ➔ $S_{SE}=-k_B/e \ln 2$

3. e-like transport from the hot to the cold reservoir
   $\Delta S = k_B(\ln g_f - \ln g_i) = k_B(\ln 1 - \ln 2) = -k_B \ln 2$

   ➔ $S_{SE}=k_B/e \ln 2$

4. h-like transport from the cold to the hot reservoir
   $\Delta S = k_B(\ln g_f - \ln g_i) = k_B(\ln 2 - \ln 1) = k_B \ln 2$

   ➔ $S_{SE}=k_B/e \ln 2$

R. Scheibner et al., PRL **95**, 176602 (2005)
R. Scheibner, PhD-Thesis, Würzburg 2007

Spin entropy contributions

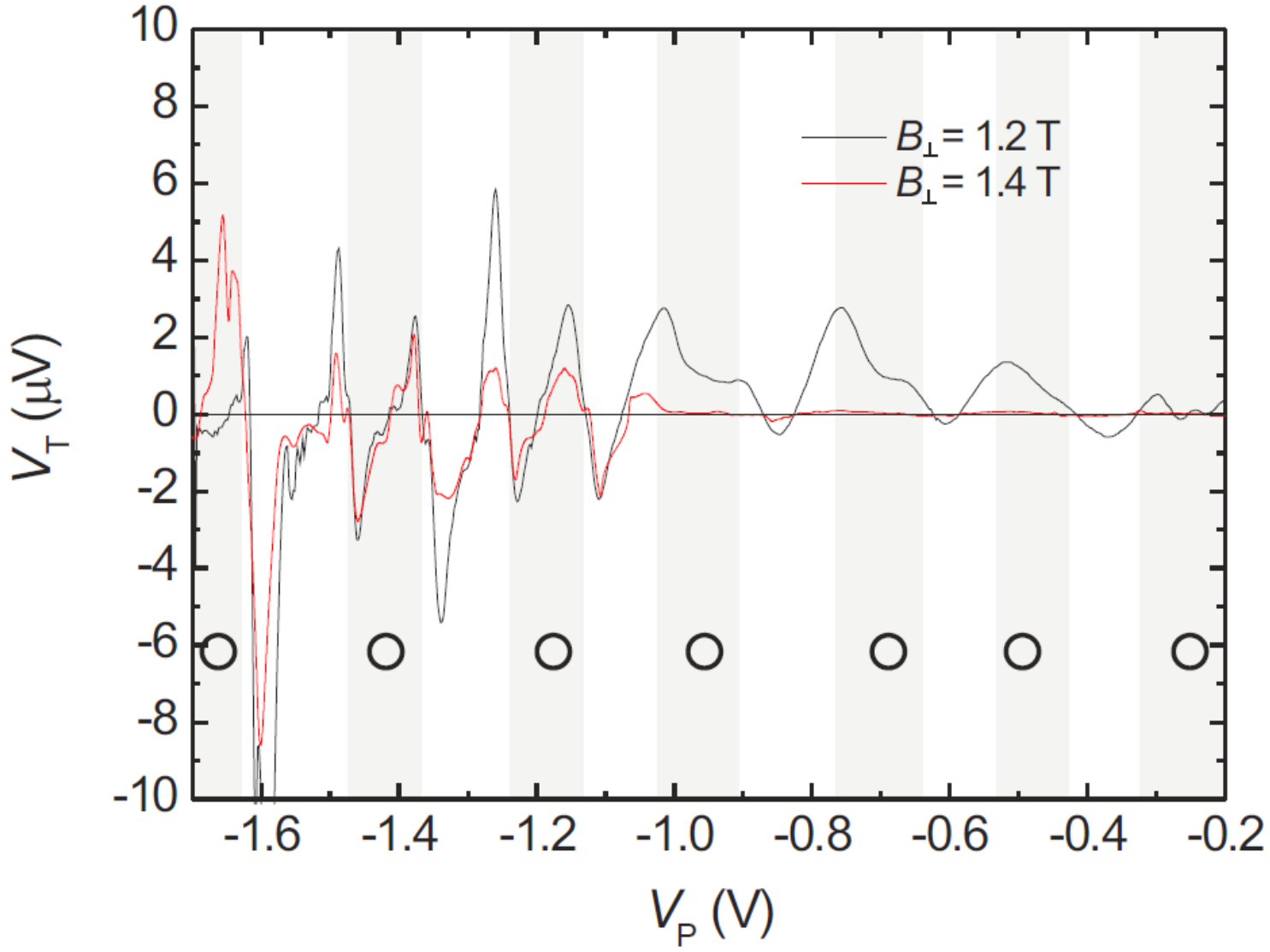

Thermal Rectifier

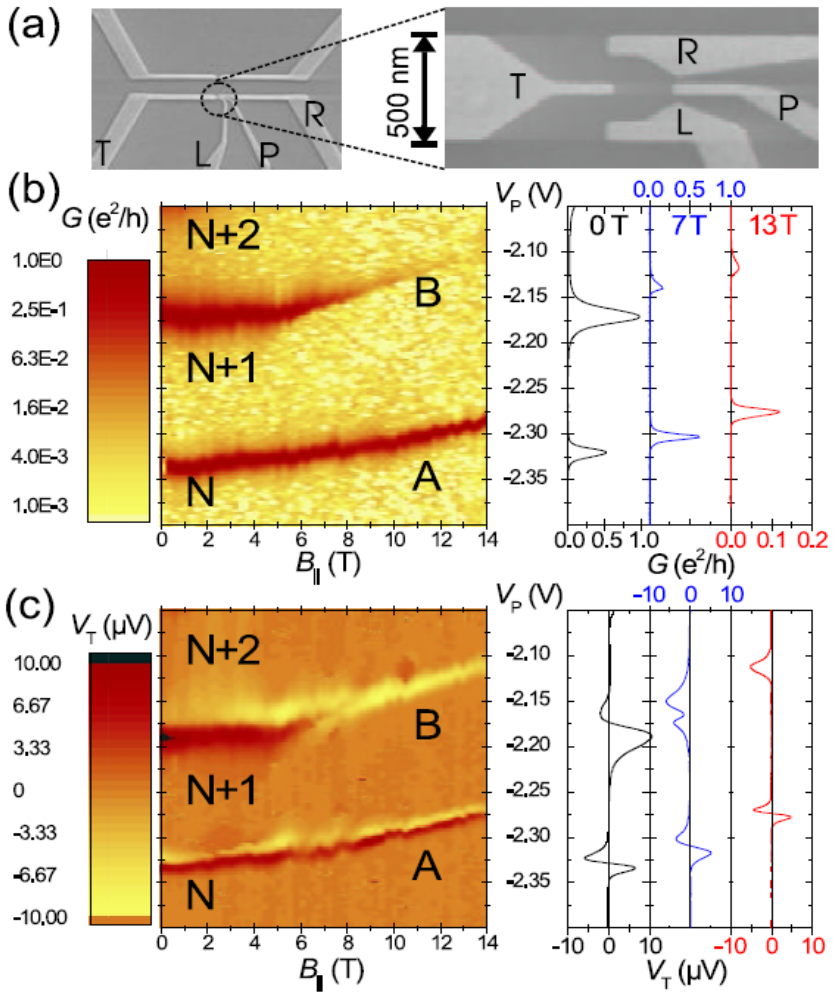

R. Scheibner et al., NJP **10**, 083016 (2008)

Thermal Rectifier

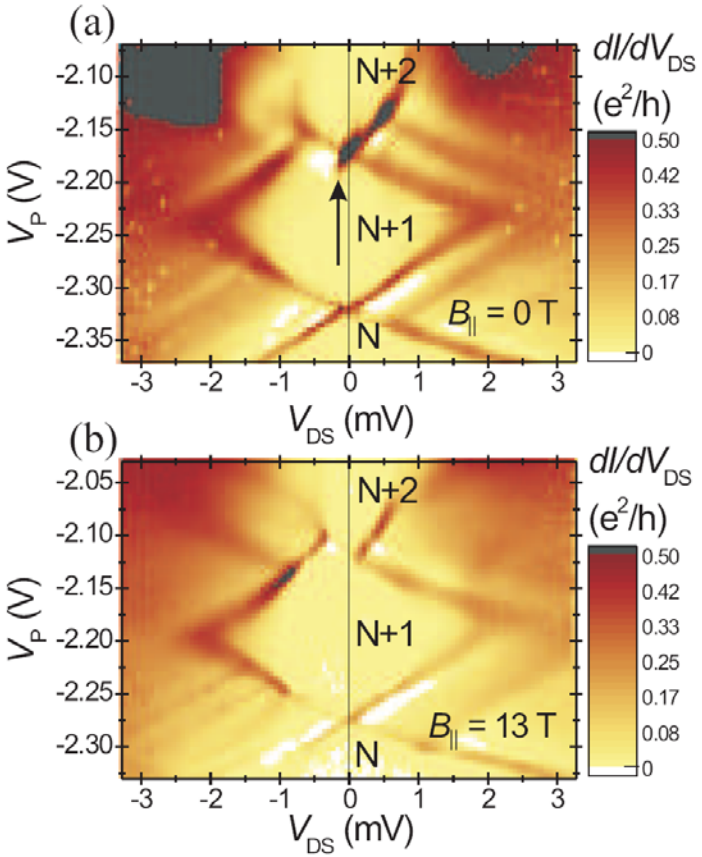

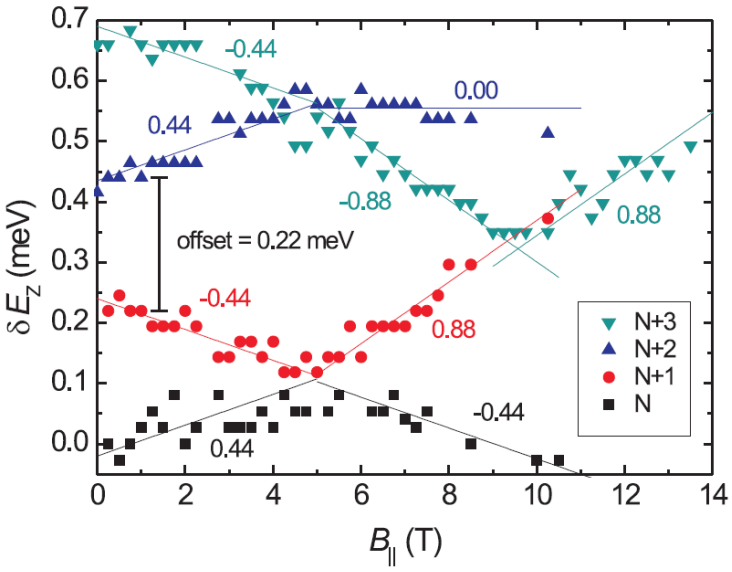

R. Scheibner et al., NJP **10**, 083016 (2008)

Thermal Rectifier

asymmetrically coupled states

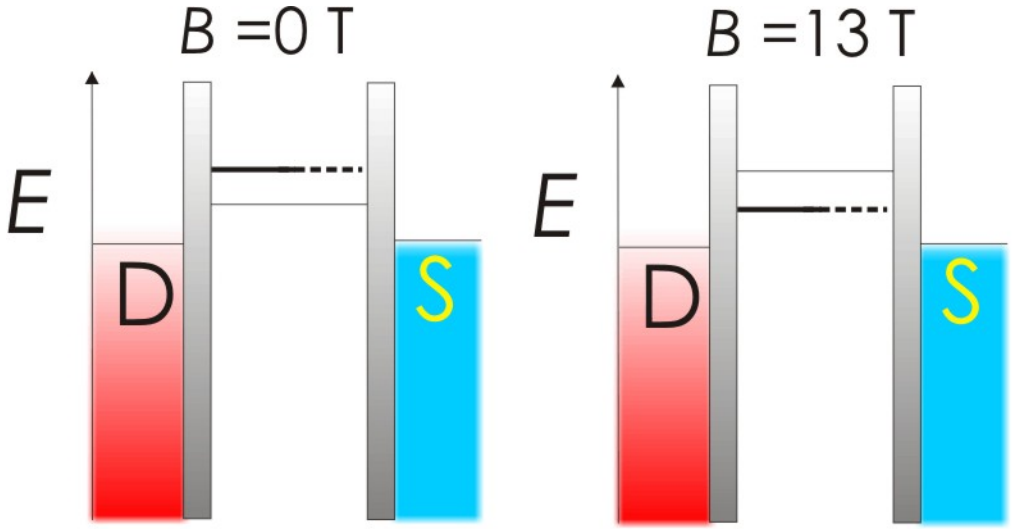

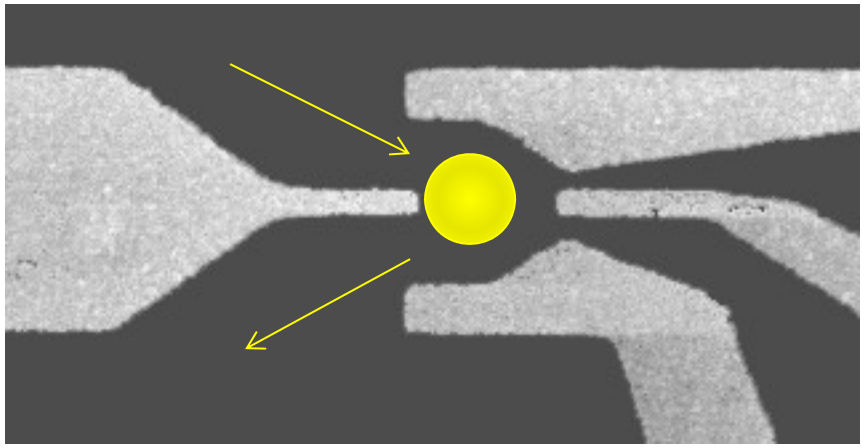

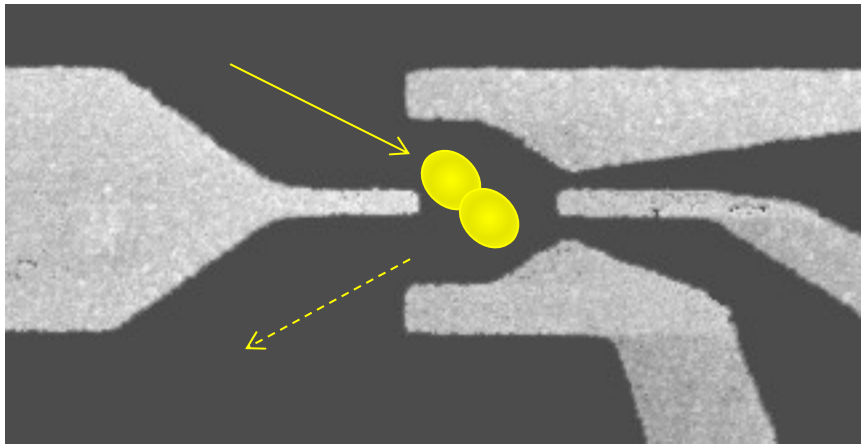

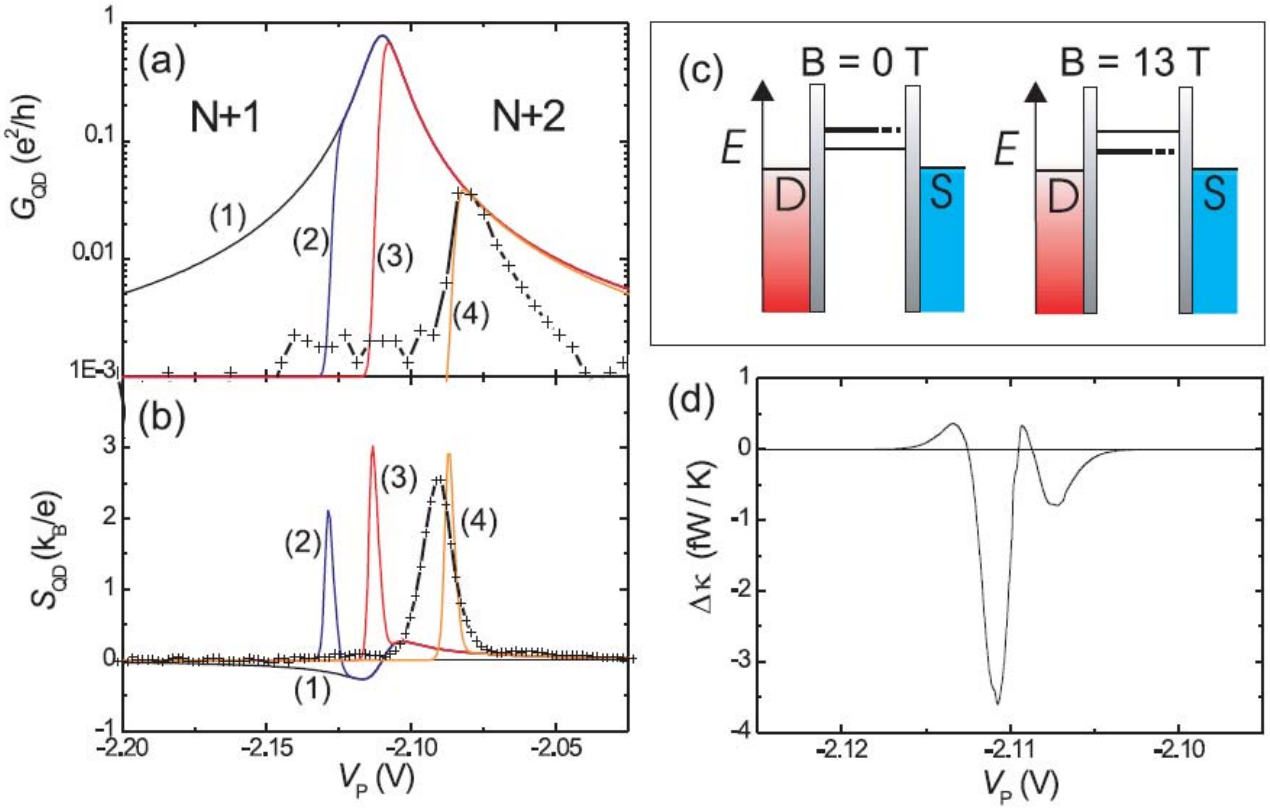

Figure 4. Calculated conductance G (a) and thermopower S (b) for $T_e = 80$ mK, $\Delta T = 30$ mK and various energy separations between the symmetric and asymmetric (blocking) states: (1) without blocking state, (2) $\delta E_Z = -250\,\mu$eV, (3) 0 μeV and (4) 400 μeV. The crosses represent the measurement at $B_{||} = 13$ T. (c) presents a schematic energy diagram of the QD close to the $N+1 \leftrightarrow N+2$ SET resonance at $B_{||} = 0$ and 13 T. The blocking state is symbolized by the thick broken line. (d) displays the difference of the thermal conductances $\Delta\kappa$ for a reversal of the temperature difference.

Thermal Rectifier

$$\delta E_Z = -250,\ 0,\ 400\ \mu eV$$

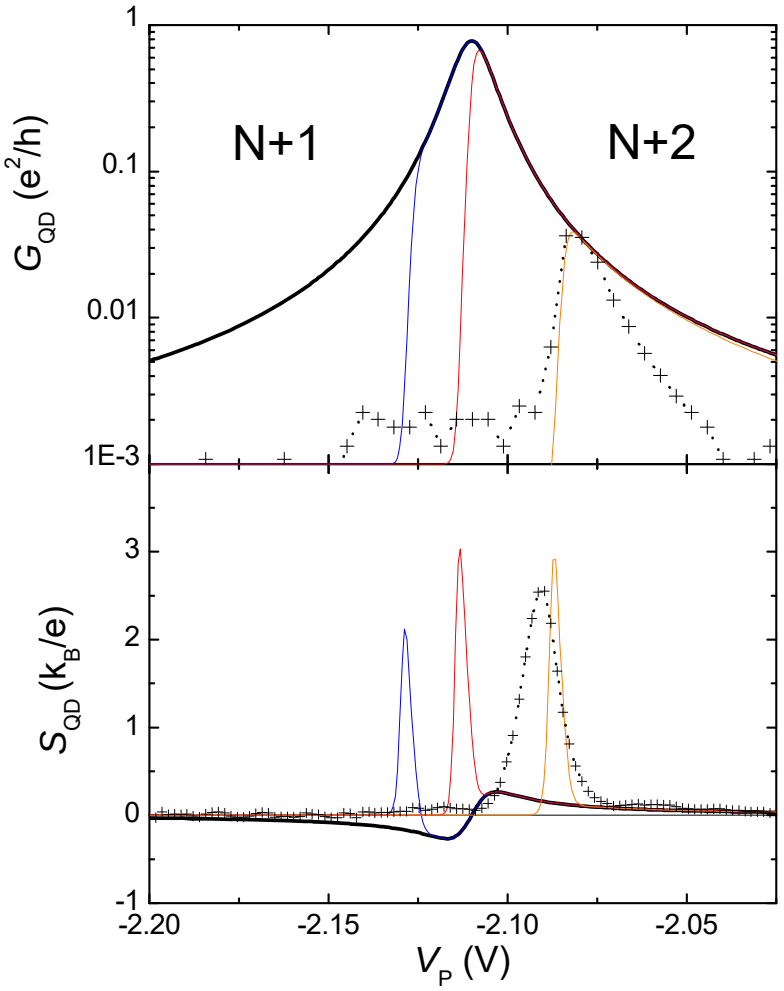

$$J_{tot} = \int_{-\infty}^{\infty} dE \left(\frac{\Lambda}{h}\right)\left[f_L(E,T) - f_R(E,T)\right]t(E)$$

$$\Lambda = \begin{cases} -e & \text{(electron)} \\ E-\mu & \text{(energy)} \end{cases}$$

$$\begin{pmatrix} I \\ Q \end{pmatrix} = \begin{pmatrix} L_{11} & L_{12} \\ L_{21} & L_{22} \end{pmatrix} \begin{pmatrix} \mu_L/e - \mu_R/e \\ T_L - T_R \end{pmatrix}$$

$$S = -\frac{L_{12}}{L_{11}} = -\frac{\left(-\frac{e}{Th}\right)\int_{-\infty}^{\infty} dE\,(E-\mu)t(E)\left(-\frac{df}{dE}\right)}{\left(\frac{e^2}{h}\right)\int_{-\infty}^{\infty} dE\,t(E)\left(-\frac{df}{dE}\right)}$$

$$t(E) = A\frac{(\Gamma/2)^2}{(\Gamma/2)^2 + E^2} \times f\left(E - \delta E_Z, T\right)$$

R. Scheibner et al., NJP **10**, 083016 (2008)

Thermal Rectifier

thermal conductance, L_{22}, for a temp. reversal

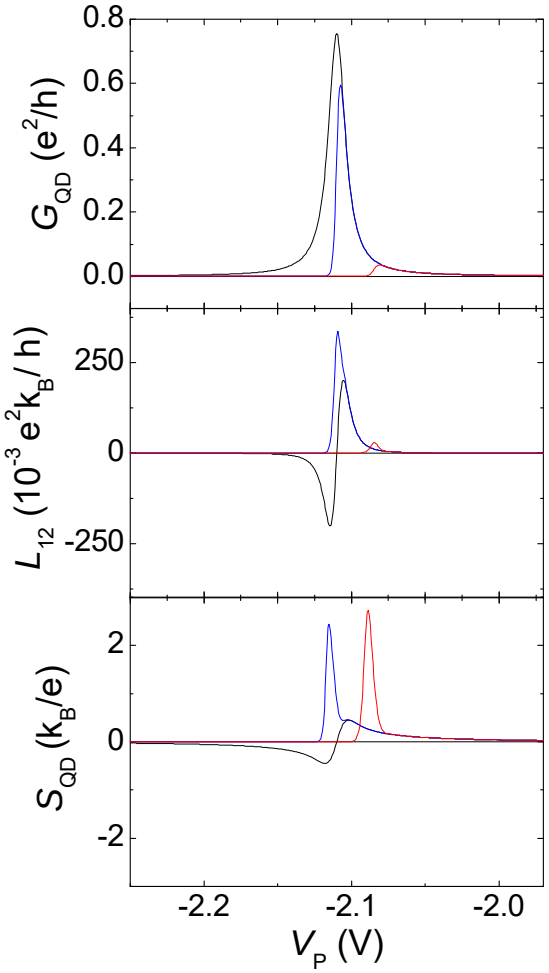

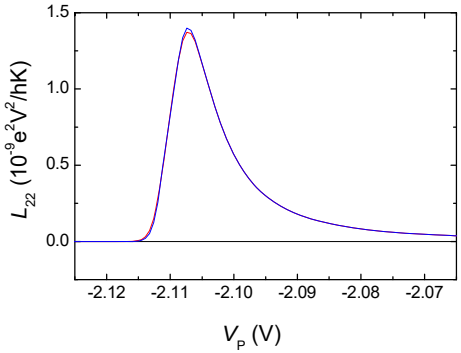

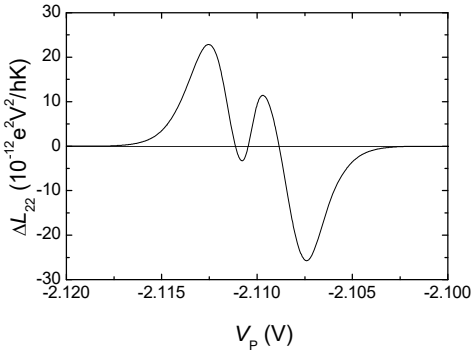

thermal conductivity

$$\kappa = L_{22} - \left(L_{12}L_{21} / L_{11}\right)$$

$$\Delta\kappa = \kappa_{T_1T_2} - \kappa_{T_2T_1}$$

$$\Delta\kappa / \overline{\kappa} \approx 0.1$$

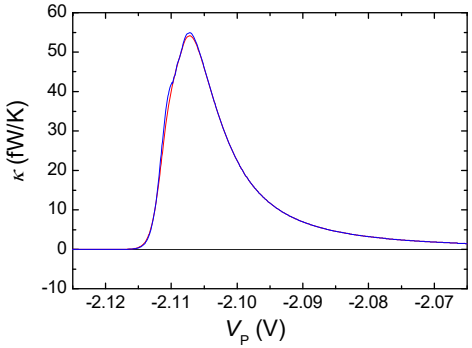

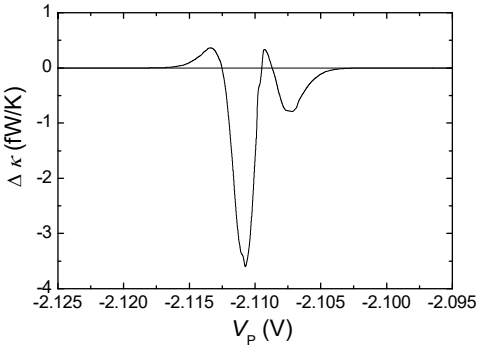

R. Scheibner et al., NJP **10**, 083016 (2008)

Double Quantum Dot: towards multi-terminal thermoelectrics

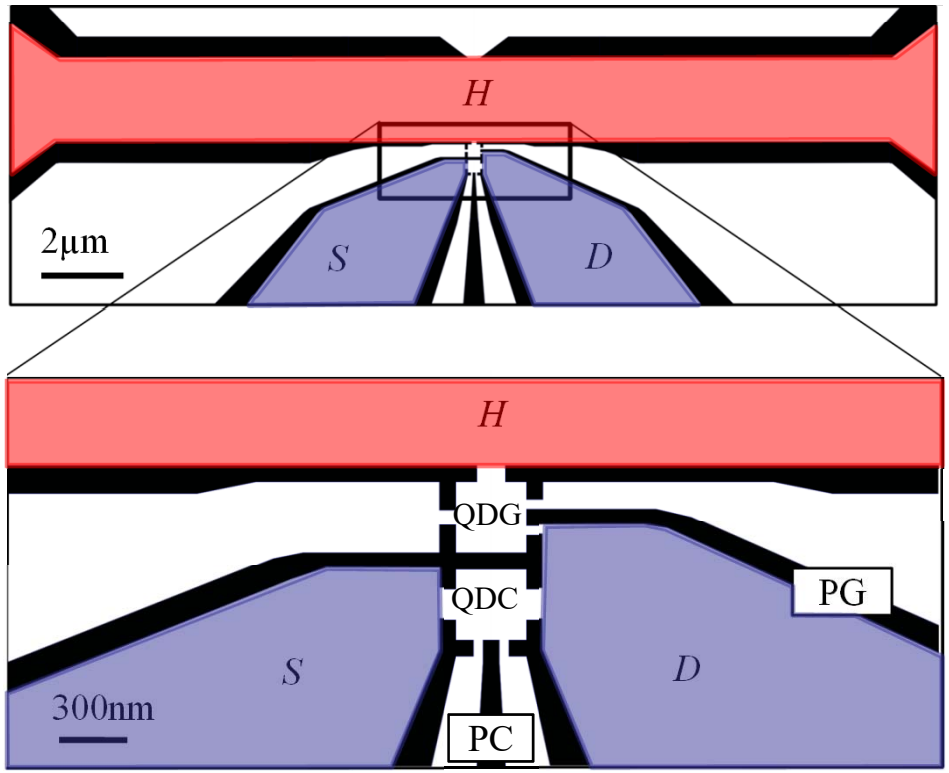

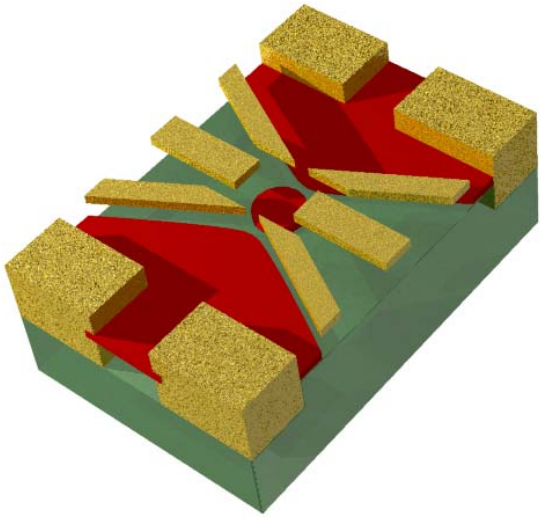

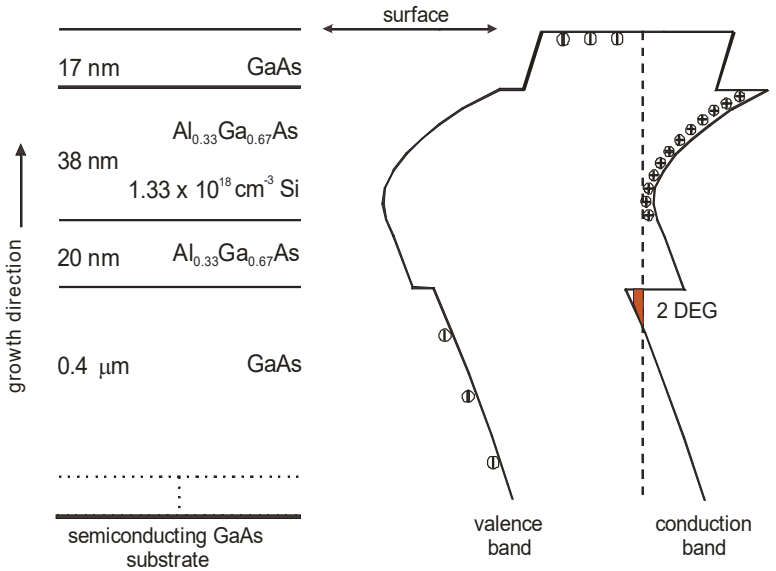

- GaAs/AlGaAs - 2DEG
- $n = 2.1 \times 10^{11}$ cm^{-2}, $\mu = 7 \times 10^5$ cm^2/Vs
- Ti/Au-surface electrodes (opt. and e-beam lithography)
- Au/AuGe - ohmic contacts

Characterization

All reservoirs at T_C = 80 mK

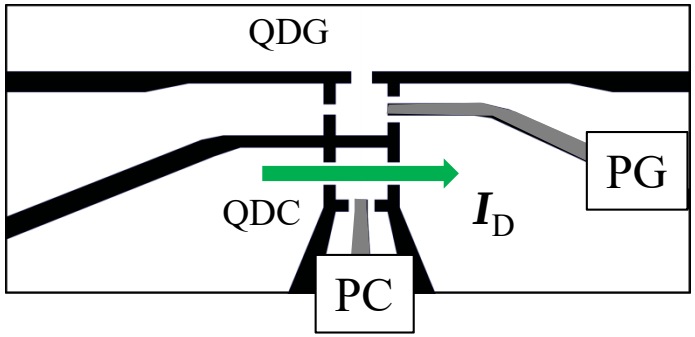

U: single QD charging energy

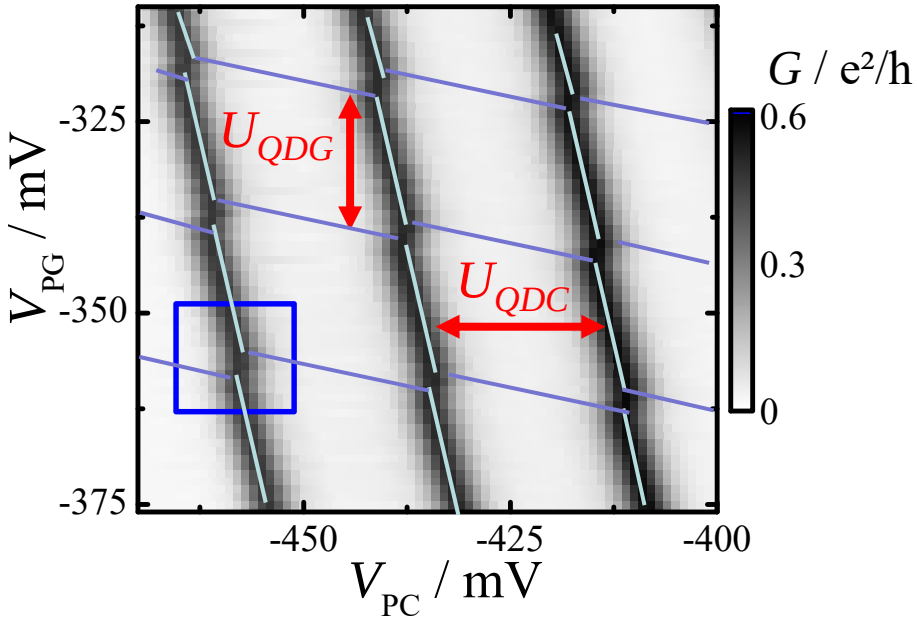

Stability Diagram: Regions of high conductance delimit regions with fixed charge configuration

Characterization

All reservoirs at T_C = 80 mK

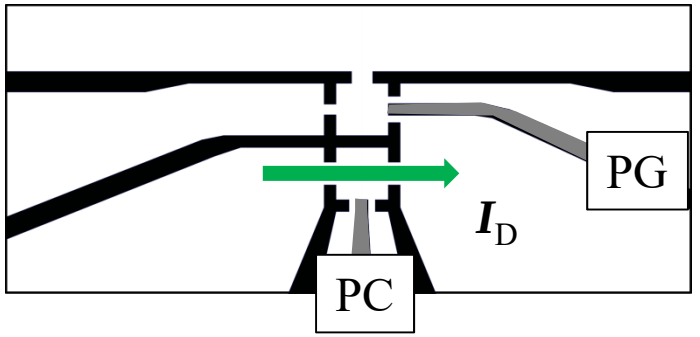

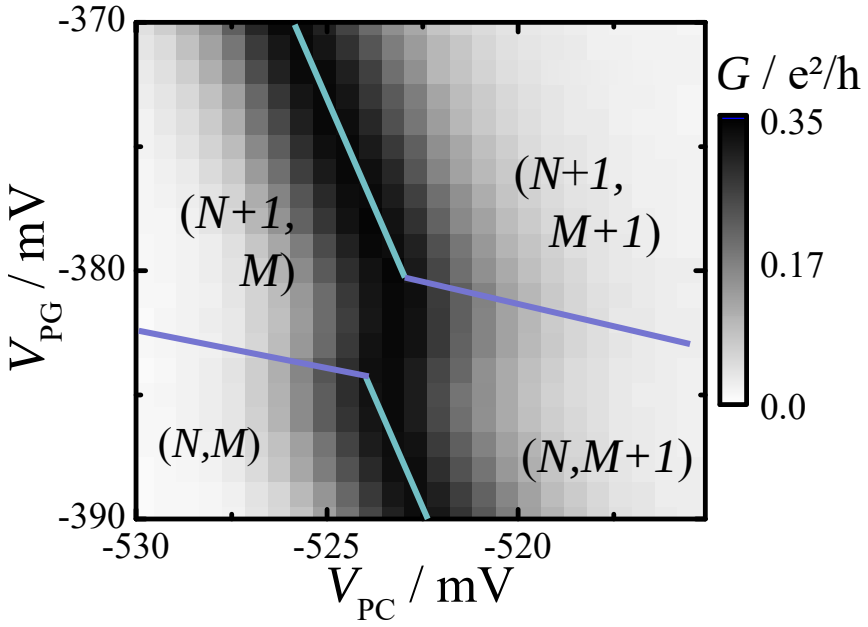

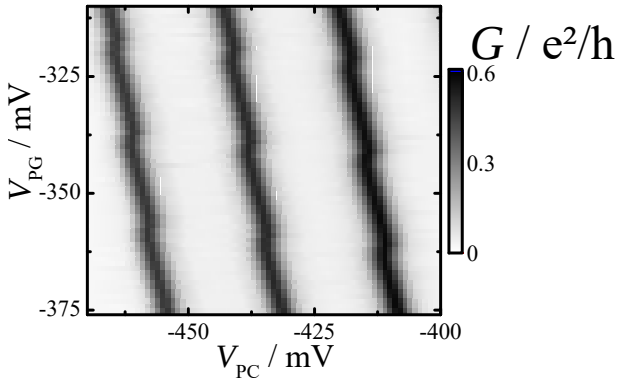

occupation numbers
QD_C: M
QD_G: N

Characterization

All reservoirs at T_C = 80 mK

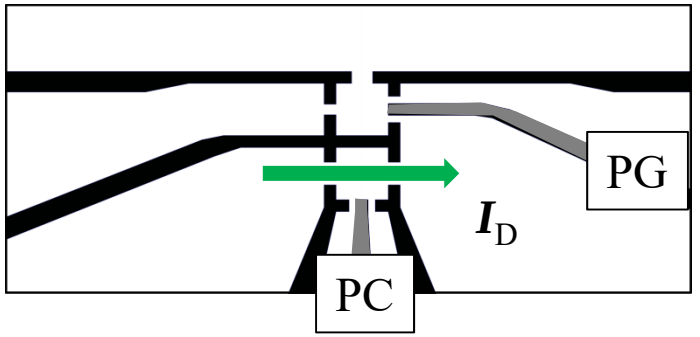

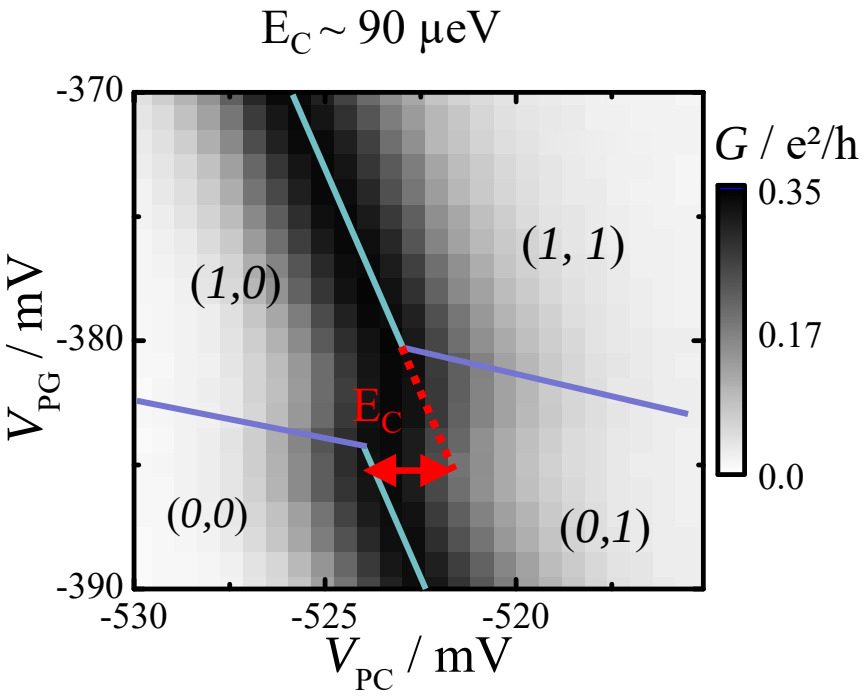

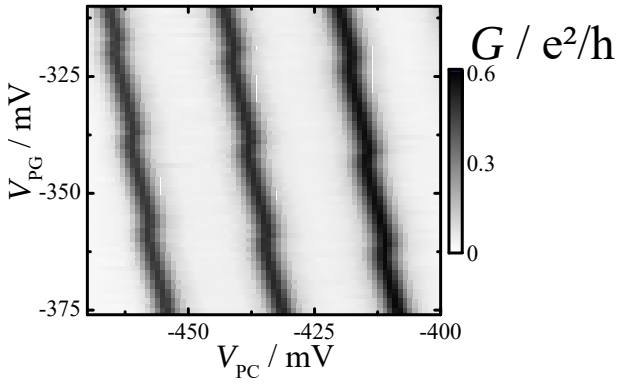

occupation numbers
QD_C: $M = 0$
QD_G: $N = 0$

Stability Vertex

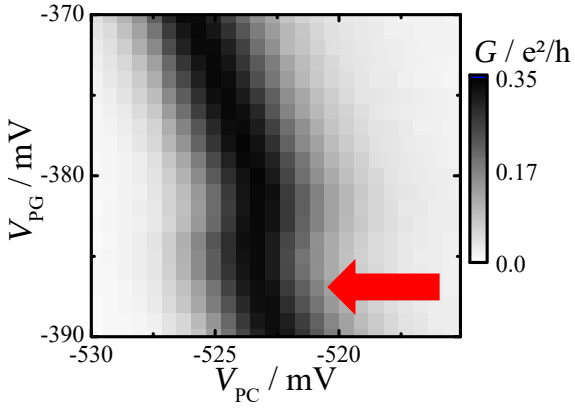

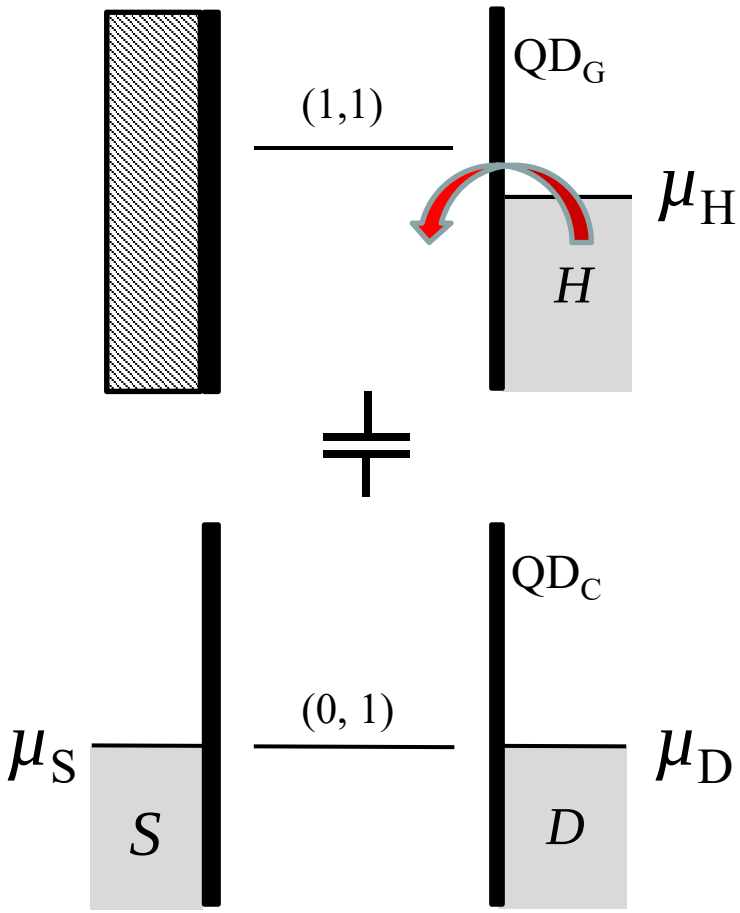

Stability Vertex

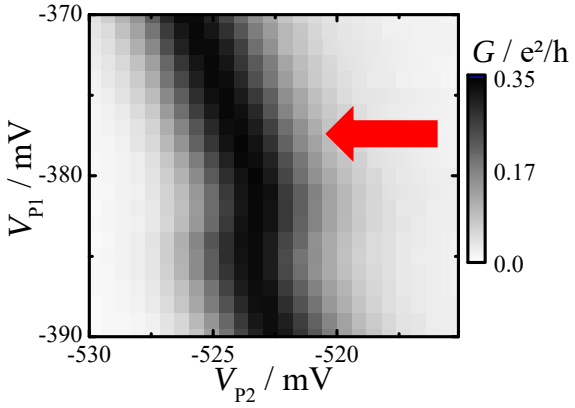

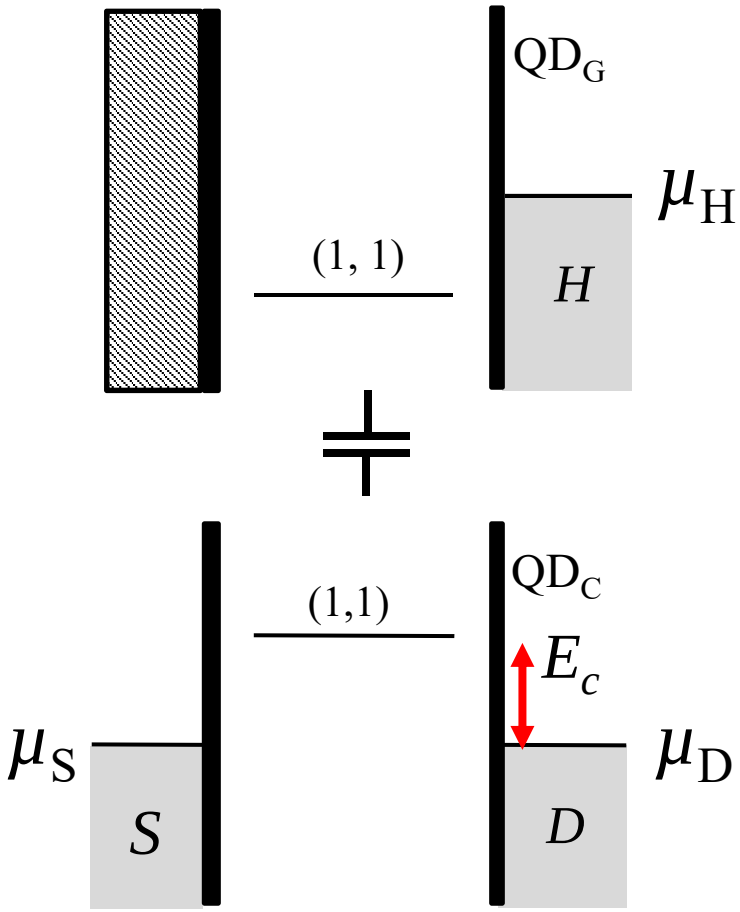

occupation numbers
QD$_G$: N
QD$_C$: M

Stability Vertex

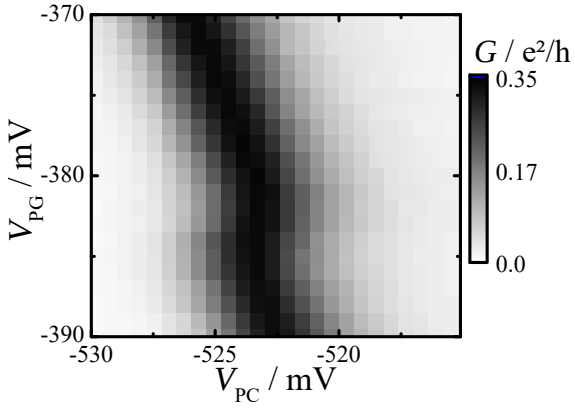

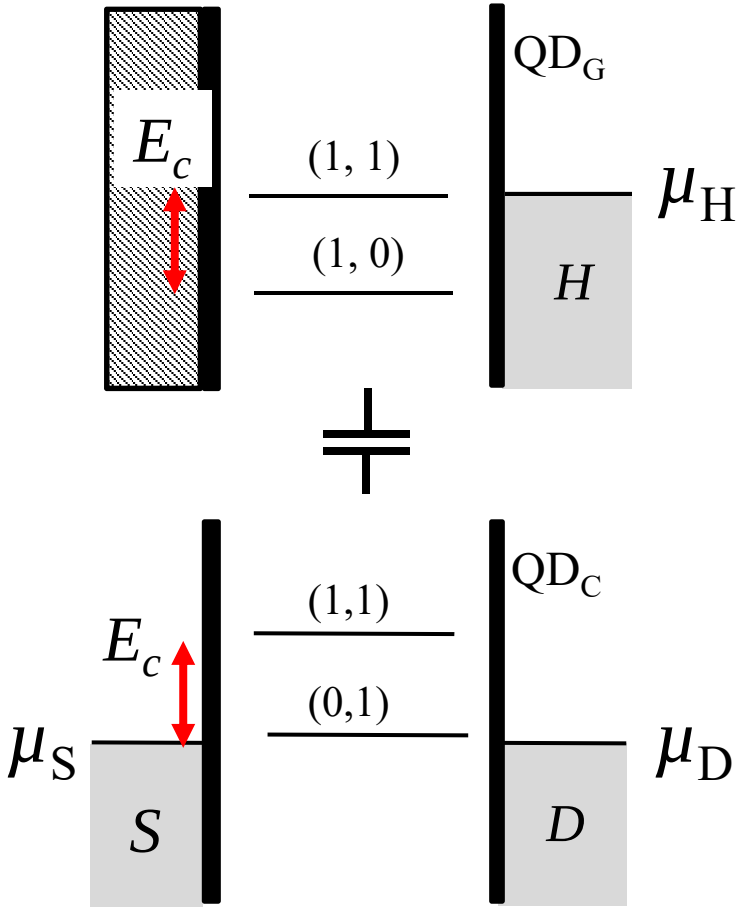

Hunting an Energy Harvester

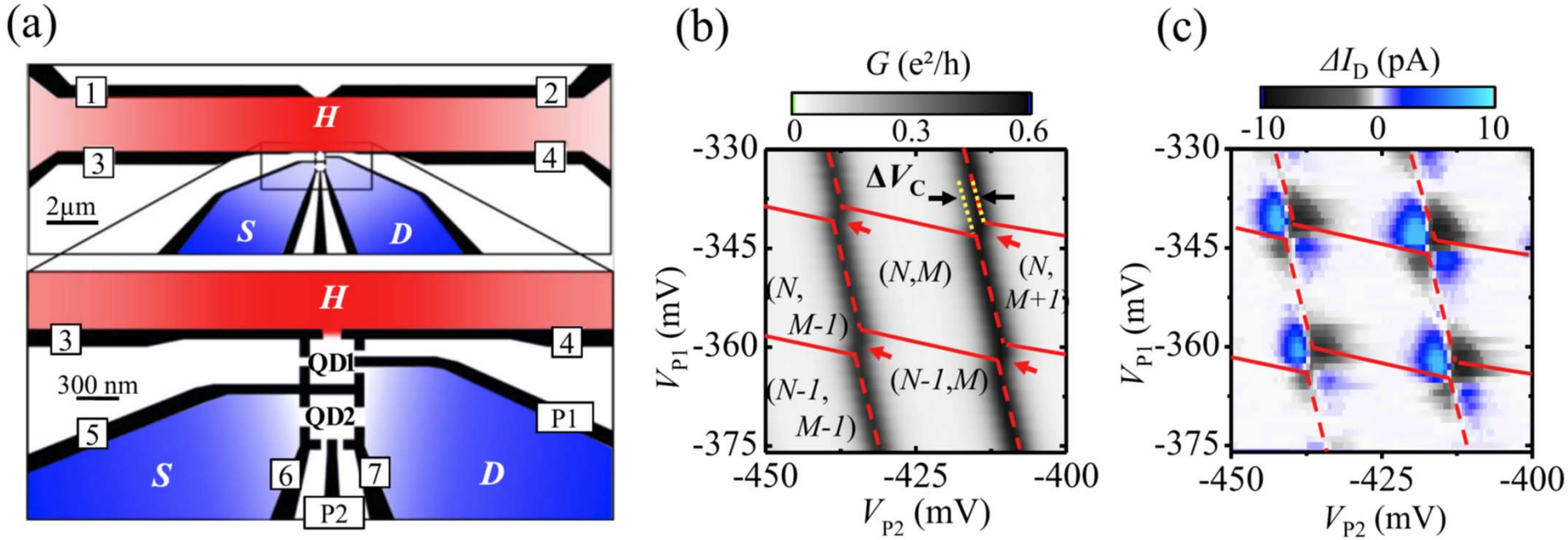

Figure 1. (a) Schematic design of the gate structure (black). Gates are labeled with numbers 1–7, P1 and P2. Electronic reservoirs are denoted S, D (both blue) and H (red). (**b**) Stability diagram of the QD-system showing the conductance of QD2. The characteristic honeycombs are indicated with red lines. QD occupation numbers are denoted with N, M. ΔV_C indicates the capacitive inter-dot coupling energy. (**c**) Current signal ΔI_D in reservoir D with $V_{S,GND} \approx -30\ \mu V$ for $T_H \approx T_{S,D} + 100$ mK.

New J. Phys. **17** (2015) 113003 doi:10.1088/1367-2630/17/11/113003

New Journal of Physics
The open access journal at the forefront of physics

Deutsche Physikalische Gesellschaft DPG
IOP Institute of Physics
Published in partnership with: Deutsche Physikalische Gesellschaft and the Institute of Physics

PAPER

Thermal gating of charge currents with Coulomb coupled quantum dots

H Thierschmann[1,3], F Arnold[1], M Mittermüller[1], L Maier[1], C Heyn[2], W Hansen[2], H Buhmann[1] and L W Molenkamp[1]

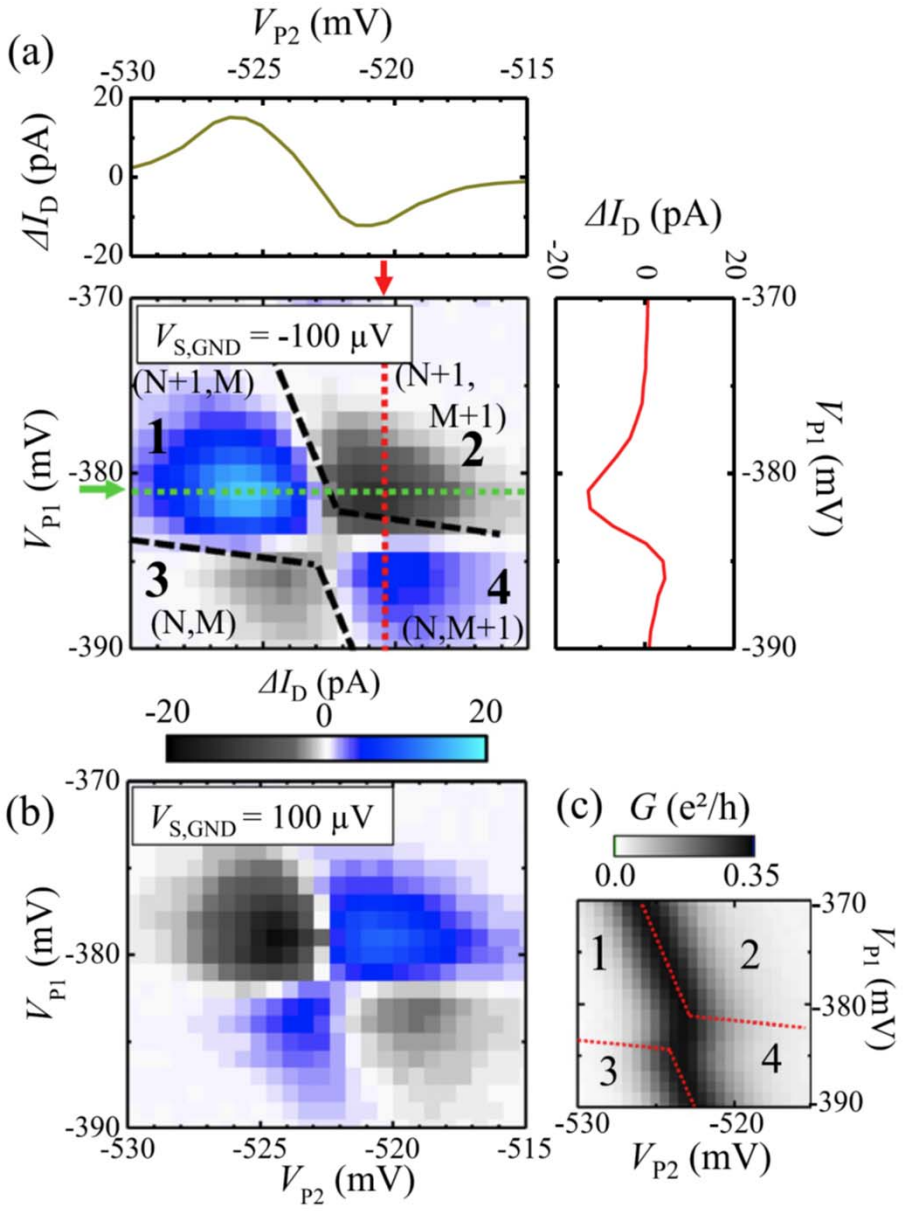

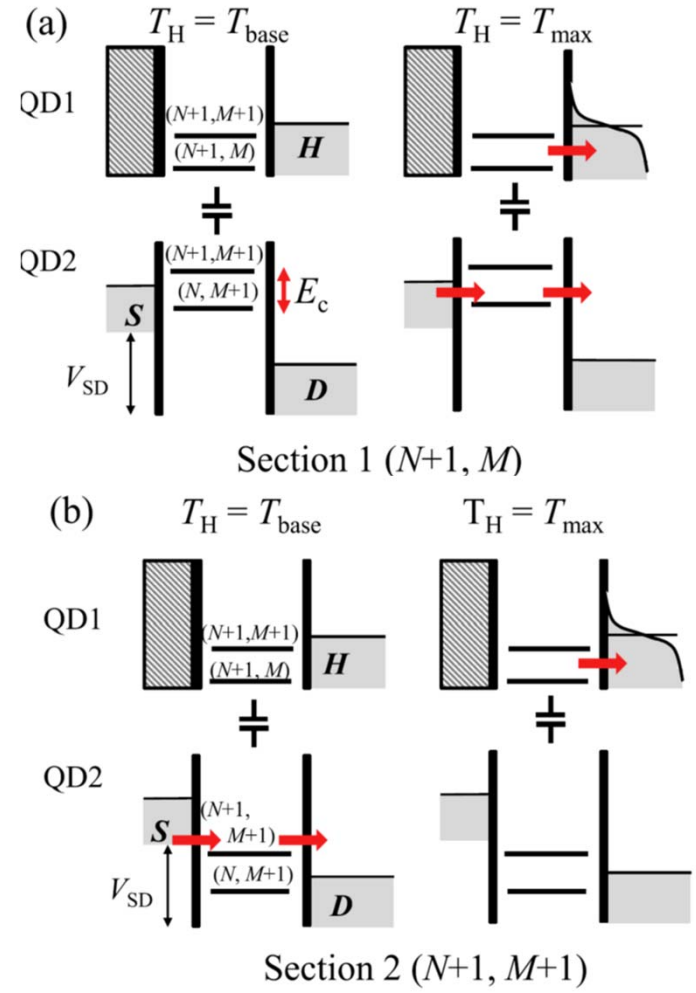

Allowing charge fluctuations on dot 1 enables (disables) charge transport through dot 2

Energy harvesting

What we really wanted is slightly different:

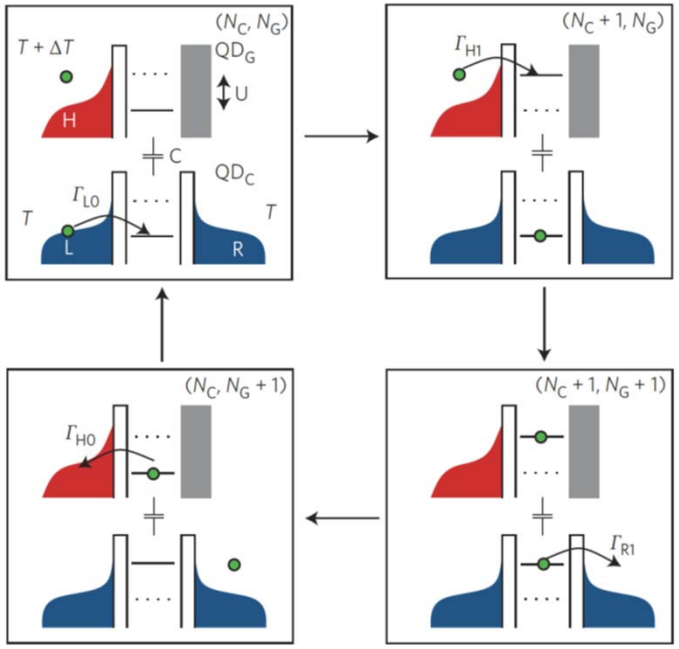

Figure 1 | Operating principle of the energy harvester. Two quantum dots are capacitively coupled, exchanging energy in packages of U, but not particles. One quantum dot (QD_C) is connected to two terminals, L and R. The other (QD_G) is coupled to a third terminal, H, which is at a higher temperature. When charge fluctuations occur according to the depicted four-stage sequence, an energy package is extracted from reservoir H and is delivered to the cold subsystem. There, these fluctuations are rectified and converted into a charge current when the product of tunnelling coefficients $\Gamma_{L0}\Gamma_{R1}$ differs from that of the opposite process $\Gamma_{R0}\Gamma_{L1}$ (not shown), that is, when both particle–hole symmetry and left–right symmetry are broken.

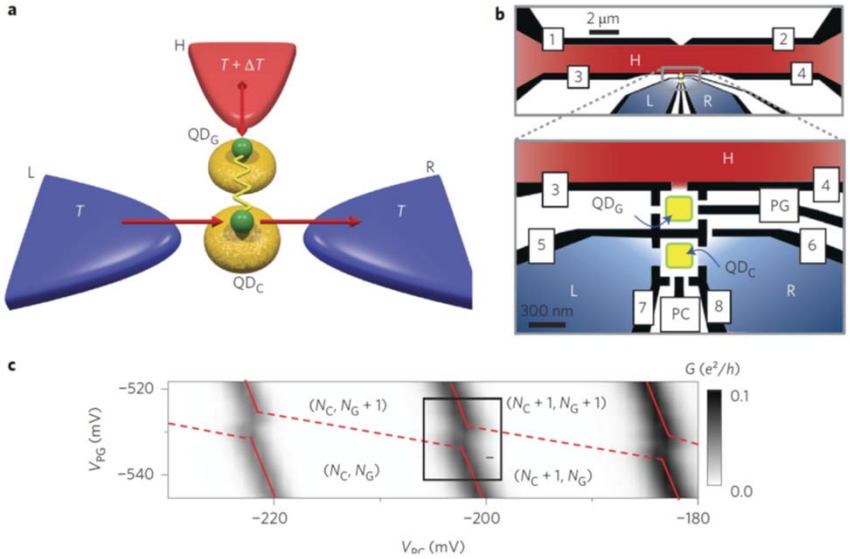

Original proposal:
R. Sanchez, M.Büttiker, Phys. Rev. B 83, 085428 (2011)

Energy harvesting

and it actually occurs in between the triple points,
where thermal gating is not dominant – but only for asymmetric barriers:

LETTERS NATURE NANOTECHNOLOGY DOI: 10.1038/NNANO.2015.176

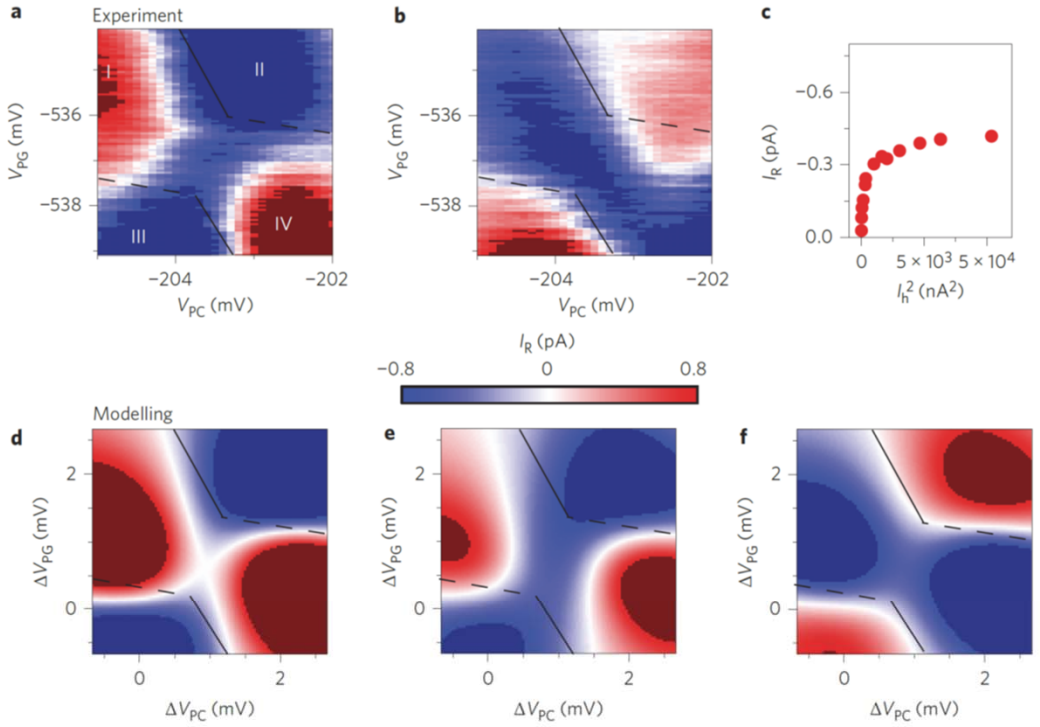

Figure 3 | 2*f* current in reservoir R (I_R) for configuration A in the vicinity of a TP pair. Black lines denote the stability region borders as obtained from the conductance data. **a**, Experimental data for $0 < \Delta\mu_{LR} < 10$ μV. The signal around the TP pair is a result of thermal gating (regions I–IV). **b**, The signal becomes reversed if $\Delta\mu_{LR}$ is inverted (-10 μV $< \Delta\mu_{LR} < 0$). The signal between the TPs is due to the proposed mechanism of energy harvesting. It stays negative, irrespective of the sign of the voltage bias $\Delta\mu_{LR}$. **c**, I_R as a function of squared heating current I_h^2 between two TPs for slightly different Λ. **d**, Model calculation for energy-dependent tunnelling barriers of QD_C, symmetric with respect to L and R. The signal between the TPs is zero, and only the effect of thermal gating is present. **e**, Calculation using asymmetric and energy-dependent tunnel barriers as obtained for configuration A with $0 < \Delta\mu_{LR} < 10$ μV. **f**, Model calculations for -10 μV $< \Delta\mu_{LR} < 0$.